Characterization of Biofilm Structure Developed under Varying Concentrations of Fe(III) on Different Support Materials

By

Iqra Sharafat

Department of Microbiology
Faculty of Biological Sciences
Quaid-I-Azam University
Islamabad
2015

Characterization of Biofilm Structure Developed under Varying Concentrations of Fe(III) on Different Support Materials

A thesis submitted in partial fulfillment of the requirements for the

Degree of

Master of Philosophy

In

Microbiology

By

Iqra Sharafat

Supervised by

Dr. Naeem Ali

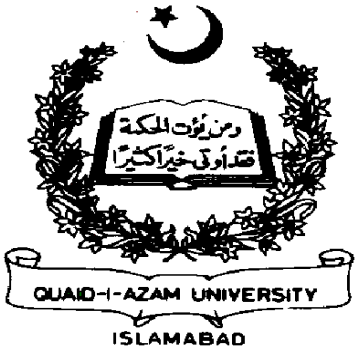

Department of Microbiology
Faculty of Biological Sciences

Declaration

The material and information contained in this thesis is my original work. I have not previously presented any part of this work elsewhere for any other degree and the material presented in this thesis has not been copied from any other source.

Iqra Sharafat

Contents

Certificate

This thesis submitted by Iqra Sharafat is accepted in its present form by the Department of Microbiology, Quaid-i-Azam University, Islamabad, Pakistan; as satisfying the thesis requirements for the degree of Master of Philosophy in Microbiology.

Supervisor: _____
(Dr. Naeem Ali)

External Examiner: _____
(Dr. Syeda Sabahat Zahra Kazmi)

Chairperson: _____
(Dr. Rani Faryal)

Dated: 15-06-2015

Dedicated to

My honorable Teachers,
Family and Friends

List of Tables

List of Figures

List of Acronyms

ABC	ATP binding cassette
ABBR	Aerobic batch biofilm reactor
AHL	N-Acyl-Homoserine lactone
AOB	Ammonium oxidizing bacteria
BAS	Biofilm Airlift Suspension
BFB	Biofilm Fluidized Bed Reactor
CLSM	Confocal laser scanning microscope
DCB	Divalent cation bridging
DAPI	4',6-diamidino-2-phenylindole
DPD	4,5-dihydroxy 2,3-pentanedione
FISH	Fluorescent *in situ* hybridization
FTIR	Fuorier transform infrared spectroscopy
NOB	Nitrite oxidizing bacteria
OTR	Oxygen Transfer Rate
Pss	*Pseudomonas syringae*
PVC	Polyvinyl chloride
PE	Polyethylene
SBBR	Sequencing batch biofilm reactor
SEM	Scanning electron microscope

SRT	Sludge Retention Time
SS	Stainless steel
TCP	Tissue culture plate
TDS	Total dissolved solids
TSS	Total suspended solids
TR	Tire rubber
WWTP	Wastewater treatment plant
WWT	Wastewater treatment

Acknowledgements

First praise be to Allah, the Almighty, on whom ultimately we depend for sustenance and guidance. Second, I would like to express my deepest gratitude to my supervisor, Dr Naeem Ali, for his guidance and stimulation throughout the course of this work. Sir has always made himself available to clarify my doubts despite his busy schedules. I found him instrumental in transforming a rough idea into a full-fledged framework. His emphasis on a sound evaluation motivated me to look at every system artifact from the point of view of an eventual experiment. Thank you Sir, for all your help and support.

All faculty members of the department have been very kind enough to extend their help at various phases of this research, whenever I approached them, and I do hereby acknowledge all of them, especially, Dr Fariha Hassan Chairperson department of Microbiology, Professor Dr. A. Hameed, Professor Dr. Safia Ahmed, Associate Professor Dr. Rani Faryal, Dr. M. Imran, Dr. Qaiser (Head department of environmental biotechnology NIBGE Faisalabad), Dr.Sajjad Ahmed (senior scientist NIBGE Faisalabad), Dr. Asma Imran (senior scientist NIBGE), Dr. Sumera Yasmeen (senior scientist NIBGE Faisalabad) for their assistance.

Furthermore, friends at the campus who have metamorphosed my sojourn here into a tour de forc academically, socially and intellectually merit my special gratitude. My coursemates in the M.Phil, especially, Mona Karim, Zara Rafaque, Afshan Ahmed, Sobia Ali, Hajira Zain, Sanam Khan, Faiza Mushtaq, Tooba Hayat, Tehseen Usman, Aysha Yousuf and others have also ever ceased to amaze me with their aptitude and support.
I feel a special mention and acknowledgment should be made to Dania Khalid Saeed, who as a good friend, was always willing to help and give her best suggestions. Thank you Dania.
In the same vein, completing this work would have been all the more difficult were it not for the support and help provided by my senior PhD colleagues, Noshaba Hasan, Aneela Younus, Saima Khalid and Nazia Khatoon at soil and Environmental Research Laboratory, with my questions . I am indebted to them for their help.
I owe a lot to my parents, my very dear brother and sisters who encouraged and helped me at every stage of my personal and academic life, and longed to see this achievement come true. This dissertation is dedicated to them.

Iqra Sharafat

Abstract

Biofilms are described as consortia of microorganisms adherent to biotic or abiotic surfaces embedded in a self-produced extracellular matrix containing polysaccharides, proteins and DNA. Biofilms can be harmful or useful depending on their area of existence. Biofilm formation is a nuisance, of particular relevance to human health, when found in drinking water reservoirs and distribution systems as these become a source of contamination and hinder the efficient operation of these systems. In addition, they may also pose a health risk to public by providing a habitat for pathogenic microorganisms. Conversely, however, biofilms are positively exploited in processes as diverse as biofilteraion, waste water treatment, production of fine chemicals and biofuel production. The overall objective of the study conducted here was to investigate the coupled effects of exogenous supplementation of different concentrations of Fe(III) and different support materials on microbial community structure and architecture of biofilms. The complexity of multispecies biofilm development and implications of microbial interactions on biofilm performance and their three dimensional structure were also underlined in this study.

Four laboratory scale aerobic batch mode biofilm reactors (ABBR) (four liters each) were run under test and control modes at varying conditions of ferric iron 0, 2.5, 6.5 and 8.5 (mg/l) for biofilm development on Stainless steel (SS), Polyethylene based plastic (PE), Polyvinyl chloride (PVC), Iron (Fe) and Tire rubber (TR) by taking activated sludge as an inoculum. After 90 days of incubation results revealed that parametric variation i.e. concentration of Fe^{3+} and attachment surface properties exerted a significant effect on bacterial density in biofilms ($p<0.05$). Polyethylene accumulated more bacterial density with increasing concentration of Fe^{3+} being highest at 8.5 mg/l (1.77131E+11 CFU/ml cm^2) whereas Fe and PVC, on the other hand showed a significant decrease in bacterial count with an increase in concentration of Fe^{3+} across the specified range (Fe = 2.241E+08 CFU/ml cm^2, PVC = 8.84E+08 CFU/ml cm^2). Biochemical identification of isolated bacteria from biofilms and activated sludge showed a wide diversity of bacteria which were mostly Gram negative and dominant species in biofilms included *Pseudomonas* sp., *Vibrio* sp., *Shewanella* sp., *Providencia* sp., *Serratia* sp., *Klebsiella* sp., *Bacillus* sp. and *Staphylococcus* sp. Sludge digestion indicated 38 percent more reduction in COD and BOD_5 in the reactor fed with 8.5 mg/l of Fe(III) than untreated reactor representing the undergoing physiological activities of microorganisms. Molecular characterization of autotrophic nitrifiers and denitrifiers based on phylogenetic sequencing analysis indicated the presence of genera *Nitrobacter, Bradyrhizobium* and *Rhodopseudomonas* in biofilms on TR in reactor treated at different concentrations of Fe(III), however, more diversity of species was observed at 8.5 mg/l. Likewise, PE at Fe^{3+}-8.5mg/l showed greater species of nitrifiers and denitrifiers related to the genera *Bradyrhizobium, Nitrobacter and Rhodopseudomonas* in addition to the genera *Nitrosomoas* and *Nitrospira* at Fe^{3+}-6.5 mg/l.

Fluorescent *in situ* hybridization (FISH) coupled with high resolution quantitative technique, confocal laser scanning microscopy (CLSM) of biofilm developed on TR revealed a significant increase in density of eubacteria from 3.00E+01 cells/cm^2 at 2.5 mg/ to 1.05E+02 cells/cm^2 at 8.5 mg/l and beta proteobacteria from 8.10E+01 cells/cm^2 at 2.5 mg/l to 1.42E+02 cells/cm^2 at 8.5

mg/l as the concentration of Fe(III) increased. Whereas, gamma proteobacteria demonstrated an inverse relationship between their cell density and ferric under different iron treatments (7.30E+01 cells/cm^2 at 2.5 mg/ to 3.40E+01 cells/cm^2 at 8.5 mg/l). Scanning Electron Microscopy (SEM) of biofilm on PVC showed greater diversity of microorganisms, EPS content and different cell sizes in biofilm developed on TR at 8.5 mg/l than at 0 mg/l. Similarly, effect of Fe^{3+} and different support materials were noted on biofilm and EPS development through FTIR that varied specifically in the region of 3270 cm^- -3384.2 cm^- in case of PVC, Fe and PE depicting carboxylic acids. Predominance of amines (1644.38 cm^-, 1636.49 cm^-) was observed in biofilms on SS and TR at lower concentrations of Fe(III) whereas significant abundance of carboxylic acids (3271.47 cm^-) and ethers and esters (1035.03 cm^-)in SS and TR, respectively, at its increased concentration. Further studies to understand how different support materials and Fe(III) concentrations mechanistically affect biofilm microbial community structures and functional performance are needed to devise strategies to control biofilms and enable the rational design of new generations of substrata for the improvement of biofilm based biological treatment processes.

A biofilm is a heterogeneous, highly structured sessile community of microbially derived cells embedded within a self-developed extracellular polymeric matrix composed mainly of proteins and polysaccharides with fewer contents of nucleic acids, lipids and humic mixtures (2)**,** (40), (41), (42), (38), (4)**.** Microorganisms use biofilm formation as a mechanism to survive indefinitely under harsh environmental conditions that implicates a progressive interplay within the microbial community structure at molecular level to facilitate the acquisition of new genetic traits (1)**,** (2). Biofilm formation is a dynamic process and is a result of a series of steps i.e. conditioning of surface, reversible and then irreversible adhesion of cells, microcolony formation, maturation and finally detachment and dispersal of cells (37), (38)**.**

Biofilms have gained much attention in medical science due to their adverse impacts on public health as these harbor infectious pathogens and are involved in around 65 percent of all diseases in human beings (3) such as, Native Valve Endocarditis (NVE), Otitis Media disease, Cystic Fibrosis , Bacterial Prostatitis, Periodontal diseases (4). Biofilms ease transport of genetic material, act as a barrier against antibiotics giving rise to antibiotic resistant strains of bacteria (3). Likewise, biofilms have negative effects in industrial and environmental sectors. These are associated with eutrophication (5), biofouling, hygiene and technical problems deteriorating the quality of water and piping materials in water distribution systems (6) and thus need the application of mitigation strategies to control these.

Not all biofilms are bad. The benefits of growing in biofilms are many. These are being used extensively in a diverse range of disciplines spanning environmental, biotechnological and medical industries. (7) Biofilms are obliging us for microbial enhanced metal and oil extraction and leaching of ores in mining industry [5], (3), microbial fuel cell technologies (8), (9), bioremediation (10), (11) and in biotransformation processes by sub surface biofilms (3), (2), (12) and many more. In the field of environmental biotechnology, attached growth processes (biofilms) have achieved special attention of scientists because multispecies biofilms provide the advantage of greater activity than planktonic bacteria, high biomass retention within the bioreactors and capacity to treat enhanced volumes of aqueous solution(s) (13). Various studies on attached growth bioreactors and enrichment cultures have proved

that biofilms are associated with production, degradation, cycling and mineralization of nitrogen, phosphorus, sulfur and various other organic and inorganic compounds of wastewater and sewage by adsorption and absorption mechanisms (14).

The formation of activated sludge flocs such as aerobic/anaerobic granules in waste water treatment (WWT) processes is a renowned positive application of biofilms which increases the treatment and separation efficacies of the waste water treatment plants (WWTP) (15), (7). Contemporary biological WWT techniques rely on application of biofilm(s) as a catalytic medium. (2).

Activated sludge process, a heterogeneous combination of microorganisms, colloidal particles, cations and organic polymers, comprised of two stream units for biological transformation of pollutants and separation of solids from liquid is capable of reducing organic matter to low levels and a very high quality effluent is generated due to flocculent nature of biomass (16)**,** (15)**,** (17)**.** Typical conventional systems, used for this purpose discharge insufficiently treated effluents rich in Ammonium-nitrogen (NH_4^+-N) and poorly biodegradable carbon to the environment causing problems such as eutrophication (18). Therefore, there is an ongoing demand for the development and implementation of sustainable waste water reclamation technologies to further improve the quality of effluents before their disposal in the environment and meet the demands of environmental conservational regulations (5)**,** (19)**.** In this scenario, urban and industrial WWT processes based on the development of active biofilms have emerged and now a days become a fertile field of research for water and waste-water researchers and is being resourced by governments and people (17) (5)**,** (20).

Current developments in the field of biotechnology have accelerated biofilm research in a diverse range of new directions. One out of several aspects of biofilms weakly understood is the structure of biofilm(s) previously considered as homogeneous and planar structure according to conceptual and mathematical models leading to its irrational revelation. Experience over the years with biofilm study has gradually made it obvious that biofilm structure holds the key to address conversion rates and mechanisms of mass transfer taking place within biofilms. However, making prediction of biofilm architecture is a difficult task due to a complex interplay among diverse processes that affect structural and architectural characteristics of biofilm(s). Hence, understanding and assessment of impact of different factors on biofilm

structure is crucial (21). Various theoretical models have been proposed to describe an idyllic biofilm structure, with the recognition that biofilms are heterogeneous (22). Logic behind the heterogeneity nature of biofilms advocates the concept that various process elements including cell physiology govern the structure of biofilm(s). Therefore, it becomes imperative that conditions prevailing the system be identified, and structure(s) of biofilms related to these respective conditions, as a first step in elucidating the composite interactions which administer the biofilm processes and ultimately, their structures (21), (23).

It has been proved that miscellaneous biological, physical and chemical parameters influence its structure to varying degrees. The physical parameters include mass transfer, substratum properties (type of attachment surface, quality and roughness), hydrodynamic forces and detachment while chemical factors include nutrients type and concentration. It is very candid to investigate into each of these factors individually with respect to their impact on biofilm structure yet, the dilemma of biological elements (microorganisms and EPS, physiology of cells) remains melded with the above ones and is challenging. Previously, several studies have been undertaken to reveal the impact of these parameters on biofilm structure by conceptual modeling yet, significant experimental data is unavailable (24), due to problems in designing and developing new methodologies, to study how and to what extant these conditions play their role to affect the biofilm structural composition (21). Recent investigations have focused on a key goal of revealing the phenomena of microbial cell–cell, cell–surface (7) and metal–microbe (25) interactions and their impacts on biofilm growth and stability (7).

Iron (Fe), one of the vital nutritional elements for bacteriological growth acts as an electron acceptor coupling oxidation of organic matter with iron reduction during respiration. For instance, Fe is a part of all heme enzymes including hydro-peroxidases and cytochromes. A comprehensive review of previous work on the structural profiling of biofilms under a diverse range of Iron concentrations revealed that Iron promotes or controls biofilms at its narrowly defined range of concentrations. Lack of Iron limits microbial growth where bacteria display iron scavenging mechanisms such as siderophores (Fe chelators) production for its acquisition (26). Moreover, negatively charged surfaces of bacteria and extracellular

polymeric substances exhibit a substantial sorption tendency towards positively charged monovalent, divalent and multivalent cations (Na^{+}, K^{+}, Mg^{+2}, Ca^{+2}, Fe^{+2}, Fe^{+3}, Al^{+3},) in a particular ratio as proposed in postulates of divalent cationic bridging theory (DCB theory), it also results in an enhanced activated sludge flocs stability and active biomass (27), (25). Consequently, in order to enhance biofilms and attached growth processes, supplementation of activated sludge with Fe(III) has been proposed as a state of the art strategy (28)**.** Likewise, the contribution of metal ions bound with EPS, in direct electron transferal from the metals and other compounds to appropriate electron acceptors has been greatly ignored (29)**.**

One more aspect, which has been attached with less attention uptill now, is the positive and negative influence of support materials on the densities of attached biomass of biofilms. To control biofilms, various natural and synthetic substrata are used. Materials based on plastics e.g. Polyvinyl chloride (PVC), Polyethylene (PE) and rubber are some of the synthetic materials proposed for this purpose due to their reduced biodegradable and recalcitrant nature, large surface area, hydrophobicity and adsorption properties in challenging environments (5), (30), (2).

Similarly, few researches have reported the structural integrity and accumulation of biofilms on the surfaces of Stainless steel (6) and Iron commonly employed as piping materials in water distribution, plumbing systems and municipal buildings (31). Furthermore, previous studies have concentrated exclusively on interactions between surfaces and clinically relevant monospecies biofilms whereas few studies have focused on waste water treatment processes comprised of multispecies microbial communities that include studies of biomass, their distribution and subsequently treatment efficacies of bioreactors (32).

In this study, we aimed to use conventional and molecular techniques i.e. fluorescent in situ hybridization (FISH) combined with confocal laser scanning microscopy(CLSM), molecular sequencing, fourier transform infrared Spectroscopy (FTIR) and scanning electron microscopy (SEM) in order to assess the positive as well as negative impacts of properties of bio carriers (Stainless steel, Iron, PVC, PE and Tire Rubber) and different concentrations of Fe(III) as a nutrient and bridging agent on biofilm microbial community structure and EPS components and measure physicochemical parameters (nitrification rate, COD, BOD5, volatile fatty acids

(VFA), total dissolved solids (TDS) and total suspended solids (TSS) and dissolved oxygen (DO)) to monitor functional efficiency of laboratory scale aerobic batch biofilm reactors (ABBR).

This phenomenological study will establish relations between physical, chemical and microbial processes of surface-microbe and metal–microbe interactions which are an important precursor to the development of processes in a wide range of environmental and biotechnological applications. Since biofilm structure and its associated role varies from surface to surface and also on different Fe^{3+} concentration, therefore, it is highly important to study it when it is unwanted on surfaces like pipelines in water distribution systems (WDS) in order to develop effective mitigation strategies to control it and for the selection of sustainable and cost effective piping materials. Moreover, it becomes equally important to fully understand its development, detailed bacterial interactions, catalysis and associated role of limiting environmental factors when biofilm is present on any attached growth reactor. Considering this dual role of biofilm as bio catalytic matric the present study is planned.

Aim and Objectives

The study was undertaken to extend previous works in the field of waste water treatment and environmental biotechnology to a comprehensive set of measures that define biofilm structure with the aim to find suitable carrier material and Fe(III) concentration for biofilm development as well as for its control and to evaluate development of biofilms in batch mode on different support materials under varying concentrations of Fe(III).

Specific objectives of the work presented here included;

i. Development of biofilms on selected substrata in aerobic batch biofilm reactors (ABBR) under the influence of Fe^{3+} as a nutrient, electron acceptor and coagulant in activated sludge.
ii. Determination of microbial community composition of biofilms by conventional and molecular methods i.e. heterotrophic plate count method (HPC), phylogenetic sequencing and florescent *in situ* hybridization (FISH) coupled with confocal laser scanning microscopy (CLSM) and digital image analysis.
iii. Characterization of biofilms structure developed on the support materials by scanning electron microscope (SEM).
iv. To assess the biofilm forming capability of all isolated bacterial species by biofilm development assays.
v. To monitor the treatment efficiency of different reactors in terms of removal of nitrogen, COD, BOD5 and volatile acids.
vi. Characterization of extracellular polymeric substance (EPS) of biofilms developed on different support materials under varying Fe(III) Concentrations by fourier transform infrared spectroscopy (FTIR).
vii. To further investigate the ability of each biofilm on its respective surface under the influence of varying Fe^{3+} concentrations in ammonium removal by enrichment technique.

Biofilms, metaphorically termed as “city of microbes” (1) with EPS as “house of the biofilm cells” were observed by Antonie van Leuwenhoek as early as in 1674, to describe minute invisible ‘animalcules’ with his primitive microscope (2). Since then, an array of development made in the field of research on microbial slimes has accelerated yet the term “biofilm” was typically formulated in 1984 (3). Various descriptions of the term biofilm have been proposed. According to Omniscient Encyclopedia Wikipedia (OEW), a biofilm is a well-structured microbial community trapped in a matrix of polymeric substances attached to surfaces. (http://en.wikipedia.org, 2090205) (3). The new definition of biofilm is a microbially derived sessile community characterized by cells that are irreversibly attached to a substratum or interface or to each other, are embedded in a matrix of extracellular polymeric substances that they have produced, and exhibit an altered phenotype with respect to growth rate and gene transcription (4).

More than 99 percent of microbial population on Earth has been found in its attached growth form viz. biofilm.(Vu et al., 2009) (5). Both Gram negative as well as Gram positive bacteria ae capable of biofilm formation. (6). Both autogenic and allogenic factors of ecosystem play their role in successional changes of microbial communities leading to the formation and establishment of biofilms as has been demonstrated in the case of biofilms developing in water distribution pipelines (7). Diverse range of microorganisms e.g; bacteria, fungi, viruses, algae and protozoans intricate biofilm but primarily, bacteria predominate (Kerr et al. 2003) and in response to favorable environmental conditions such as nutrients, polymeric matrix, temperature and moisture start biofilm establishment (8). Bacteria flow towards their respective substrates through Brownian pedesis and chemotaxis (9).

2.1. Why Bacteria Prefer to Grow as Biofilm?

Bacteria prefer to grow in their benthic form as biofilm has been documented as a protective method of cellular growth allowing them to survive under adversarial circumstances and hostile conditions such as nutrient starvation. Moreover, biofilm assists cells to inhabit new niches after dispersal from their sessile structures. (Abee et al., 2011), (10)

One key positive influence of substrata on bacteria (attached growth) is enhanced activity within biofilms due to (i) modified physiology of cells due to switching on of certain genes (ii) altered concentrations of enzymes and nutrients in their local environment (iii) selective impact of EPS that acts as a molecular sieve towards toxic componds and protects cells against extreme conditions such as, pH, temperature and starvation (11)**.**

2.2. Diversity of Bacteria in Biofilms

A great phenotypic variety is exhibited in biofilms depending on the specific genotypic system studied under the influence of environmental factors. (10). Transcriptional profiling records have revealed that regulation of a number of gene(s) in bacterial communities leads to their altered phenotypes, such as increased/decreased cell growth and sometimes EPS production (9), (12)(13). YneA gene, the SOS responser that mediates bacterial cell elongation and biofilm development, was found responsible for two types of Listeria monocytogenes biofilms when grown under flowing and static growth conditions (14). Similarly, densely packed and heavily layered cells of Lactococuss lactis and Lactobacillus plantarum in extracellular polymeric matrix were reported by Habimana and his coworkers under flowing and static conditions of flow (15). In liquid media, some Bacillus species form pellicle assemblies floating on the surface whereas other species develop colonies and sporulation sites on agar media (10).

2.3. Determinants of Biofilm Structure

Considering the contribution of various environmental and genetic factors in the diversity of biofilm structural development, biofilm determinants is an ongoing debate (16). Transposon mutagenesis, identification of gene loci, 16SrRNA, gene knock-out and various other molecular techniques have been utilized to investigate the functions of gene(s) in the formation of biofilm components. Genes are assigned their particular role(s) by comparing a mutant strain's biofilm formation ability with its wild type isogenic strain (17). Additionally, Davies et al. found that the quorum sensing system plays a vital part in its differentiation (18), (10). Quorum sensing and two component

regulatory machineries in bacteria are mainly involved in regulation of biofilm formation processes (19), (1)**.**

2.3.1. Quorum Sensing

The process of Quorum sensing (QS) has been recognized as a central cell- to-cell communication and networking system in both gram positive as well as gram negative microorganisms, governed by the synthesis and detection of a certain threshold of low molecular weight signaling molecules termed as autoinducers thereby regulating the expression of specific genes(s) related to biofilm development, motility and other virulence determining factors. (20)**,** (21)**,** (22), (23).QS is the main factor involved in process of biofilm regulation (24) and was first described for Vibrio fischeri, a marine bacterium. Luciferase complex enzyme has been reported responsible for bioluminescence that is governed by the process of QS (21)**.**

2.3.1.1. Common Themes in Bacterial Quorum Sensing

Bacterial QS systems have been categorized into three general classes: (i) LuxI/LuxR QS system found in gram-negative bacteria (ii) oligopeptide mediated two component QS system in bacteria that are gram positive (iii) autoinducer 2 (AI- 2) encoded by *lux S* QS in both gram positive bacteria and gram negative bacteria (25), (21)**,** (1)**.**

2.3.1.2. Quorum sensing (QS) in Gram Negative bacteria

Signalling moieties employed in gram negative bacteria are either homoserine lactones (HSLs), heptylhydroxy-4-quinolones, or di-ketopiperazine (23). Autoinducer synthases typically designated as, Lux I proteins, induce AHL moieties which are recognized by lux R proteins in response of their binding to DNA promoter regions and activation of transcription of certain genes in gram negative bacteria (20). In *Vibrio fischeri* [72], several studies have reported three types of AHL signals, 3- oxo - hexanoyl- HSL, *N*- octanoyl- HSL and *N*- hexanoyl-L- HSL. [78-80]. (20). Whereas, in biofilms of *P. aeruginosa* QS system (PQS), 2- heptyl-3- hydroxy-4- quinolone has been discovered as the signaling molecule [90] by the transcription of *rhlI* genes (20)**,** (21)

2.3.1.3. Quorum sensing (QS) in Gram Positive Bacteria

First type of QS system in gram positive bacteria involves the production of precursor auto-inducing oligopeptides (AIP), their slicing from the respective concensus sequences, sensing by two- component transduction system and finally, their release into extracellular environment through an ABC i.e. ATP binding cassette transporter as cell membrane in these bacteria is not freely permeable to the movement of AIPs contrary to gram negative bacteria (20)**,** (25)**.** Second type of QS in gram positive bacteria is ComRS, identified recently in various Streptococcus spp., in which a tiny pheromone oligopeptide signal XIP is internalized into the cell, ComR which is a *Sig X* regulator binds with XIP leading to transcrioption of target genes (21), (26). This type of QS was observed in *S. mutans* (21)**.**

2.3.1.4. Bacterial Inter Species Communication

In addition to intraspecies communication systems as described above, there is another system called AI2 (autoinducer-2) system for interspecific signaling and communication found in both gram positive as well as gram negative bacteria in which Lux-S encoded protein plays a role in synthesis of AI-2 precursors i.e. 4,5-dihydroxy 2,3-pentanedione (DPD) and homocysteines (27).

2.3.2. Two Component Systems and Biofilm Regulation

2.3.2.1. GagS/GacA

Around sixty two component regulatory systems have been described for the spp. of P.aeruginosa. [70] Among all of these, GacS/GacA (transmembrane sensor kinase) is the super regulator of QS and biofilm in these strains. GacS receives a phosphate from GacA after its autophosphorylation, because of which expression of micro RNAs, RsmZ and Rsm-Y, is upregulated to capture Rsm-A gene encoded Rsm-A protein. Inactivation of Rsm-A by GacS/GacA system governs the control on the production of C12- HSL and C4-HSL (28), (1)

2.3.2.2. RetS/LadS

Ret-S, a hybrid sensor stifles biofilm development. On the contrary, Lad-S has proved itself to be its antagonist (29). *Ret-S* mutant of P. aeruginosa PAO1 strain and PA14 strain lacking in lad-S, manifested an attenuation in biofilm forming capability as compared to their respective wild type strains and Lad-S+ strains (30)

2.4. How Microorganisms Develop Biofilms

Pseudomonas aeruginosa is a model organism for biofilm study because of its ubiquity in nature and its biofilm structural scaffolding cycle may be divided in five steps during its establishment (1). Creation of base layer termed as "conditioning film" on substrate surface is considered the very first step of biofilm fabrication containing several organic particles and ions (31)**.** This film is formed because of interactions between medium and surface immersed into it leading to modification of substrate properties viz. surface tension and charge properties and thus enhances deposition of cells (31)**.** A possible mechanism proposed for the adhesion of bacterial cells with any substrate is based on hydrophilic/hydrophobic characteristics of the later and the phenomenon of overcoming of repulsive attractions between electrical conditioning film and bacterial appendages (flagella, pili and fimbriae). (31)**,** (2)**.**

After reversible attachment of planktonic cells in the second stage, it is then progressively followed by an irreversible adhesion phase of cells in the third stage mediated by the process of polymer bridging between cells and EPS. As a result of this attachment, microcolonies (discrete growth of cells in extracellular matrix of polymers) are formed. Bacteria grow constructing three dimensional communities, occupying non-colonized surfaces and cover the whole area (13)**.**

Ultimately, when a biofilm reaches a certain threshold thickness, dispersion of attached cells occurs to colonize new niches in the final stage as represented in Fig. 1 (1), (2)**.**

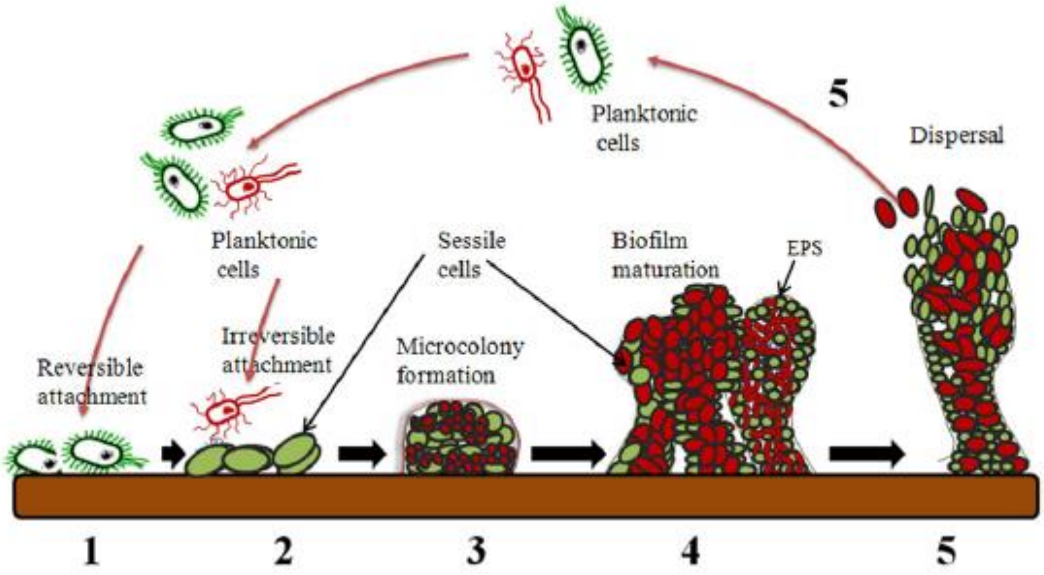

Figure 2.1. Hypothetical model representing a mixed sp. biofilm development in five distinct stages (32)**.**

Both multispecies and monospecies types of biofilms follow the same sequence of successional modifications and exhibit similar structural manifestations (13)**.**

2.5. Resistance Mechanisms in Biofilms

General resistance mechanisms employed in both monospecies and multispecies biofilms include slow penetration of substrate into the medium, 3-D structure of biofilm, resistance phenotypes, resistance against disinfectants and antibiotics, horizontal transfer of gene(s), mechanism of programmed cell death, internalization into protective sites and changed environment such as pH and nutrients and production of enzymes (32)**.**Yet, mechanisms employed in biofilms comprised of multispecies for greater resistance include unique process of quorum sensing for communication within and across the species, greater volume of formed biofilms, extra eDNA production application of protocooperation among species, dense 3-D structures (33) interaction of EPS with superoxides and antibiotics to set them at their sublethal concentrations, formation of persister phenotypes (10) and irregulation of cAMP / CRP operon to increase the resistance against higher fluid pressure (32)**.**

2.6. Biofilms and Our Environment

Biofilms may be harmful or useful depending upon their area of presence (34). Around 65% -80% of microbial infections have been stated to involve the engagement of biofilms (34). Biofilms harbor pathogens that cause numerous diseases such as, endocarditis (by Streptococci, Staphylococci, Aspergillus and Candida sp.), Otitis media (disease of ears caused by Moraxella spp., Haemophilus influenzae, group A streptococci, S. aureus and enteric bacteria), cystic fibrosis (by H. influenza and S. aureus), other diseases of respiratory tract and numerous others (4), (35), (36), ease transfer of genetic material (34), provide resistence against antibiotics, perturb water quality, cause corrosion in water distribution pipelines hence, permit scientists utilize strategies for the control and mitigation of biofilms. (2).

At the same time, usefulness of biofilm has also been exploited in several fields of biotechnology and environment e.g., microbial enhanced extraction of oils and metals, bioremediation and for many biotransformation purposes etc. (34), (2).

2.7. Biofilms in Wastewater Treatment

Municipal and industrial wastewater treatment (WWT) is one of the major research topics focused by biological scientists and resourced by public and governments in this age (11). Because, untreated or not sufficiently treated wastewater and sewage, if discharged to the main streams and environment roots a number of problems such as damage to marine life and eutrophication. Therefore, there is need for proposal and implementation of cutting-edge technologies for enhanced wastewater reclamation and in order to meet the criteria of environmental conservational regulations (37), (11).

Typical old systems, used for this purpose liberate effluents with abundant Ammonium-nitrogen and poorly biodegradable carbon (38) so in this situation of prompt plea of developing sustainable WWT processes, biofilms development from activated sludge have been proposed as a satisfactory solution to the problem and are proved to be very promising biotechnologies. Biofilms provide us with the benefits of excellent capability of biomass retention in system, operational flexibility, better control over reaction rates (13), (3), lessened hydraulic retention time, less

sludge production, resilience to environmental vicissitudes, resistance against shock organic load (39), improved biodegradation of recalcitrant compounds, minimum energy consumption and many more. Therefore, there is a growing need to devise approaches to enhance biofilm(s) growth under stressed conditions by chemical, physical and mechanical means and to explore the heterogeneous microbial composition, spatial distribution, physiological and architectural features of biofilms developed from activated sludge during wastewater treatment (WTT). (34), (13), (3).

2.7.1. An Overview of Activated Sludge Process

Activated sludge structure consists of three levels: bacteria, micro- colonies and activated sludge flocs (40), (41). Bacteria strongly bind together with the aid of polymeric substances to form micro colonies that are further interconnected by cations, polymers and polyelectrolytes to produce floc(s) (40), (42). Flocs assist bacteria to obtain substrate and protect them from environmental strains such as dehydration and predation (43).

Biological process of wastewater treatment (WWT) reduces multitude of contaminants from the influent in three steps, fueled by bacteria that act as biocatalysts. In the first step, oxidation of complex organic matter converts it into more easily removable products followed by second step of flocculation. In the third step, elements i.e. phosphorus and nitrogen, causative agents of eutrophication in receiving water bodies are removed biologically (44), (41).

2.8. Extracellular Polymeric Substance (EPS) Components and EPS Characterization

EPS, a hallmark of activated sludge process (>90 % of biofilms), are defined as the polymers that can be isolated from EPS secreting microbes, without which microorganisms can still remain viable. (1), (45). EPS serves as a sink for nutrients, provides protection to cells against predators and the effects of biocides (31) and helps in the cohesion and adhesion of cells to the surfaces irreversibly by the phenomenon of polymer bridging (45), (46), (1). Polysaccharides in EPS have been found either as homo-polysaccharides as found in Salmonella species or hetero-polysaccharides as in Pseudomonas spp. Heteropolysaccharides have further been

categorized as anionic or cationic in nature (Staphylococcus spp.) (47), (45). Sheng et al., 2010 carried out calorimetric assays to assess the role of carbohydrates and proteins in the strength of biofilms, carbohydrate to protein ratio showed that protein constituents played major part in flocs stability than carbohydrates (48).

Important enzymes detected in biofilms include polysaccharases, phosphatases and peptidases that serve as a digestive system for organic compounds and upsurge the availability of nutrients to bacteria (49). Production of "lectins" peptides that bind with sugars, in biofilms have been detected for their role in biofilm stabilization (45). Bacterial adhesins such as appendages and EPS have been verified for their part in cohesion and adhesion of cells among themselves and with surfaces (50), (41). Application of rotational viscosimetry has demonstrated that hydrogen bonding, weak Vander Waals forces and polar interactions were involved among polymer components that affect biofilm stability, mechanistically (51),(45).

Qualitative and quantitative measurement of concentrations of EPS components is a difficult task (1). There is need of extensive research for the characterization of its components and understanding the interactions among these polymers of biofilm by using techniques such as FTIR and various others (3).

2.9. Important Engineering Aspects for Biofilm Development

According to Saravanan and Sreekrishnan (2006), biofilm modeling is tailored with flow dynamics in the system that gives a prediction of the WWTP performance (52).The difference between attachment and growth of biofilm and detachment is described as development of biofilm. Reliable operation of bioreactors depends on high biomass on carriers and biofilms must be smooth so that active mass is not easily washed out of reactor (53). Biofilm grows in a reactor when rate of dilution i.e. DH = =Q/V) exceeds μ_{max} (maximum growth rate): $DH = Q/V > \mu max$

Occasionally, formation of biofilm is found at dilution rates less than μmax but still most of the conversion processes occur in solutions (54).

2.9.1. Aerobic Treatment vs. Anaerobic Treatment

Treatment under aerobic conditions has been recommended for WW with lower than 1500 mg/L COD whereas anaerobic treatment at COD concentration upto 50,000 mg/L (55). Aerobic treatments result in better quality effluents due to high activity within the films. Practically, temperature effects and mixing also impact efficacy of batch reactors (56). Substrate conversions are dependent on the rate of mass transfer within the biofilms. Thicker biofilms posit more limitations of mass transfer. This limitation presents hindrances in the movement of substrate and product into and out of the biofilm, respectively, subsequently this step becomes a rate determining step of the process (57) (52).

2.9.2. Condition for particle retention

Lower velocity of liquid i.e. u = Q/A is required than settling velocity of particles (ut) for particle retaining in the bioreactors; $\mu < \mu t$

2.9.3. Dissolved Oxygen (DO) and Oxygen Transfer Rate (OTR)

Organic stuff becomes rate limiting for bacterial growth if greater than 3 mg/L of DO is present in media. DO is recommended to be maintained at 2 mg/L or above for greater removal of organic matter (41)**.** Product of biofilm specified surface area (A) and flux (N) is termed as volumetric (OTR) i.e. OTR = NA

For biofilms having low surface area, liquid–solid (L-S) mass transfer becomes a rate limiting parameter (54). Oxygen transfer occurs from air bubbles through liquid into biofilm matrix. Consideration of mass transfer coefficients of liquid – solid and gas – liquid phases is an important design parameter of biofilm based reactors (54).

2.9.4. Sludge Retention Time (SRT)

Minimum SRT for the degration of organic matter is four to ten days whereas longer SRT is used in case of nitrifying biofilms. Advantages associated with longer SRT include improved removal of organics due to more oxygen transfer (52).

2.10. Biofilm Models

2-D or 3-D structure of biofilms depends on the characteristics of their support materials. Prior information related to microbial community structure, active biomass, substrate conversion kinetics and stoichiometry of biofilms is crucial to develop and propose biofilm models (58). 2 dimensional model of biofilm was formulated on the basis of degradation of substrate and diffusion kinetics (52). Multilayered model states biofilms composed of three layers of bacteria, each layer with different microbial communities, for an up-flow anaerobic sludge blanket (UASB) reactor put forwarded by Guiot et al. 1992 (59). Nucleation centers are occupied by methanogenic bacteria with least growth rate, central layer by hydrogen associated bacteria and the outermost layer by miscellaneous bacterial species with highest growth rates as witnessed by fluorescence in situ techniques (42), (52).

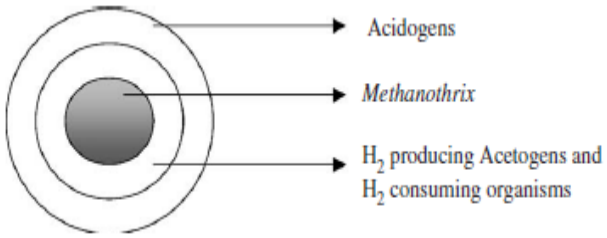

Figure 2.2. Three-layered structure of bacterial aggregates (59)

Microcolony syntrophic model explains that efficient break down of complex biodegradable compounds is dependent upon a synergistic coherent relationship amongst different microbial communities within microcolonies. Microcolonies deal with thermodynamic and kinetic requirements for transfer of intermediates and effective substrate transformation (60), (52). According to Non-layered Structure of Biofilm, anaerobic protein fed granules with non-stratified architecture of granules have been reported too under anaerobic conditions by *fluorescent in situ hybridization* integrated with confocal scanning microscope (58).

2.11. Biofilm Reactors

"Biofilm reactors" are considered a class of bioreactors in which microorganisms in their attached growth form (biofilms) are used as a catalyst to carry out the processes (transformation of compounds, biodegradation, fermentation processes). Biocatalysts either grow on substrata (support materials, walls of reactor, baffles) or attached to

each other forming biogranules (52). Biofilm reactors are generally divided into two types based on the form of biofilm carriers:

2.11.1. Fixed Bed and Mobile Bed Biofilm Reactors

On fixed beds, media in their static form such as rocks, plastic, rubber, sponges, metals, membranes or granular carriers are utilized to develop biofilm i.e. non-enclosure method. Influent flowing through the static media delivers nutrients to microorganisms. (31)**,** (3), (55), (42). Mobile beds are comprised of constantly moving media, which are maintained by mechanical stirring, water or air velocity. For instance, upflow anaerobic sludge blanket reactors (UASB) and biofilm airlift suspension (BAS) reactors (55), (42).

2.11.2. Continuous VS. Batch Reactors

Two major classes of bioreactors used in biofilm based WWT processes are continuous and batch mode processes. Systems operating in continuous mode e.g. Upflow Sludge Blanket (USB) (55)), Biofilm Airlift Suspension (BAS) and Biofilm Fluidized Bed Reactor (BFB) reactor (42) make available dynamic fluid conditions like natural systems but are sophisticated to operate. Batch on the other hand are simple and easier in operation (12).

Reduced cost, reaction times, flexibility of reusing the reactor for different products and yield are some of the major factors that dictate the selection for batch and fed batch processes over continuous. Although, control and regulation of batch processes is more challenging than continuous with respect to maintenance of operational conditions. Yet, characteristic flexibility of batch processes that allows to tailor the reaction variables according to requirement and meet the market demand alongwith progress in computer controlled processes and developments in hardware are in favor of batch processes (56). Further reason in favor of batch and semi-batch process belong to their more R&D attitude and practice. Reactions are first carried out in laboratory batch equipment and are then scaled up. Processes in fed batch mode also have the advantage of enhanced productivity but reactant overdose can cause a potential runaway situation in case of exothermic reactions (61).

2.12. Factors Affecting Biofilms

There are quite a large number of factors which have been found to influence the development of biofilms e.g. light and temperature (31)**,** velocity of medium (34), pH (41), microbial composition (36) Yet this study intended to investigate the impact of type and concentration of nutrients and characteristics of biofilm beds on its development because previous knowledge in this regard is insufficient to conclude their role in biofilm development.

2.12.1. Nutrients

Nutrients are necessary for the growth and establishment of microbial films. Proliferation of cells depends on an optimum level of nutrients. Limitation or excess of nutrients limits cellular growth (31)**.** Different nutrients such as calcium, iron, magnesium and oxygen affect biofilms to variable ranges. As Shukla and Rao (2013) found in their study using CLSM that calcium at its varying concentrations affected the architectural characteristics of Staphylococcus aureus (bap positive strain) biofilms (62).

2.12.1.1. Impact of Fe as a Nutrient and Electron Acceptor on Biofilm

Iron is a nutrient essential for the growth of bacteria like several other nutritional elements such as nitrogen, phosphorus and carbon. For instance, Fe is a component of heme enzymes e.g. cytochromes. Bacteria exhibit iron scavenging mechanisms under extreme deficiency of iron such as production of iron chelators termed as siderophores. Fe is also an electron acceptor that chains oxidation of organic matter with reduction of Fe(III) during the course of anaerobic respiration (63)**.** Fe reducing bacterial sp. utilize iron as their energy source so it has been anticipated that improved reduction of iron by bacteria can be a more achievable mechanism for enhanced biofilms (64)**,** (63)**.**

Recent studies have shown that iron also plays a significant role in biofilm establishment (65) and that lack of Fe compromises formation of biofilm (22). Very little is known about the Staphylococcus epidermidis iron scavenging processes,

however receptors to acquire Fe from the receptor bound transferrins, and production of siderophores for chelation of iron, have been reported in it (65)**.**

Studies suggested that P. aeruginosa strain K1120 yields low biofilm if supplemented with declining Fe concentrations (less than 8 µM) in medium suggesting importance of iron in biofilm production (22)**.** Patriquin and coworkers also reported that biofilms needed more Fe than planktonic cells (their growth declined at amounts at less than 1 µM) (22).

Oxidation of iron that produces ferric hydroxide and Fe(III), plays an important role in iron respiration by serving as electron acceptor species and ferric iron which is produced as result of iron oxidation was consumed by acidophilic bacteria (66). Reduction of iron generates lower redox conditions, making environment appropriate for the growth of SRB. Subsequently, numerous facultative iron respiring bacteria switch from aerobic to anoxic respiration. This iron respiration also results in rise of pH. Ku sel et al. observed pH increase (3.2-5.8) and Fe(II) production when they cultivated Acidiphilium cryptum JF5 on various carbon containing media (67), (64).

2.12.1.2. Stoichiometry of Fe^{3+} as an electron acceptor

Speciation of ferric hydroxide may explain fates of Fe(III) as a terminal electron acceptor, consuming glucose as a carbon source and ignoring bacterial growth. It predicts consumption of 2 moles of acidity per one mole of Fe(III) reduction;

$$24Fe(OH)_3 + C_6H_{12}O_6 + 48H^+ \longrightarrow 24Fe^{2+} + 6CO_2 + 66H_2O$$

However, in case of free ferric ion, one mole of iron reduction results in one mole of acidity as shown below;

$$24Fe^{3+} + C_6H_{12}O_6 + 6H_2O \longrightarrow 6CO_2 + 24Fe^{2+} + 24H^+$$

Langmuir has described production of substantial concentration of iron hydroxide in its solubilized form at pH values larger than 2.2 in addition to neutral $Fe(OH)_3$ and Fe^{3+} ions (68).

Massonet et al.carried out an experiment in 2006 in which Fe-linked genes (sirR and sitABC operon) expression was observed in planktonic Staphylococcus epidermidis and sessile bacteria in vivo as well as in vitro in a rat model. In vitro studies showed higher expression of sirR and independence of Fe concentration in case of attached growth bacteria while sitC expression was not inversely associated to sirR expression whereas in vivo studies, expression of sitABC and sirR was found higher during the primary phase when implanted and, after a brief reduction, was found stable for more than a period of two weeks (69). In vivo and in vitro study showed that the requirement of iron as a growth factor is different for both sessile and planktonic cell growth because biofilms show different phenotypic and genotypic variations (69).

Bollinger et al. in 2001 described culturing of biofilms using drip flow reactor system and included stainless steel slides as support materials to observe the override impact of iron on biofilm related gene(s). In their study, they investigated regulatory mechanisms of oxidative stress response and that how potentially coupled processes of quorum sensing and stressed conditions of nutrients were overlapped in Pseudomonas aeruginosa by using sodA that codes manganese cofactor super-oxide dismutase (Mn-SOD) and Mn-SOD as a reporter gene and reporter enzyme, respectively.

The reporter enzyme, Mn-SOD, was detected in wild type planktonic cells grown in Trypticase soy broth yet not in lasI or lasR mutants. On the contrary, the reporter enzyme was constitutively expressed in lasI and lasR mutant biofilms but its activity was completely inhibited with supplementation of 25µM ferric chloride in the growth medum. Limitation of iron increased the expression of lasI in the wild type P. aeruginosa about 30% -35% (23)**.** In another study, Musk and his colleagues reported that for proper growth and metabolism of P. aeruginosa iron was needed**.** They proved with help of in vitro experiments that both depletion of iron (<1µM) and repletion of iron (>100µM) results in retarded biofilm development. (65)**.**

Yun Cai reported in 2010 relation between iron and quorum sensing (QS) system in P. aeruginosa, he explained that those P. aeruginosa strains deficient in QS system are less virulent and form undifferentiated, smooth biofilms and are less stable contrary to well differentiated biofilms in wild type strains (Yun Cai, 2010).The author conducted

an experiment to show that QS regulates biofilm development in bacteria. For this purpose, he grew a wild type PAO1 (a pili mutant) and a lasR and rhlR mutant strains of *P. aeruginosa* under normal conditions and iron depletion conditions created by the addition of iron quencher compounds in media.

Wild type and pili mutant strains displayed similar capacity of biofilm formation under normal conditions of iron availability whereas lasR and rhlR exhibited less biofilm suggesting that pili are not required for biofilm formation instead QS is responsible for biofilm development. On the other hand, in iron depleted media, all strains showed decreased biofilm that was again recovered upon repletion of iron in media. This study revealed the fact that QS genes lasR and rhlR are the principal regulators of biofilm formation in P. aeruginosa consistent with the results of other studies (Yun Cai, 2010). Above findings were consistent with the results of Patriquin and coworkers 2008 in which they demonstrated that rhlI mutant strain , defective in twitching motility on low iron media, restores twitching on supplementation of C4 homoserine lactone (22). Therefore, It can be concluded from the above findings that under depletion of iron caused an increased expression of QS-related rhlR gene and concomitant C4-HSL production might resulting in up regulation of twitching and down regulation of biofilm development (Yun Cai, 2010)(22).

Iron levels affect auto induction process in *Pseudomonas syringae* (Pss). Biofilm forming ability of *Pseudomonas syringae* pv. syringae (*Pss*), a plant pathogen that utilizes QS signal molecules AHLs for autoinduction, was tested under varying iron concentrations in the growth media. Two AHL biosensor strains, containing PahlI:gfp reporter gene fusion quick to respond to AHLs, were used to gauge the process of autoinduction and AHL production in Pss on KB media alone or supplemented with 2µM of FeCl3.

In low/no iron media, all mutant strains, aefR-, ahlIR-, and gacA- did not produced AHLs with no visible green fluorescence on KB in the proximity of colonies. On iron supplemented media, wild type strains gave a significant green fluorescence and ahlIR- mutants still produced no AHL signal. The same experiment was replicated by using E.coli as a biosensor to the curiosity of the demonstrators that the response of AHL biosensor based on E.coli and Pss, were different to known quantities of AHLs

in the presence of iron in the experimental media (smaller fluorescence zone in the absence of iron).

One interpretation of this phenomena is that the response of the Pss ahlI:gfp biosensor is higher than E.coli LuxI:gfp fusion to AHL amounts and more prominent fluorescence zones are displayed by the Pss- biosensor that reflects enhanced response to AHLs in the presence of iron. Thsu, *Pss.* regulated genes responsible for EPS production and motility by QS and becomes pathogenic to bean only when cells achieve a fairly high concentration (Dulla, 2008).

2.12.2. Impact of Surface Material Properties on Biofilm Structure and Development

Features of substratum surfaces used as biofilm carriers play critical role in microbial deposition in various applications including membrane reactors for the treatment of municipal water (24). According to previous studies, factors needed to be considered prior to selection of carrier materials include their surface charge (39), hydrophobicity, biodegradability, resistance to corrosion, roughness (42), size, existence of protective coatings on surface and cost (31). Availability of water in the surfaces is also a key factor determining the growth of attached biomass. Some materials such as porous materials, capture more water content in the cracks than others favoring the microbial growth (31). These characteristics affect attachment sites leading to preferential deposition by some microbial populations over others and different depths of biofilms as well due to establishment of substrate gradient(s).(39), (70).

Rubber derived materials have been introduced as a novel and highly efficient media in wastewater and sewage treatment. In a study that involved the use of waste tire rubber chips (WTRCs) as a carrier of biofilm in a hybrid subsurface flow (SSF) constructed wetland, twofold nitrate and threefold phosphorus removal efficiency was achieved than that in the same system with gravel as a biofilm medium (71). Andersson et al. (2008), in their study on assessment of materials for enhanced biofilm, have proposed plastic and rubber as the most suitable carriers for biofilm development as they contain low densities and large surface area (13).

Polyethylene has also been tested as a carrier material for biofilming. It has been hypothesized that degradation of compounds can be improved if microorganisms are cultivated on polyethylene. Species of bacteria identified on PE include Bacillus spp., Micrococcus spp., Moraxella spp. while predominant fungi were Aspergillus ssp., Janibacter cremeus and Amauroclopius ornatus (72). Sen and Raut, 2015 reported 30% and 16% to 24% decrease in PE molecular weight whwn incubated with Bravibacillus borstelensis and Rhodococcus rhodochrous, respectively (72).

Properties of materials of the pipes used in water industry and wastewater treatment systems influence the densities of biofilms (73). Pipes made up of cast iron have been extensively used due to their cost effectiveness for decades. For this reason, it is very difficult to replace them with stainless steel or plastic pipes instantly. Very few data is available about the microbial community of iron biofilms due to the complications associated with their DNA extraction and PCR. Furthermore, due to their wide usage in water distribution systems and municipal buildings, more research about the iron corrosion and effect of iron on biofilm stability is required (70).

Rusty iron offers large number of attachment sites for bacteria that protects them from oxidation. The species of Arthrobacter were found as dominant biofilm formers in galvanized and cast iron distribution pipelines (74). Seth and edyven (2006) cited that the Pseudomonas genus might alter the oxygen reduction reactions. Sulfate reducing bacteria and two iron respiring bacteria (Leptospirillum ferrooxidans and Leptospirillum ferriphilum) were isolated from water distribution systems that explained microbially influenced corrosion (MIC) process (75). Activity of enzymes in biofilms was shown to play a significant part in ennoblement of iron (70).

Percival et al. compared total and viable cell count on 2D matt stainless steel with count on 2B smooth stainless steel and did not found significant difference of cell counts on both types of stainless steel (74). Bacterial species found in stainless steel biofilms included Methylobacterium spp., Pseudomonas spp., Arthrobacter, Corynebacterium and Acinetobacter spp. on 304 grade of steel whereas pathogens found on 2D and 3D grades of steel included Corynebacterium spp., Staphylococcus spp., Micrococcus spp. and spp. of Acinetobacter (74).

With the failure of copper based pipes due to pitting corrosion on their surfaces, there is growing interest in water industries for the utility of stainless steel as an alternate. Consequently, scientists are focusing on effects of biofilm on deterioration of stainless steel and vice versa (74). A number of studies have shown that plastic based materials support biofilms, however growth on plastic materials was found similar or lesser than on steel, iron, and cement (36).

Vander Kooij et al., 1995 detected that the materials in connection with water, boost biofilm formation by liberating biologically degradable compounds into liquid streams and affect the configuration of microbial populations within biofilm (76). Niquette and coworkers 2000 measured bacterial densities on PVC, PE and iron and steel and found iron as the material that supported biofilm the most. Steel coupons had densities half of those on iron (45 times greater) whereas lowest counts were found on PVC and PE. (73). Similar findings have been reported by Zacheus et al. 2000. Their group compared biofilms on PVC, PE and stainless steel and found no considerable difference between cell counts. Although volume of cells was slightly less on PE than on PVC (35).

According to Beech and Sunner MIC study 2004, their study demonstrated the presence of mixed surface associated species of novel sulfur oxidizing bacteria, bacteria that reduce sulfate and iron reducing/oxidizing bacteria capturing electrons from iron metal surface via both mechanisms i.e; with the involvement of hydrogen or directly. The authors reported significantly different biocorrosion rates on steel surfaces under identical environmental parameters ranging from 0 .05 mm per year to 3 mm per year in two similar reactors. (77). These studies indicate there is need for more biodegradation studies to find out economical materials that allow improved biofilm growth for WWT purposes.

2.12.3. Cation Induced Bioflocculation

Negatively charged surfaces of cells and EPS have rendered metallic ions, particularly those with multiple valency, of great significance in flocculation of sludges because they play role in building ionic bridges of EPS and their maintenance adding to the strength of granules (78). Interaction of substituent cations with exopolymers

mechanistically affects physical properties and stability of biogranules and films (45)**,** (79)**.**

However, each type of cation has its characteristic properties such as charge-valence, redox-potential, diameter and hydrolysis end products that result in their different chemical and biological behavior in the process of bioflocculation (45)**,** (78)**.** At extreme low pH values (less than 4), cations such as Calcium are removed from the granules resulting in reduced settling (40)**.**

Nguyen and coworkers in 2008 reported an increase in activated sludge floc stability, size and microbial activities with an increasing concentration of Ca(II) from 5 mM to 25 mM (that reached at steady state rate at higher concentration) (80)whereas removal of polyelectrolytes from the activated sludge flocs caused deterioration of their structures (81).In another study by Phong and his colleagues, Ca^{2+} was found more bound to the polymers in sludge than Mg^{2+} (40).

Park et al., 2006 described that flocculation and WWT performance of plants also relies on the type of the cation coming with the influent (Al^{3+}, Fe^{2+}, Fe^{3+}, Na^{+}). Therefore, role of cations in flocculation and mono/multispecies biofilm formation needs further investigation (78)**.** There was an increase in granulate biofilm in laboratory scale activated sludge reactor with the addition of Al^{3+} in 0.25-0.5 mg/L concentration, as reported by Nguyen and his coworkers (82). Lecompte (1966) patented a process for using magnesium carbonate as a coagulant with concentrations of Mg ranging between 5 to 44 mg/L (83), (A.R., 1966).

2.12.3.1. Cations and Extracellular Proteins

Cation-proteins interactions involve binding in negatively charged functional groups of EPS associated proteins (glycerate, carboxyl, pyruvate etc.) and metallic cations (77)**.** Both acidic and hydrophobic amino acids of extracellular proteins contribute to flocculation by electrostatic interaction with metal ions (41)**.**

2.12.3.2. Cations as Electron Shuttles

Metallic ions result in different redox potentials in their varied oxidized states in the EPS. For instance, redox potential of Fe lies in the range between 0.2-0.4 V in its

Fe(III) and Fe(II) states. For that reason, Metallic ions may work as electron "shuttles" opening up unique redox pathways like direct transfer of electron from the shuttlers (e.g. Fe) to microorganisms (77)**.** EPS binding with metals affects microbially influenced corrosion termed as (MIC) (41), (77)**.**

2.12.3.3. DCB Theory

The Divalent cation bridging concept commonly called DCB theory postulates that divalent cations (Mg^{2+} , Ca^{2+}) link with anionic functional moieties of biofilm matrix and encourage sludge settling (84), (78)**.** This theory posits deflocculation, a result of bivalent cationic displacement which are important constituents of flocs, by high amounts of monovalent ions including K^+ and Na^+ due to ion exchange mechanism (85), (41)**,** (79)**.**

2.12.3.4 Monovalent/Divalent Ratio of Cations - An indicator of Sludge Physiognomies

Above theory has been supported by subsequent studies, ascertained by external addition of monovalent ions and subsequent release of divalent ions along with decay of flocs. This phenomenon also provided basis for the possible explanation of electrophile-induced glutathione gated potassium (K^+) efflux stress process (GGKE) where K^+ released through channels present in plasma membranes of cells into sludge milieu lead to disruption of bridged flocs (85).Authors observed sludges with monovalent to divalent ratio greater than two had poor settling ability because both classes of cations compete for the common attachment sites in EPS. Thus, M/D ratio of cations can predict sludge properties and efficacy of WWT operations (85).

2.12.3.5. Role of Trivalent Cations in Bioflocculation

Since each cation possesses its unique biochemical characteristics and form different hydrolysis products so it becomes very important to consider their nature, quality and concentration before their selection. Multivalent cations such as $Fe^{3+,}$ Al^{3+}, due to their outstanding affinity with multi-dentate negatively charged ligands in EPS lead to extra stability of granules in sludge and are of great significance in this regard (78), (77). As Hol brook et al. (2004), reported that alum addition in an activated sludge

process resulted in more abridged structure of granules and removal of polysaccharides (Holbrook RD, 2004). Recent studies have proposed also the likely involvement of divalent/trivalent ratio of cations together in increase of biomass aggregation (82).

2.12.3.6. Fe (III) in Bioflocculation

Fe in its oxidized form makes quite different impact in cation based flocculation by virtue of its specific redox characteristics (63)**.** Previous studies showed that sludge deficient in iron resulted in more turbidity of solution which accounted for decline in sludge dewatering suggesting the pronounced role of iron in granule stability and is considered as an important cation than Ca^{2+} and Mg^{2+} (78)**.**

Two separate studies conducted previously have reported more turbidity of the liquid when Shewanella alga (86), a bacterium that reduces iron and sulfide, was applied in the liquid (78)**.** Muller (2001) have shown that Fe(III) had a superior flocculation capability as compared to Fe(II) (87)**.** Consistant with the above, according to Novak and his research group, 2003 reduction of Fe (III/II) leading to deflocculation was also coupled with loss of volatile solids during anaerobic assimilation of sludge (78)**.**

Park and coworkers (2006) indicated that different cationic groups are linked with sludge digestion under different conditions. They showed that how concentration of Fe was imperative in granulation process under anaerobic conditions while aerobic conditions sustained sludge digestion with the breakdown of materials linked with Mg^{2+} and Ca^{2+} (78)**.** Surface proteins in some bacteria have been postulated for their affinity of binding with Fe^{3+}. S. alga RAD 20, a strain lacking adhesins, exhibited no significant attachment tendency with Fe(III) due to excessive coating of EPS on its surface while its wild type strain having hydrophobic proteins on its surface bound with much Fe(III) (86). Role of Fe concentration also became evident from the findings of a study devoted on quantifying the expression level of surface carbohydrates in Corynebacterium diphtheriae. Provision of low or no Fe had modulated the expression level and types of carbohydrates on its surface (78)**.**

2.13. Microbial Community Composition of Activated Sludge Biofilm(s)

Characterization of microbial community profile within biofilm also predicts the functional performance of activated sludge process. Bacterial sp. generally detected from activated sludge biofilms are comprised of α, β and γ proteo bacteria including Actinobacteria and Bacteroidetes. Lim et al. (2012) reported prevalence of Enterobacter sp. and sp. of Dyella genera in cake collected from MBR by cultivation methods (88). Members of Beta-proteobacteria have been reported for their key role in biofilm development in MBR reactors for WWT (89). Typical bacteriological sp. isolated from activated sludge include sp. of the genera Klebsiella, Aeromonas, Citrobacter, Acinetobacter, Pseudomonas, Neisseria and Malikia (24).

Dolinsek et al., 2013 incubated sludge with radio labelled bicarbonates and determined the composition and spatial organization of eubacteria and nitrifiers with the application of FISH coupled with CLSM. This stuy showed the association of Microvirio heterotrophic organisms with Nitrospiras (β proteo bacteria) in the biogranules (90). A sequential FISH study combined with visualization by CLSM showed the presence and coaggregation patterns among AOB (Nitrosomonas spp.) and NOB (Nitrospira lineage) in biofilms established in trickling filter reactor and MBBR (91). Nogueira et al., 2005, quantified distribution of heterotrophic bacterial populations and nitrifiers in biofilm reactors in situ, by using 16S rRNA targeted probes and statistical analysis of CLSM images. Reactor run at very short HRT showed 100% communities comprised of nitrifiers while the second reactor that was operated at longer HRT, contained 73% populations of AOB and NOB, with the rest as heterotrophs (92). FISH with MAR (Microautoradiography) showed the distribution pattern of autotrophic nitrifiers and heterotrophs in biofilm reactors fed only with ammonium under carbon deficiency. AOB and NOB comprised 50 % of total bacteria while the remaining percentage included members of proteo bacteria (23 % γ and some species from α proteo bacteria, 9 % from Cytophaga- Bacteroides – Flavobacterium group, 2 % unknown bacteria) (93). Similarly CLSM alongwith 16S rRNA sequencing of microbial populations within biofilm reactors revealed the presence of strains phylogenetically associated with Nitrosospira, Nitrosomonas or Nitrosococcus pedigrees from β group of proteo bacteria (94). Manz and his team, 1993, pioneer of using FISH on environmental samples, used molecular probes for eukaryotes, β and γ subdivisions of bacteria combined with DAPI staining. Results

indicated that majority of biofilm bacteria (70 %) attached more with probes than free bacteria (bound only 40 %) due to more rRNA contents in them (95).

2.14. Biological Nitrification/Denitrification Process – A Catalyst for the Change of the Paradigm

Biological removal of nitrogen is accomplished by the process of nitrification coupled with denitrification. Nitrification produces nitrite as a result of ammonia oxidation by the activity of chemolithotriphic ammonia oxidizing (AOB) bactria such as, Nitrosomonas spp. and Nitrosococcus spp. Nitrite is oxidized into nitrate by the activity of nitrite oxidizing bacteria (NOB) e.g. Nitrobacter spp., Nitrococcus spp. and Nitrospina spp. (96), (41), (97), (97), (98), (3), (99).

In AOBs, ammonium monooxygenase enzyme (AMO enzyme) plays role in ammonia oxidation into NH_2OH i.e. hydroxyl-amine, further catalyzed by hydroxyl-amine oxidoreductase enzyme (HAO) into nitrite (NO_2^-) (100). Ancestral hierarchy and phylogeny of AOB developed based on the analysis of 16S rRNA sequencing and sequence divergence can be exploited by using amoA gene as a phylogenetic and functional marker (101).

The "amo" operon is comprised of three genes i.e. amoA, amoB and amoC (99). The subunit having the putative active site of the amo enzyme is encoded by amoA gene (101). amoC gene is located in an open reading frame present upstream of amoA gene (99). All AOB strains form β group of Proteobacteria have been found with identical,2 to 3 copies of amo regulon whereas AOB from γ division contain only single copies of the operon (99). Gene encoding catalytic site and subunit for amo enzyme i.e. amoA gene, has appeared as an appropriate marker for determining the AOB population composition in different environments (102).

ATCC 19718 strain of N. europaea, a model strain has conveyed fundamental understanding of AOB physiology and genetics. In this strain, ncg-ABC-nirK gene regulon coding for nitrite reductase has been found under the control of a protein NsrR, acting as repressor of nitrite reductase, governed by the concentration of NO_2^-. Not any other gene in this strain has been found part of this operon except norB. The norB gene was found significantly expressed with supplemented NO_2^- (97). 16S

rRNA sequencing of genes from environmental sample showed majority of sequences related with AOB species except one lineage from Nitrospira genus and two clusters from nitrosomonads (101). Detection of particular 16S rDNA fragments can be used to identity NOB (103). Cebron and Garnier (2005) found dominance and equal distribution of spp. of genera Nitrobacter and Nitrospira in the influent as well as effluent of a WWTP by q-PCR (103).

In biological denitrification process, nitrates are reduced into molecular nitrogen which serves as an alternate terminal electron acceptor under oxygen limiting conditions due to its low redox potential than oxygen. (3), (104), (97). This process is catalyzed by a series of four enzymes which include nitrous oxide- reductase, nitric oxide reductase, nitrate reductase and nitrite reductase. The product of genes nirK having copper and gene nirS (cytochrome cdI) can reduce nitrite into NO (104).

2.14.1. N Removal in the Activated Sludge and Waste Water Treatment Process

Ammonia is harmful to life on earth and causes loss of nutrients in agriculture. It damages nerves and is associated with several pathological conditions and even death (105), (104). Although nitrification is a nuisance for life yet it is favorable in WWT for removal of nutrients (104), (100), (41). WWTP all around the world are required to discharge effluents with total concentrations of nitrogen as low as 3 g per m^3 (57), (41). Therefore, it becomes imperative to apprehend the composition of AOB and NOB communities that play key role in nitrification/denitrification dynamics in WWT (105).

Zou and his coworkers have surveyed recently the community of AOB in a batch biofilm reactor based on CANON process and determined phylogenetic affiliations of main bacteria in biofilm. Phylogenetic relations determined on the basis of hao and 16S rDNA marker genes indicated that majority of AOB were related to species of Nitrosomonas genus while those of amoA based gene were related to uncultured novel bactaria although 88 to greater than 90% resemblance with spp. of Nitrosomonas was also obtained (100). Laboratory MBBR reactors when operated at 35℃ - 40℃ temperatures, removed more than 90 % ammonium nitrogen from both industrial and synthetic WW. Nitrosomonas spp., (N.nitrosa and N. oligotropha) were

found as the prevailing species in biofilms during the course of operation when analysed by quantitative PCR. Rise and decrease in nitrite quantities correlated well with the high and low populations of Nitrospira species (106). Gujer, 2010 concluded from his modeling derivations that higher nitrification potential of RBCs and Trickling Filters is achievable if heterotrophic biomass is replaced with mass of nitrifier organisms (107). The Efficacy of biofilms for removal of N was compared on RBCs operated in continuous and batch mode. The former showed 89% removal of N_2 from the solution per day while the later oxidized 147.8 and 76.5 mg NH_{4+} -N under aerobic and anaerobic conditions yet no oxidation of nitrite (38).

As total N removal is an important goal in industrial and urban WWT, therefore, further work is required in this aspect to improve the efficacy of bioreactors for nitrogen removal.

To carry out the research work and meet the objectives, following experimental set up was established and protocols were followed as below;

3.1. Sampling

Activated sludge was collected from waste water treatment plant located at I-9, Islamabad, Pakistan in containers at low temperature, immediately transported to laboratory within half an hour of collection and stored at 4˚C. The sludge was shifted to the already designed sterile aerobic batch biofilm reactors on the same day of sampling.

3.2. Aerobic Batch Biofilm Reactor (ABBR) Setup and Start-up for Biofilm Development

Four laboratory scale, 4 liter aerobic batch biofilm reactors (ABBR) were set up at the Environmental and Soil Laboratory, Department of Microbiology, Quaid-i-Azam University, Islamabad, Pakistan. Three reactors were used as test whereas one was run as control. Configuration of reactors is shown in fig. 1. The reactors consisted of plastic material, with a flat bottom (length: 9 inches, width: 6.2 inches, height: 5.5 inches) and a cover with holes on its both sides through which metallic wires were passed to hang the biofilm carriers in vertical position. Selected support materials consisted of iron, PVC, stainless steel, tire rubber (TR) and polyethylene (PE). Specificities of support materials are shown in table 1 and 2 below. Size of these carriers was selected such that their three fourth volumes were covered with sludge into the ABBR.

ABRs were filled with two liter of activated sludge. 200 ml of minimal salt medium (MSM) was added in each reactor along with 5 gram of starch and technical agar (Oxoid) each. Composition of MSM is described below. Reactors were covered with black paper and kept in dark to inhibit algal growth and left initially for 2 days at 30˚C temperature in incubator as an acclimation period for microorganisms to grow in activated sludge. Then $Fe(OH_{3)}$ was weighed in its specific concentrations (2.5 mg/l, 6.5 mg/l and 8.5 mg/l) and supplemented into three test reactors, with no addition into the control.

Iron was selected for biofilm development due to two reasons. Firstly because it serves as a source of nutrient and electron acceptor for bacterial growth and secondly because it has been hypothesized for its role in enhanced bio flocculation during activated sludge process (as described in chapter 2). Reactors were run for further 90 days at 30˚C. Stirring was performed periodically for aeration for 10 minutes by mechanical aerators. Sampling process and reactor set up was kept under sterile conditions to avoid contamination of microorganisms from environment.

Table 3.1. Volume of selected support materials determined by displacement method

MATERIAL	VOLUME(m^3)=V_{wf}-V_{wi}	V_{AVG}(m^3)=(V1+V2)/2
Stainless steel	V1=357-350=7 V2=405-400=5	7+5/2= 6
Polyvinyl chloride(PVC)	V1=265-255=10 V2=255-250=5	10+5/2=7.5
Tire rubber	V1=270-255=15 V2=270-260=10	15+10/2=12.5
Polyethylene (PE)	V1= 220-215=15 V2=300-285=5	15+5/2= 10
Iron	V1=23.2-22.0=1.2 V2= 23.7-23.0=1.7	V1=1.2+1.7/2=2.06

Table 3.2. Surface characterization (Length, width and thickness were measured by using a Vernier caliper)

MATERIALS	LENGTH (cm)	WIDTH (cm)	THICKNESS(cm)	SURFACE AREA(cm^3)	Average surface area (cm^3)
Stainless steel (SS)	L_1= 10.94 L_2= 11.00	W_1= 3.86 W_2= 3.58	D_1= 0.06 D_2= 0.04	$S.A_1$= 86.23 $S.A_2$= 79.93	83.08
Polyvinyl chloride (PVC)	L_1= 10.83 L_2= 10.86	W_1= 4.09 W_2= 4.06	D_1= 0.10 D_2= 0.17	$S.A_1$= 91.58 $S.A_2$= 93.25	92.42
Iron	L_1= 12.04 L_2= 12.12	W_1= 1.70 W_2= 1.78	D_1= 0.06 D_2= 0.08	$S.A_1$= 42.58 $S.A_2$= 45.37	43.98
Tire rubber	L_1= 11.0 L_2= 11.00	W_1= 3.97 W_2= 4.16	D_1= 0.13 D_2= 0.14	$S.A_1$= 91.23 $S.A_2$= 95.76	93.48
Polyethylene (Plastic)	L_1= 11.00 L_2= 11.22	W_1= 4.09 W_2= 3.86	D_1= 0.03 D_2= 0.03	$S.A_1$= 90.88 $S.A_2$= 87.52	89.20

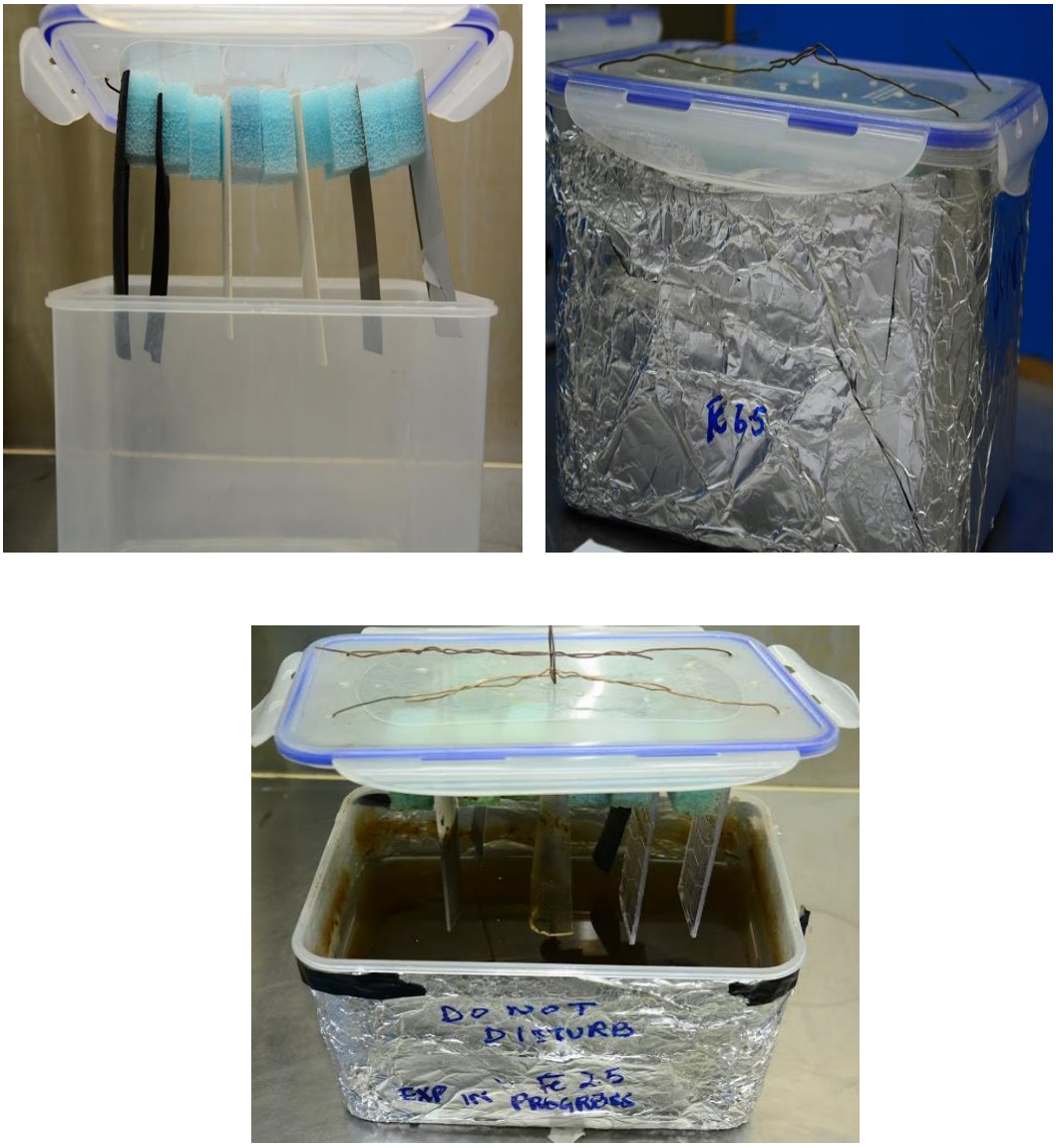

Figure 3.1. Aerobic batch biofilm reactors (ABBRs) before and during operation supplemented with different concentrations of Fe(III).

3.2.1. Minimal Salt Medium

Added sterile $MgSO_4$ (2 ml), 20 % glucose (20 ml), 1M $CaCl_2$ (100µl) into 700 ml distilled autoclaved water and 200 ml of prepared sterile M9 medium. Composition of M9 salts and micronutrients is mentioned in table 2 and 3, respectively.

Table 3.3. Ingredients of M9 salt

No.	Ingredients
1	64g $Na_2HPO_4.7H_2O$
2	15g KH_2PO_4
3	2.5g NaCl
4	5.0g NH_4Cl
5	Total volume 1000 ml (in dis. water

Table 3.4. Components of Micronutrients

No.	Components (mg/l)
1	$ZnSO_4$. $7H_2O$ (10.0)
2	$MnCl_2$. $4H_2O$ (3.0)
3	$CoCl_2$. $6H_2O$ (1.0)
4	$NiCl_2$. $6H_2O$ (2.0)
5	NO_2MoO_4. $2H_2O$ (3.0)
6	H_3BO_3 (3.0)
7	$CuCl_2$. $2H_2O$ (1.0)
8	$CuSO_4$ (1.0)

3.3. Digestion of Sludge under Varying Concentration of Fe(III) in Aerobic Batch Biofilm Reactors (ABBR)

Main physicochemical parameters that were monitored regularly include pH and dissolved oxygen as these parameters were not controlled. Performance of reactors was investigated by comparing their initial and final COD, BOD_5, total biomass of biofilms, nitrogen removal rates and by calculating their volatile acids and alkalinity levels.

3.3.1. COD and BOD_5 Determination

Chemical oxygen demand (COD) and Biochemical oxygen demand ($BOD_{5)}$ measure the content of oxygen that is used to reduce organic compounds in the solution. COD of sludge at the initial and final stage of experiment from both test and control reactors was determined by using commercial kit (Merck Co.) in triplicate having a measuring capacity range within 25 to 2500 mg/l. 3 ml filtered samples were added into COD vials and mixed well for ten minutes. COD vials were placed in sludge digester for digestion at 145 ˚C temperature for two hours. COD values were recorded using spectroquant Pharo 300 (Merck) after cooling of vials. A conversion factor of 0.69 was applied on COD values to achieve BOD values.

3.3.2. pH and Dissolved Oxygen Profile within Aerobic Batch Biofilm Reactors (ABBR)

The pH of test and control ABRs was monitored periodically by using digital Sartorius (pp 15) pH meter and dissolved oxygen (DO) with electrode of digital DO meter. Whole data was subjected to statistical analysis with Microsoft Excel (2013) program. Student's t-test was applied to compare mean values where a P value of <0.05 was regarded as default level of significance.

3.3.3. Floc Dynamics within Aerobic Batch Biofilm Reactors (ABBRs)

Relative speed of settling of flocs at the bottom of aerobic batch biofilm reactors was recorded on the basis of visual observations.

3.3.4. Alkalinity and Volatile Fatty Acids (VFA)

Alkalinity and volatile fatty acids (VFA) were determined by using the ASTMD 1067-02 method B. 20 ml of sludge samples at the start and end of experiment was taken into 100 ml flasks and pH was measured by using digital pH meter. pH was lowered down to 4.3 and then up to 3.5 by adding 0.1N H_2SO_4 from burette and volume of H_2SO_4 used was observed. Heated the samples till boiling and let the temperature be 60˚C to 70˚C. Used 0.1N NaOH to surge the pH of samples 7.0. Recorded the NaOH volume used. Formulas were used to calculate VFA and alkalinity values as shown below.

Alkalinity (mg/l) = Vol. (ml) of H_2SO_4 used × N of H_2SO_4 × 5000 / volume of sample (ml)

VFA = Vol. (ml) of NaOH used × N of NaOH × 5000 / volume of sample (ml)

3.3.5. Nitrification Rate of Activated Sludge During Digestion of Sludge in Aerobic Batch Biofilm Reactors (ABBR) under varying Concentrations of Fe(III)

3.3.5.1. Nitrite-Nitrogen (NO_2^--N) Measurement

To measure NO_2^--N nitrogen concentration within the reactors and in case of biofilms in enrichment medium, APHA standard method number 3500 (2005) was used.

Reagents Prepared

- **Stock Solution:** 0.5 g of sodium nitrite was dissolved in 1000 ml of distilled water i.e. 100ppm to prepare nitrite stock solution. Different volumes were taken from the stock solution (0.2ml, 0.4ml, 0.6ml, 0.8ml and 1.0ml) to make several dilutions (0.2, 0.4, 0.6, 0.8, 1.0 and 2.0 ppm) by dissolving in 100 ml distilled water.

- **Buffer' s Color Reagent:** 105ml of HCl (conc.) was dissolved with 0.5 g 1-naphthyl- ethylene diamine dihydrogenchloride and 5 g sulfanilamide into 250 ml of dis. water followed by addition of 136 grams of sodium acetate by continuous shaking. Final volume was made upto 500 ml using distilled water.

Procedure

50 ml filtered sample was taken into Nesseler's tube (100 ml), 2 ml color solution was added and shaken well for 15 minutes until the appearance of color. Absorbance was measured finally, at 540 nm. Nitrite concentrations were determined from the standard curve.

3.3.5.2. Nitrate-nitrogen (NO_3^- -N) Measurement

EPA standard method number 4500 (20005) was applied to measure NO_3^- -N concentrations in the samples.

Reagents Prepared

- KNO_3 standard solution was prepared by mixing KNO_3 (3.61 g) into 500 ml of distilled water i.e. 100ppm. 0.5 ml, 1.0 ml, 1.5 ml, 2.0 and 2.5 ml volume was taken from the standard stock solution and the corresponding ppm dilutions were prepared with 100 ml distilled water.
- Ammonia solution (concentrated)
- Phenol disulphonic acid solution

Procedure

- 50 ml sample was evaporated and dried on hot plate in a china dish. 0.5 ml solution of phenol disulphonic acid was added carefully to the sides of china dish and let it be cool at room temperature. The sample was diluted with 100 ml of distilled water after addition of concentrated ammonia solution (6-8 ml) and absorbance was determined at 410 nm wavelength.

3.3.6. Total Dissolved Solids and Total Suspended Solids

Total suspended solids (TSS) and total dissolved solids of activated sludge were determined by using the protocols of national environmental quality standards (NEQS).

3.3.6.1. Measurement of Total Dissolved Solids (TDS)

Washed filter paper. Dried evaporating dish and weighed. Stirred sample. Pipette out 50 ml while stirring. Filtered and washed three times.

Transfer filtrate to evaporating dish & dried. Let it cool, weighed and calculated in mg/ L. Formula used for calculation of TDS is as follows;

$$TDS\ (mg/l) = (WB-WA)1000 \div 100$$

Where, WB= weight of filter paper + residue, WA= weight of filter paper.

3.3.6.2. Measurement of Total Suspended Solids (TSS)

Washed filter paper & dried it. Weighed filter paper after letting it to cool. Assembled filtration apparatus. Wet filter paper with distilled water and stirred sample. Pipette out 50ml while stirring. Filtered and washed three times.Transfered filter to evaporating dish & dried. Let it cool, weighed and calculated in mg/ L. Repeated all steps 1 to 10 using 10 ml aliquot. Formula used to calculate TSS is as follows;

$$TSS\ (mg/l) = W2-W1\times1000\div100$$

Where, W1= weight of beaker+ residue, W2= weight of beaker

3.4. Microbiological Characterization of Activated Sludge and Biofilms

Chemicals, reagents and culture media utilized in this work were purchased from DIFCO laboratories (Michigan, USA), Sigma Chemicals Co., St. Louis, BDH Laboratory Division (Dorset, England) and Oxoid chemical company UK. All the media were prepared and incubated overnight before use at 37˚C temperature to test the sterility.

3.4.1. Estimation of Bacterial Biomass by Heterotrophic Plate Count (HPC) Method

The heterotrophic plate count (HPC) method is considered as an indirect method to estimate the biomass and activity of cultivable microorganisms within the samples. Conventional serial dilution technique was used to determine the HPC of biofilm samples developed on different materials and activated sludge as colony forming units (CFU/ml).

$1cm^2$ of materials with attached biofilms were washed with sterile distilled water three times to remove loosely attached planktonic bacteria. Biofilms were scraped off from the surfaces by using a scalpel blade along with brief sonication of materials to remove biofilms and dislodge the clumps in capped sterile tubes with sterile distilled water. After tenfold serial dilution up to $10^{-8,}$ 0.1ml of samples was spread plated on nutrient agar plates and incubated at 30 ˚C for 24 hours. CFU/ml was quantified using digital colony counter EKDS (DC-3). Activated sludge was briefly vertexed, serially diluted and spread on agar count plates and incubated at 37˚C temperature for specified time period. HPC was determined by using the following formula;

CFU/ml cm^2 = (No. of colonies × dilution factor) / dilution volume

3.4.2. Bacterial Density and Diversity of Activated Sludge Using Various Techniques

In order to investigate that what impact vertex and centrifugation exert on microbial diversity and density in activated sludge, sludge was processed, serially diluted and spread on agar plated in two sets. First set involved direct tenfold serial dilution of the sample and spreading on plates whereas the second set involved brief vertexing and centrifugation for two to three minutes at 10,000 rpm. The pellet was discarded and supernatant was serially diluted and spread on nutrient agar plates. CFU was calculated per ml in both cases and data was compared.

3.4.3. Identification of Bacterial Isolates

Colonies were selected from each spread plate based on their morphological characteristics and differences and restreaked further to acquire purified growth of

isolates. Isolated bacteria were then identified and characterized based on their morphology, differential staining (Gram's staining), growth on selective media such as, MacConkey agar, Pseudomonas citrimide agar (PCA), Eosine methylene agar (EMB) and biochemical tests. After carrying out all biochemical tests, bacteria were characterized according to Bergey's manual of bacteriology (Bergey et al. 1994).

3.4.3.1. Morphological Characterization

Morphological study of bacterial isolates involved considering the following physical characteristics as shown in table below;

Table 3.5. Morphological characteristics of bacterial isolates for their identification

No.	Feature	Description
1	Size of colony	Small, moderate or large, pinpoint
2	Form	Irregular/regular, circular, rhizoidal, filamentous
3	Pigmentation	Color of colony or medium (due to diffusion)
4	Elevation	Flat, convex, raised
5	Opacity	Opaque translucent, transparent

3.4.3.2. Light Microscopy

Smears of bacterial isolates were prepared on glass slides followed by heat fixation using a sterile technique. The smears were flooded with crystal violet and rinsed with tap water after 45 seconds to one minute. Gram's Iodine was applied then as a mordant and then 95% ethyl alcohol was applied as a decolorizer after washing with tap water. Finally, slides were flooded with safranine, washed with tap water, dried and observed under microscope.

3.4.3.3 . Biochemical Analysis

Biochemical analyses involved Simmon citrate utilization test, Methyl red and Voges – Proskauer test, SIM test, urease test, oxidase and catalase production test, nitrate test, triple sugar iron (detection of glucose and/or lactose fermentation)test.

i) Triple Sugar Iron (TSI) Test

TSI test is used to detect glucose or lactose fermentation by microorganisms. TSI agar slants were prepared with supplementation of 55 NaCl. The bacteria were inoculated by stab-streak inoculation method and incubated at 37˚C for 24 hours. Alkaline reaction was indicated by a pink red coloration in the slant and acidic fermentation by a yellow color. The slope reactions occurred due to lactose fermentation and that of butt were because of glucose fermentation.

ii) Catalase Test

To check the production of catalase enzyme in bacteria, wooden applicator was used to have a single colony on a glass slide. One drop of hydrogen peroxide (H_2O_2) was applied onto colony to record the production of bubbles which indicates positive result. The result was recorded as negative when there was no bubbles production.

iii) Urease Test

Urease broth was prepared (0.9/95g/ml) and autoclaved. After cooling down of media, 5 ml sterilized syringe filtered urea (0.2/5g/ml of dis. water) was supplemented. Test isolates were inoculated and incubated for 24 hours at 37˚C. Presence or absence of pink coloration in the media showed positive or negative test, respectively.

iv) Methyl Red-Voges Proskauer (MR-VP) Test

MR-VP broth (Oxoid) was dispensed into test tubes after its preparation and autoclaved. Bacteria were inoculated into the test tubes and incubated overnight at 37˚C. Methyl red indicator (methylred; 0.1g, 95% ethanol; 300 ml, distilled water; 2000 ml) for MR test and Barrit's reagent for VP test were prepared. Barrit's reagent was comprised of solution A and solution B. Solution A contained 5.0 g α-naphthol and 100 ml ethanol. Solution B was prepared by dissolving 40g potassium hydroxide in 100 ml distilled water. The media in the test tubes was divided in two parts into

new sterilized test tubes, after completion of incubation period. To one part prepared methyl red indicator (1 to 2 drops) was added to note the production of bright red color in the test tubes for positive result while in the second portion, 1 ml of solution B and 3 ml of solution A was added and test tubes were shaken for 2 to 3 minutes for reaction. Pink coloration in the medium was recorded as a positive reaction whereas no such coloration as a negative reaction.

v) Simmon's Citrate Test (Citrate utilization test)

Simmon's citrate test is used to know whether bacteria have the capability of fermenting citrate as a sole carbon source or not. The test isolates were inoculated aseptically into Simmon's citrate agar slants augmented with 5% NaCl and incubated at 37˚C for 24 hours to note the color change. Growth along with blue coloration was an indication of positive test while no growth and no turning of green color into blue in tube was that of a negative test.

vi) Nitrate Reduction Test

The reduction of nitrate in bacteria is mediated by nitrate reductase enzyme representing the ability of bacteria that they can utilize nitrate as an electron acceptor during respiration. The nitrate broth solution was heated, dispensed into test tubes carefully with inverted Durham tubes and autoclaved for 15 minutes. Observed for gas production into Durham tubes after 24 hours. Added small amounts of reagent A and reagent B (2-3 drops each) into each test tube and observed for the production of cherry red coloration. Reagent A was prepared by mixing 8.0 g of sulphuric acid into 1000 ml of 30% (5M) acetic acid. Reagent B contained 5.0 g α- naphtylamine dissolved into 1000 ml of 5M acetic acid. In case of no cherry red color appearance, small amount of zinc dust was introduced into test tubes. Zinc reduced any nitrate content if present in the tubes. Appearance of pink color after zinc addition indicated a negative test as the organism had failed to reduce nitrate into nitrogen.

3.5. Molecular Profiling of Microbial Community of Nitrifying and Denitrifying Bacteria in Biofilms Developed on Different support Materials under Varying Concentrations of Fe(III)

3.5.1. Whole Genomic DNA Extraction from Activated Sludge Sample

Protocol described by Singka et al. 2012 (1) was applied with some modifications to extract total DNA directly from activated sludge sample.

500µl of activated sludge sample was centrifuged at 14,000 rpm in a 1.5ml microcentrifuge tube for 10 minutes to achieve a sludge pellet. Same volume of glass beads (Sigma; ≈ 106 µm in diameter) equivalent to pellet and 500 µl CTAB extraction buffer (hexadecyl-trimethyl ammonium bromide) was added in the obtained pellet and incubated for one hour at 60℃.

500 µl of phenol:chloroform: isoamyl alcohol in the ratio of (25:24:1) was added into the tube after vertexing for one minute. The mixture was again vertexed for one min. and subsequently incubated on ice (1 minute) to avoid degradation of DNA during vertexing. This step was repeated three times.

Centrifuged the suspension again for 10 min. at 14,000 rpm and 4˚C temperature. Phenol chloroform isoamyl alcohol step was repeated. Aqueous layer was moved to a new 1.5 ml tube. Chloroform: isoamyl alcohol (500µl) in the ratio of 24:1 was added, centrifuged for 10 minutes at 14,000 rpm to remove the phenol. Finally, sodium acetate (pH; 5.5, 3M, Volume; 0.1) and isopropanol (volume, 0.6) was added to precipitate the DNA at -20˚C temperature for 30 minutes. 70% cold was used to wash the DNA pellet that was finally resuspended in TE buffer (30µl) with RNase (0.002%). Extracted DNA was electrophoresed on 1 % agarose gel. Sterile water was used as a negative control along with the sample.

3.5.2. DNA Extraction from Biofilm

DNA extraction from biofilm samples was performed with two methods. First method applied involved the use of SDS as described by Zhou et al. (1996) (2) while second method involved the use of commercial kit (Macrogen Soil DNA extraction kit)

3.5.2.1. DNA Extraction based on Sodium Dodecyl Sulfate (SDS)

5 gram of biofilm samples along with equivalent volume of sterile water as a negative control were homogenized with 13.5 ml extraction buffer (Tris HCl; 100 mM, pH 8.0, CTAB; 1%, sodium EDTA; 100 mM, pH 8.0, NaCl; 1.5M, sodium phosphate; 100 mM, pH 8.0) and proteinase K (50µl, 5 mg/ml) in 50 ml centrifugation tubes. Tubes containing suspensions were horizontally shaken for half an hour at 37 ˚C at 225 rpm, 1.5 ml of SDS (20%) was introduced and incubated for two hours in a water bath preset at 65 ˚C temperature with gentle inversions with intervals of 10 to 20 minutes. Centrifuged at 6000 g (10 min.), supernatant collected in 50 ml tubes. 4.5 ml of extraction buffer and 0.5 ml SDS were added, vertexed briefly, incubated for 10 minutes in water bath and centrifuged as previously to extract the pellets twice. Supernatants of three extraction cycles were mixed together and equivalent volume of chloroform isoamyl alcohol (24:1 v/v) was added. The suspension was subject to centrifugation to recover aqueous phase. 0.6 volume of isopropanol (1 hour at room temperature) was added to precipitate the DNA. Centrifuged to get pellet of DNA, washed with 70 % cold ethanol and finally resuspended in deionized water with final volume upto 500 µl. An aliquot of extracted DNA was run on 1 % gel.

3.5.2.2. Soil DNA extraction kit (Macrogen) was used to extract DNA from biofilm samples according manufacturers protocol and visualized on 1% agarose gel containing ethidium bromide. Sterile water was utilized as a negative control.

3.5.3. PCR amplification of genes related to nitrification and Sequencing

The extracted DNA from both sludge and selective biofilm samples were used as templates in PCR amplification. Primers used were selected after comprehensive literature review and using primer basis local alignment sequencing tool (BLAST) tool services (http://blast.ncbi.nlm.nih.gov/Blast.cgi). Primers and their sequences are

shown in table 5. Samples were shipped to carry out their phylogenetic sequencing commercially by Macrogen, Korea.

Table 3.6. Specificities of primers used

No.	Primer	Sequence	Specificity	TM (˚C)	Reference
1	Nso190f	GGAGCAAAGCAGGGGATCG	AOB, 16S rDNA	60.3	(3)
	Nso1255r	CGCCATTGTATTACGTGTGA	AOB, 16S rDNA	53.4	(3)
2	Nspra-675f	GCGGTGAAATGCGTAGAKATCG	Nitrospira 16S rDNA	57.5	(4)
	Nspra-746r	TCAGCGTCAGRWA[Y]GTTCCAGAG	Nitrospira 16S rDNA	56.7	(4)
3	Nitro-1198f	ACCCCTAGCAAATCGCTGACC	All Nitrobacter spp.	61.2	(4)
	Nitro-1423r	CTTCACCCCAGTCGCTGACC	All Nitrobacter spp.	62.6	(4)
4	amoA 1F	GGGGTTTCTACTGGTGGT	amoA	54.1	(5), (6)
	amoA 2R	CCCCTCKGSAAAGCCTTCTTC	amoA	59.2	(5), (6), (7)

3.6. Screening Bacterial Isolates for their Biofilm Forming Ability by Biofilm Development Assays

3.6.1. Test Tube Method

Tube test method describes the biofilm forming capability of bacterial isolates qualitatively as stated by Christensen and his colleagues previously (8), (9), (10), (11), (12). All bacterial isolates were inoculated into glass test tubes containing 10ml of tryptic soy broth with 2 % dextrose in it and incubated overnight at a temperature of 37°C. The test tubes were gently emptied then and washed three times with PBS (pH, 7.3) carefully. Tubes were air dried in an inverted form and stained with 0.1 % crystal violet while gently rotating the tubes. Again washed the tubes with distilled water and dried upside down in air at room temperature. An isolate was recorded as a strong biofilm former when there was a strong violet film at the bottom and wall of tube and scored as 2. Similarly, moderate film forming isolates were scored 1 and no/weak film formers as 0.

3.6.2. Congo Red Agar Method

As described by Freeman, 1989, CRA is also a qualitative test for the estimation of bacterial film formation (11), (13), (14), (10). CRA culturing medium contained tryptic soy agar (Oxoid) with 2% agar. Concentrated solution of CR indicator was prepared and autoclaved, separately at 121^{o}C temperature for 15 min. and then mixed with autoclaved TSA when it had reached 55^{o}C. All bacterial isolates were inoculated on CRA plates for 24 to 48 hours at 37^{o}C to detect EPS production. Black, crystal like, dry colonies indicated positive results whereas pink color specified weak sliming.

3.6.3. Tissue Culture Plate (TCP) Method

Micro titer 96 well plate test method generally known as TCP method designed by Christensen (12) is the gold standard test for detection of biofilm forming ability of bacteria (14). In this present work, the same method was applied with some modifications with respect to incubation period and fixation method.

All bacterial isolates were incubated in sterile test tubes containing 10 ml of trypticase soy broth with 2% dextrose as carbon source and incubated for 24 hours at 37^{o}C of temperature. Cultures from the tubes were then diluted in the ratio of 1:100 (volume 200 µl) with sterile fresh TSB into the wells of 96 well sterile polystyrene tissue culture plates (fig. 2) with flat bottoms. Sterile TSB was inoculated as negative control. After incubation of tissue culture plates for 24 hours at 37^{o}C, wells were decanted, washed with 200 µl of PBS (pH, 7.2) three times to exclude planktonic bacteria and plates were then placed in an oven set at 50^{o}C for the purpose of heat fixation.

The flms were then stained with 0.1 % crystal violet, washed with distilled water to remove the excessive crystal violet and air dried. OD of wells was quantified by using ELISA autoreader (Biorad) at 590 nm. Experiment was replicated three times. Standard deviation of average values of data was obtained. OD values were used as an index of biofilm formation of bacterial isolates.

Table 3.7. Biofilm measurement scale

No.	Average OD	Biofilm Formation
1	≤ ODc / ODc < ~ ≤ 2x ODc	Non/weak
2	2x ODc < ~ ≤ 4x ODc	Moderate
3	> 4x ODc	Strong

(Cut-off value of optical density (ODc): ODave. of negative control + 3(standard deviation of negative control) (8).

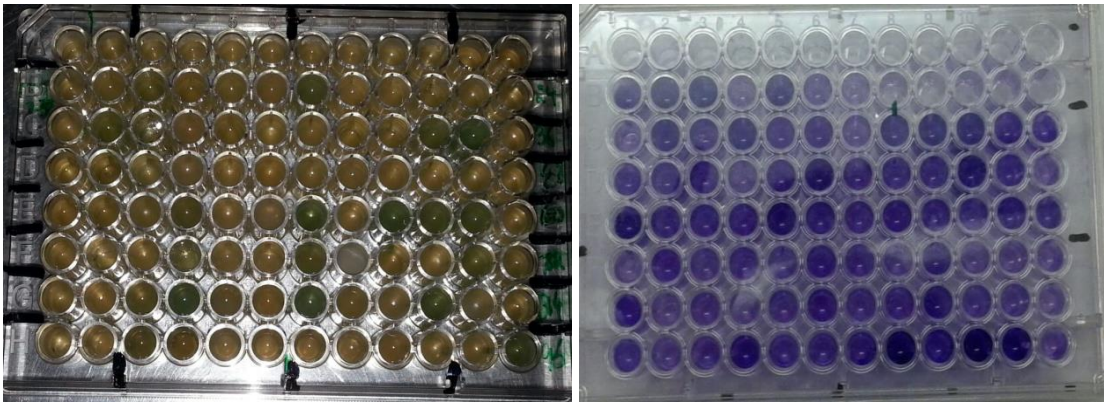

Figure 2: Biofilm formation ability of bacteria isolated from biofilms developed under various concentration of Fe(III) on different support materials by tissue culture plate (TCP) method (from left to right; micro titer plates before and after staining with crystal violet).

3.7. Activity Analyses of Biofilms

3.7.1. Nitrification Rate of Biofilms Developed on Different Support Materials under varying Concentrations of Fe(III)

Nitrogen removal rate in microorganisms depends not only on substrate conversion during respiration but also on interactions among microorganisms within biofilms. Therefore, for the quantification of nitrification activity of biofilms *in situ*, enriched cultivation technique was applied. Protocol of Ma et al., 2014 and Anderson et al., 2008 was followed with some modifications as follows (15), (16).

Composition of enrichment media used to investigate the activity of nitrifiers is shown in table 8. Biofilm was scraped off from 1cm^2 area of each biofilm carrier and collected in sterile capped glass tubes having 1 ml PBS, sonicated for 2 – 3 minutes to dissolve microorganism from the carriers thoroughly and finally, added into presterilized 250 ml flasks containing 100 ml of enrichment medium each under sterile conditions. $Fe(OH)_3$ was added in its pre-specified concentrations in flasks as in the case of reactors described above, to check the nitrification potential under the influence of iron. Flasks were covered with black paper to inhibit light and growth of algae. The cultivation conditions were: temperature, 30℃; shaker speed, 140 rpm and experiment period, 30 days. The concentrations of nitrite and nitrate were detected in each flask at day 0, 15th and 30th day of experiment using method 4500 (APHA, 2005).

Table 3.8. Composition of enrichment media

No.	Component
1	$NaHCO_3$, 13.8 g/L
2	NH_4Cl, 70.18 mg/L
3	K2HPO4, 0.236 g/L
4	0.25 ml of trace elements

3.8. Biofilm Structural Characterization

3.8.1. Characterization of Extracellular Polymeric Substance (EPS) of Biofilms Developed on Different Support Materials under varying Fe(III) Concentrations by Fourier Transform Infrared Spectroscopy (FTIR)

For the characterization of exopolymers, FTIR spectroscopy is a non-destructive technique for observing time resolved accumulation of EPS in biofilms and presence of functional groups in EPS alongwith conformational alterations if any grown on materials of interest (17). In present study, method described by Coates (2000) was used for sample treatment before performing FTIR (18).

In the first step, EPS was precipitated by taking threefold volume of cold absolute ethanol with one volume of biofilm from 1 cm^2 of each surface in sterile eppendorfs. Eppendorfs were incubated for about two hours on ice and subsequently, centrifuged at 10,000 rpm and 4℃ temperature for 20 minutes. Ethanol was evaporated by placing eppendorfs at 45℃ – 50℃ in drying oven and FTIR was performed using *TENSOR 27* FTIR apparatus.

3.9. Surface Characterization of Biofilms Developed on Various Support Materials under Varying Fe(III) Concentrations in Aerobic Batch Biofilm Reactors (ABBR) by Scanning Electron Microscope (SEM)

Scanning electron microscopy of surface attached biofilms was carried out by JEOL JSM-6490A SEM at College of Electrical and Mechanical Engineering (National University of Sciences and Technology, NUST), Islamabad, Pakistan. To visualize the surface morphology of biofilms on their carrier materials, samples were air dried in laboratory and fixed on copper stubs with sticky carbon tape, 10 × 10 mm in diameter prewashed with detergent and dried.

Then vacuum was generated by applying high voltage in ion sputtering device (JEOL, JFC-1500, auto coater) for gold deposition on biofilms. 25 mA current for approximately 50 s was used for plasma generation and subsequent gold coating on the samples. Gold coated samples were then placed under the column in chamber (vacuum generated, 15 minutes) and finally the surface morphology was observed and recorded at different magnification intensities starting from X1,00 to X20,000 and recorded.

3.10. Biofilm *In situ* Analyses and Microbial Community Visualization

3.10.1. Fluorescent *In situ* Hybridization (FISH)

3.10.1.1. Fixation of bacterial culture

Materials required

- 4% (w/v) Para formaldehyde solution
- 50%, 80%, and absolute (v/v) ethanol
- 2-ml screw-top microfuge tubes
- 2-ml microfuge tubes

- white polycarbonate membrane filters (diameter, 25 mm, pore size 0.2 µm)
- 1 x PBS (Phosphate buffer saline)

Methodology

i) Harvested 3-5 ml cells grown in tubes during logarithmic growth.

ii) Centrifuged 2ml of over-night grown culture in 2ml eppendorf (at 7000 rpm for 5 min).

iii) Pourd off supernatant, add 500ul of 1X PBS and resuspended cells.

iv) Centrifuged at 7000 rpm for 5 min, discarded the supernatant and resuspended pellet in 200ul 1X PBS and 600ul PFA (Para formaldehyde).

v) Refridgerated for 1-2 hour.

vi) Centrifuged cells (at 14000 rpm), pourd off supernatant, add 1 ml of a 1:1 mix of PBS / ethanol and resuspended cells; at this stage samples can be stored at -20°C for several months.

3.10.1.2. Preparation of cell smears and Biofilm fixation

Protocol described by Amann et al. (19), Manz et al. (20) and Wijeyekoon et al. (21) was applied for non-disruptive fixation and analysis of sessile bacteria with some modifications for optimization purposes. Biofilms were removed carefully from 1cm^2 area of each biofilm carrier and transferred in Teflon coated wells of ten well glass slides. A positive as well as a negative control were incorporated into two of the ten wells on each slide to avoid ambiguous interpretation of results. Samples were then washed with PBS, fixed with 4% paraformaldehyde (PFA) solution (2 h at -20℃) and again washed with PBS (pH, 7.2) to remove the PFA fixative. Slides were then serially dehydrated with 50%, 80% and absolute ethanol for three minutes each and stored at room temperature.

Figure 3.3. Teflon coated ten well glass slide

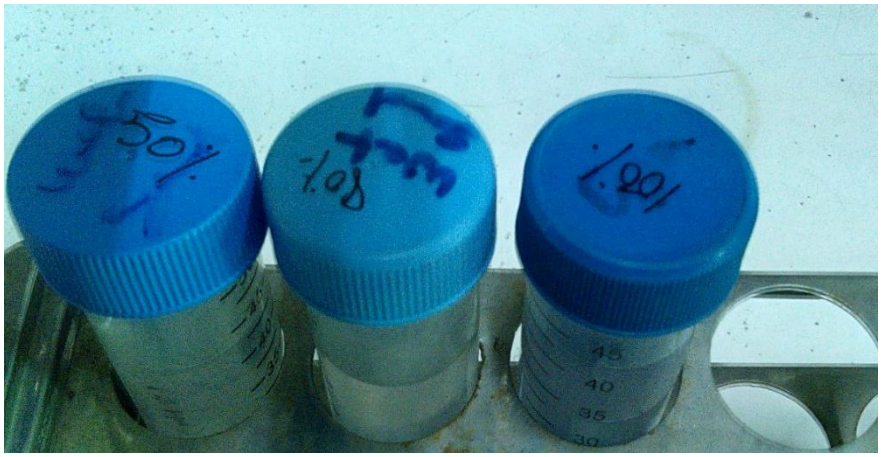

Figure 3.4. Series of different percentages of ethanol for dehydration of ten well glass slides (50%, 80%, 100%)

3.10.1.3. Hybridization with Fluorescently Labelled Oligonucleotide Probes

Protocol of Manz et al. (19) was followed with incorporation of some modifications. Hybridizations were performed in hybridization buffer solution at 46℃ of temperature for a duration ranging from one to two hours for different samples in hybridization chambers with probes 5' end labelled with fluorescent dye 5, 6- FAM (fluorescein isothiocyanate) (table 8). Probes EUB 338 I, II and III targeted all eubacteria, β-42 targeted all beta proteobacteria subdivision and γ-42 was applied to bind with all gamma proteobacteria (oligonucleotide probes purchased from α-oligos, Montrial, Canada).

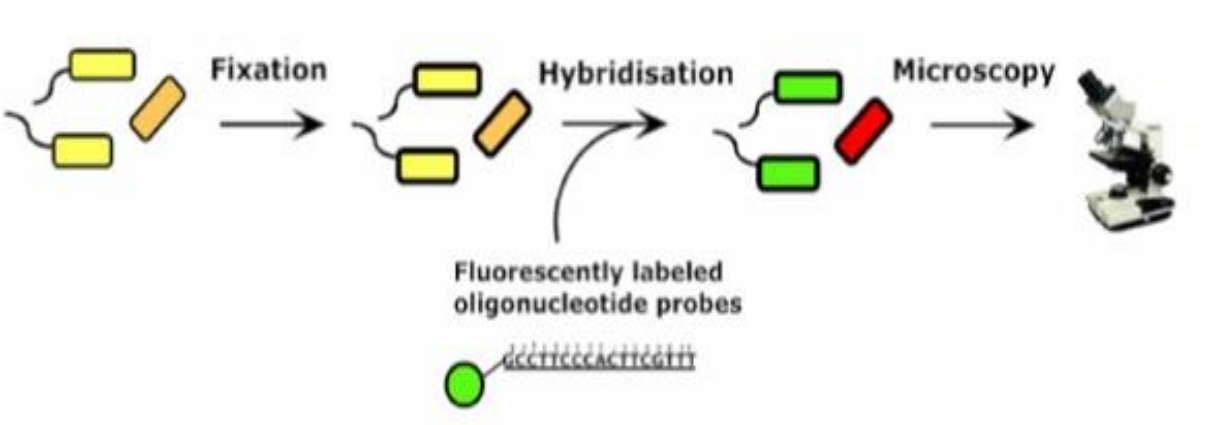

Figure 3.5. Steps involved in FISH technique.

Table 3.9. Specifications of the 5' end fluorescently labelled probes used in the study.

No.	Probe	Specificity	5'-end labelled (5,6-FAM) probe sequence
1	EUB338- I	16S rRNA, majority of bacteria	GCT GCC TCC CGT AGG AGT
2	EUB338-II	16S rRNA, bacteria not targetted by EUB338-I	GCA GCC ACC CGT AGG TGT
3	EUB338-III	16S rRNA, bacteria not covered by EUB338-I and EUB338-II	GCT GCC ACC CGT AGG TGT
4	Bet42	B-proteobacteria	GCCTTCCCACTTCGTTT
5	Gam42	γ – proteobacteria	GCCTTCCCACATCGTTT
6	Bet42 [a]	B-proteobacteria	GCCTTCCCACTTCGTTT
7	Gam42[b]	γ – proteobacteria	GCCTTCCCACATCGTTT

Bet42 [a], Gam42[b] ; competitor probes of Gam42 and Bet42 with no 5' end labelled fluorescent dye to increase the probe specificity(s).

3.10.2. Confocal Laser Scanning Microscopy (CLSM)

A Fluo *View*^{TM} (*Fv*1000) CSLM installed at National Institute of Biotechnology and Genetic Engineering , Faisalabad, Pakistan was used for optical sectioning of hybridized biofilm samples equipped with high resolution multi Argon lasers and 10 ×, 63 ×, 100 × lenses. Observations were made using 0.6 to 1.3 numerical apertures (NA) as a function of depth starting from surface. Optical sections were collected at a distance of 1.14 µm in Kalman mode. Images obtained were combined by using image analysis software digital image analysis in microbial ecology software. Total population of eubacteria, β and γ proteobacteria was quantified in sequential mode. Data obtained was edited for background noise by CLSM technique.

Parametric variation such as media supplementation with different concentrations of Fe(III) and type of support material influence microbial community composition of biofilms. Bacterial community structure of biofilms was characterized under varying conditions of ferric iron (2.5 mg/l, 6.5 mg/l and 8.5 mg/l) and different types of carrier materials viz. Stainless steel (SS), Polyethylene based plastic (PE), Polyvinyl chloride (PVC), Iron and Tire rubber (TR). Laboratory scale aerobic batch mode biofilm reactors (ABBR) were run by taking activated sludge as an inoculum. The reactors were operated for a period of 90 days and results were recorded at different phases of experiment in terms of sludge digestion and qualitative as well as quantitative bacterial diversity using conventional and advance molecular techniques. Detailed results of the study are as follows.

4.1. Digestion of Sludge under Varying Concentration of Fe(III) in Aerobic Batch Biofilm Reactors (ABBR)

4.1.1. COD, BOD_5 Removal

The aerobic batch biofilm reactors (ABBR) were compared in their performance to remove total COD and BOD_5 with respect to Fe concentration(s) at the completion of experiment. As the COD expresses total non-biodegradable and partly degradable organic contents whereas BOD_5 is the oxygen demand for biodegradable materials so, a correlation must be there between COD and BOD_5. In this present work, there was a linear association between calculated COD and BOD_5 values. A maximum of 38 percent reduction in COD and BOD_5 was observed in reactor fed with 8.5 mg/l of Fe(III). The highest COD and BOD_5 values were found in ABBR operated without exogenous supplementation of Fe (III) and at its lowest concentration i.e. 2.5 mg/l (COD; 509 and 383 mg/l, BOD_5; 351.21 and 264.27 mg/l, respectively). Minimum level of COD and BOD_5 was observed in reactors that were run at highest concentration of ferric iron (COD; 316 mg/l, BOD_5; 218.04 mg/l) with intermediate levels at middle 6.5 mg/l Fe value as shown in figure 1.

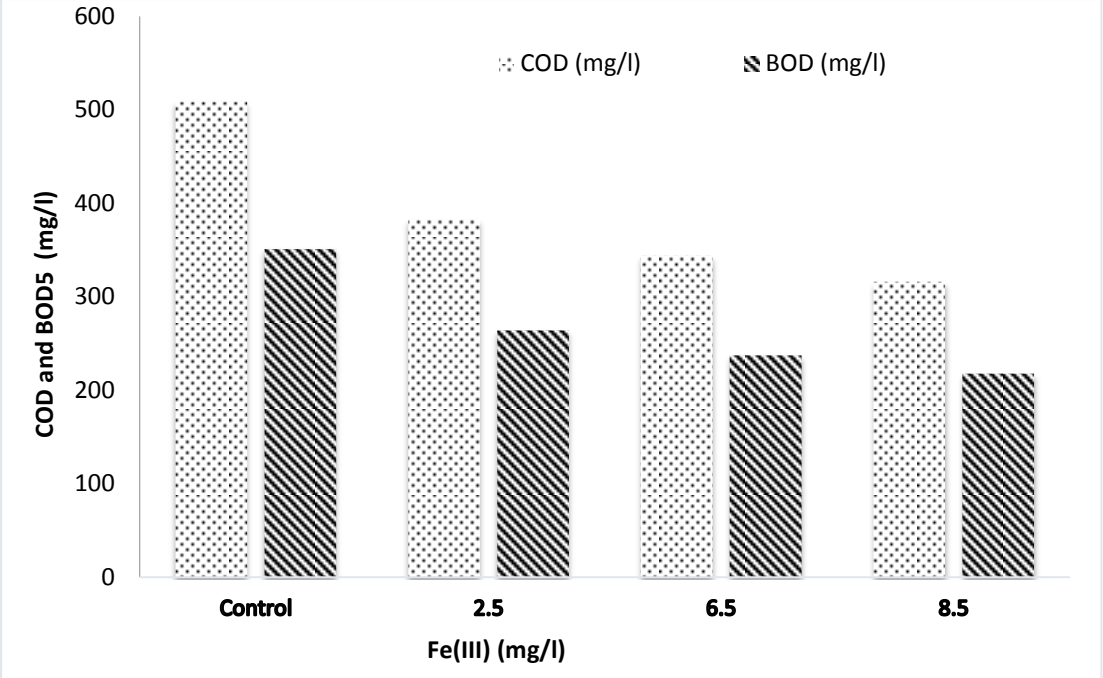

Figure 4.1. COD and BOD_5 removal efficiency of aerobic batch biofilm reactors (ABBR) after treatment **with different concentrations of Fe**(III).

4.1.2. Volatile Fatty Acids (VFA) and Alkalinity

In this study, alkalinity value declined from 9.5 in activated sludge to 7.5 in control reactor and 5 in ABBR1, ABBR2 and ABBR3 after the reactors were operated. Volatile fatty acids (VFA) increased from 27.5 mg/l in activated sludge to 275 mg/l, 250 mg/l, 475 mg/l and 147.5 mg/l in reactors containing 2.5 mg/l, 6.5 mg/l, 8.5 mg/l Fe_3^+ concentration and control, respectively.

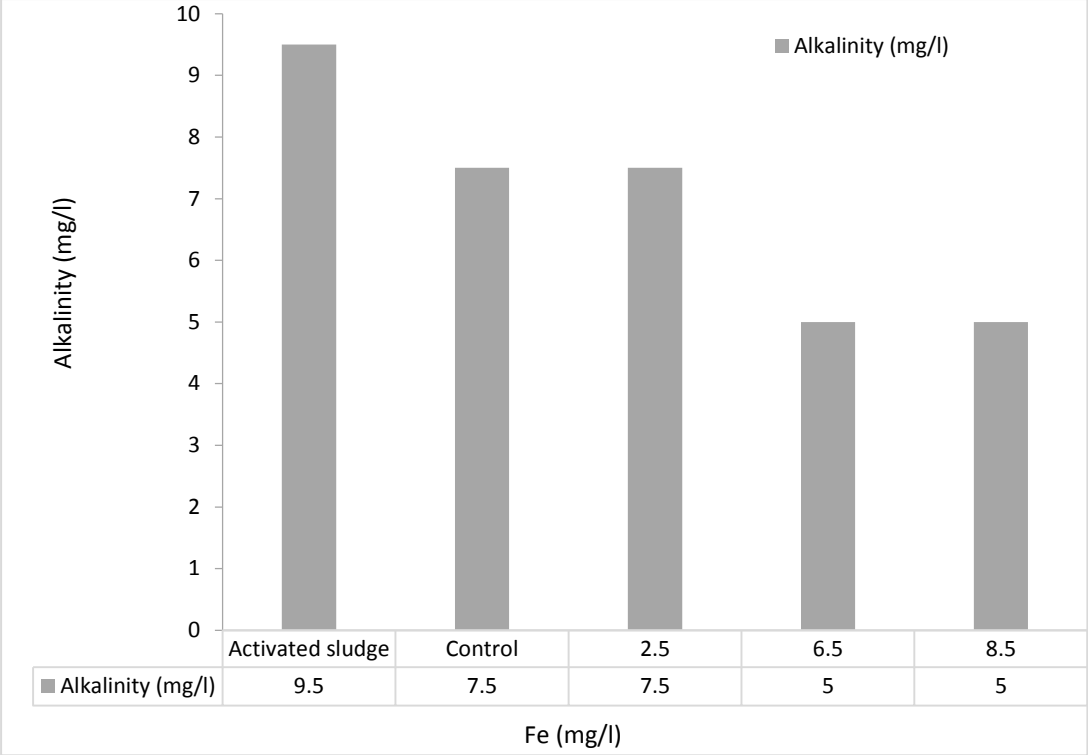

Figure 4.2. Alkalinity profile of untreated activated sludge before and after treatment with different concentrations of Fe(III) in aerobic batch biofilm reactors (ABBR).

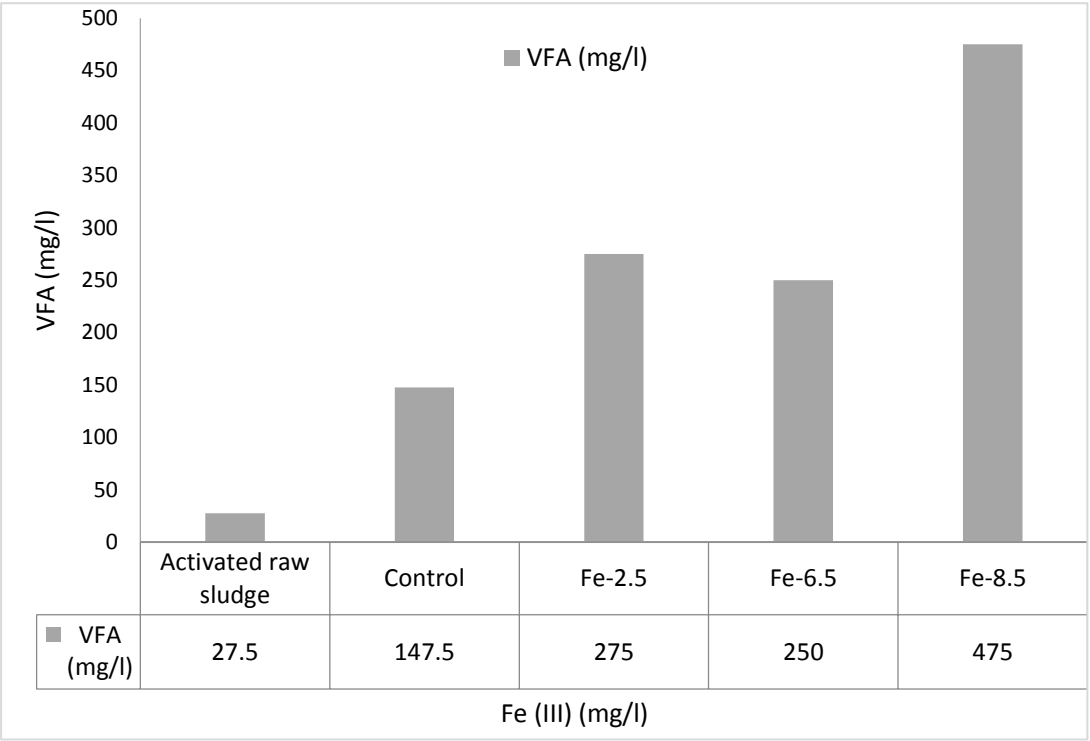

Figure 4.3. Volatile fatty acids profile of activated sludge before and after treatment with different concentrations of Fe(III) in aerobic batch biofilm reactors (ABBR).

4.5.3. Floc Dynamics within Aerobic Batch Biofilm Reactors (ABBRs)

Visual observation indicated that at higher Fe_3^+ concentration i.e. 8.5 mg/l, sludge settled more rapidly to the bottom of mechanically stirred batch reactors due to formation of larger flocs. At lower Fe_3^+ concentrations, the sludge settled slowly. Trivalent ferric iron cations become incorporated within microbe-EPS network that resulted in denser flocs.

4.5.4. Dissolved Oxygen Profile within Aerobic Batch Biofilm Reactors (ABBRs)

Penetration depth of different substrates in biofilms depends on the level of biofilm porosity, substrate concentration and rate of mass transfer at the liquid-biofilm interface in the biofilm. Random checks for dissolved oxygen (DO) measurement showed the presence of an average DO within a range of 0.25 mg/l to 2.12 mg/l. For oxygen, a poorly soluble substrate, the typical penetration depth is shallow usually in the range of 100–150 μm (4).

4.1.3. pH Profile within Aerobic Batch Biofilm Reactors (ABBR)

pH affects the performance of reactors and stability of flocs. Periodical monitoring of pH inside the reactors showed that average pH remained in the range of 7.1 to 7.32.

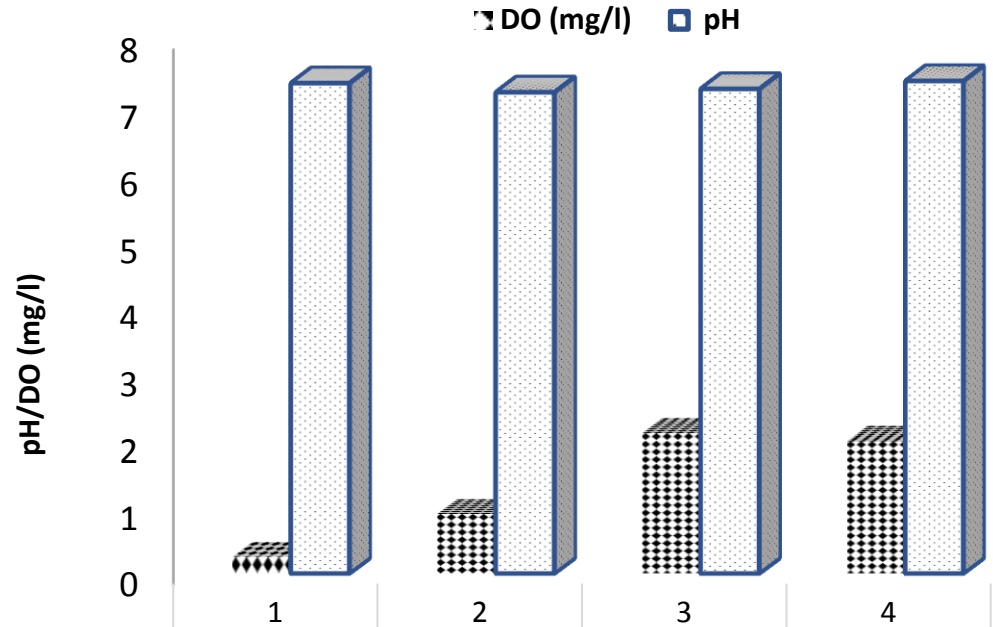

	1	2	3	4
DO (mg/l)	0.25	0.9	2.12	2
pH	7.3275	7.1925	7.2425	7.36

Figure 4.4. Dissolved Oxygen (DO) and pH Profile of Aerobic Batch Biofilm Reactors (ABBR)

4.1.4. Nitrification Rate of Activated Sludge During Digestion of Sludge in Aerobic Batch Biofilm Reactors (ABBR) under varying Concentrations of Fe(III)

Nitrite (NO_2^-) and nitrate (NO_3^-) concentrations (mg/l) were measured for a period of three weeks after the reactors were set up and operated for nutrient removal and biofilm establishment. Time lapse profiles for nitrate and nitrate concentrations are shown in figures below.

4.1.4.1 Nitrite-Nitrogen Oxidation

Ammonia oxidation results into nitrite accumulation that is further oxidized to nitrates if dissolved oxygen is present in the environment. Time lapse results indicated that under aerated conditions, in ABBR1 supplemented with 2.5 mg/l Fe(III) concentration, there was considerable decline in nitrite concentration from 75 mg/l to 17 mg/l after first week due to higher activity of NOB but after second week it showed nitrite build up (27 mg/l). The same trend was observed in ABBR2 and ABR3 run with 6.5 and 8.5 mg/l ferric iron concentrations contrary to control reactor where there was continuous decrease in nitrite quantities due to its oxidation.

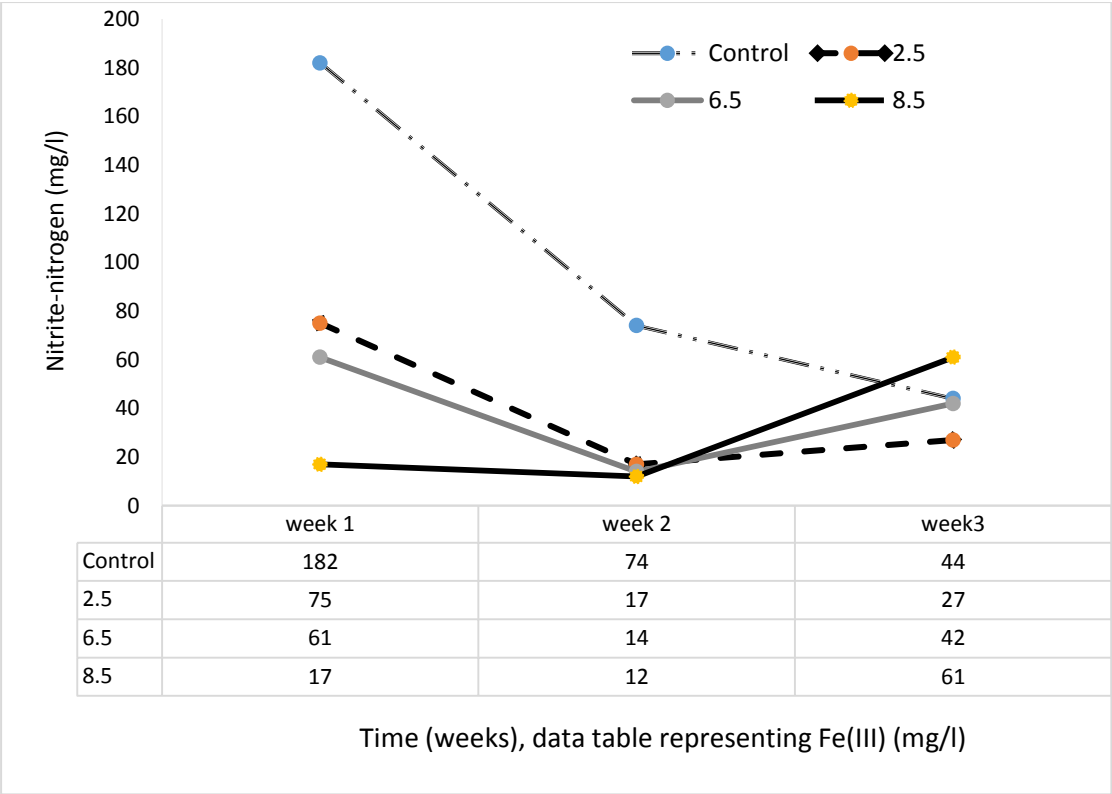

	week 1	week 2	week3
Control	182	74	44
2.5	75	17	27
6.5	61	14	42
8.5	17	12	61

Time (weeks), data table representing Fe(III) (mg/l)

Figure 4.5. NO_2^- - N production and transformation rate (mg/l) in aerobic batch biofilm reactors (ABBRs) during sludge digestion under treated and untreated conditions.

4.1.4.2. Nitrate-Nitrogen Oxidation

Accumulated dissolved oxygen (DO) facilitates conversion of nitrites into nitrates by the activity of nitrite oxidizing bacteria. Nitrate values in ABBR1, ABBR2 and ABBR3 with 2.5 mg/l, 6.5 mg/l and 8.5 mg/l Fe(III) concentrations showed a continuous reduction with time, indicating its oxidation into subsequent nitrogen compounds and finally into N gas. NO_3^--N values in ABBR1 ranged from 273.7 mg/l, the highest value at the start, to 132.6 mg/l at the end. In ABBR2, NO_3^--N concentrations varied from 220.5 mg/l at the initiation to the final 128.1 mg/l value. In control reactor on the other hand, an increase in NO_3^- concentration from 168.3 mg/l to 206.6 mg/l was recorded followed by a decrease to 163.7 mg/l again. Reduction in NO_3^- concentration after a prior increase may be attributed to the heterotrophic nitrification (discussed in detail in the following chapter).

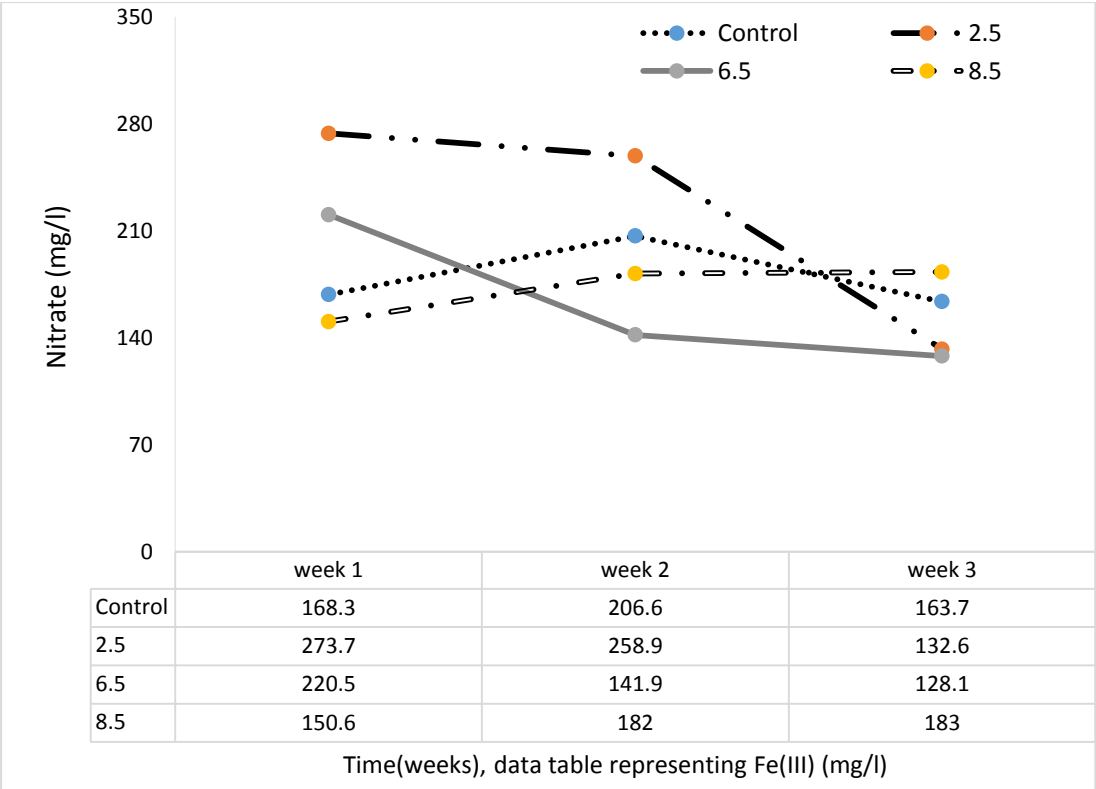

	week 1	week 2	week 3
Control	168.3	206.6	163.7
2.5	273.7	258.9	132.6
6.5	220.5	141.9	128.1
8.5	150.6	182	183

Time(weeks), data table representing Fe(III) (mg/l)

Figure 4.6. NO_3^-- N production and transformation rate (mg/l) in aerobic batch biofilm reactors (ABBR) during sludge digestion under treated and untreated conditions.

4.1.5. Total Dissolved Solids (TDS) and Total Suspended Solids (TSS)

Total dissolved solids (TDS) and total suspended solids (TSS) of activated sludge were determined by following the protocols of national environmental quality standards (NEQS). TDS value of activated sludge was found 0.05 mg/l whereas TSS was recorded as 0.015 mg/l.

4.2. Biofilm Development on Different Support Materials under the Influence of Varying Fe(III) Concentrations

Before quantifying colony forming units per ml per square meter (CFU/ml cm^2) from different biofilm(s), the aerobic batch biofilm reactors (ABBR) were successfully operated under specified conditions for the stated period in order to grow biofilm(s) on carrier materials. Figure 6, below, is presenting the microbial biomass fixed on biofilm support materials in the reactors under untreated and treated conditions. The increase in total bacterial density on certain carrier materials (explained below) at

higher Fe^{3+} concentrations must be subjected to the utilization of iron because all surfaces were incubated under same nutritional and environmental conditions.

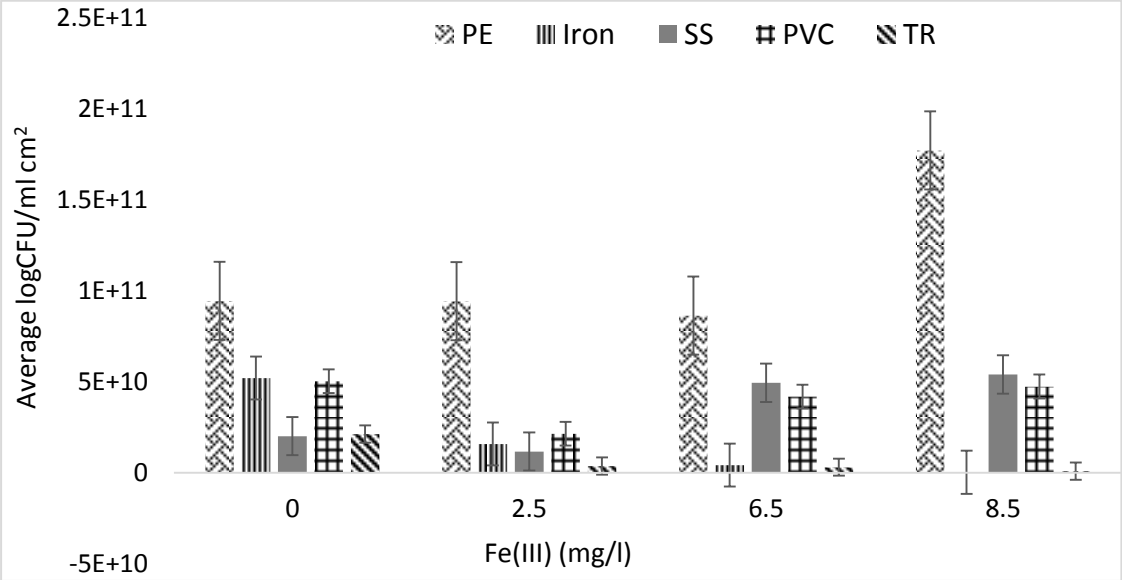

Figure 4.7. Effect of varying concentrations of $Fe(OH)_3$ relative to different support materials on biofilm development in aerobic batch biofilm reactors (ABBRs). (Support materials: PE; Polyethylene, SS; Stainless steel, PVC; Polyvinyl chloride, TR; Tire rubber)

A significant correlation was found between concentrations of Fe(III) and bacterial densities fixed on all types of attachment surfaces as the ANOVA results indicated a probability value less than 0.05 ($P<0.05$ showing that all model terms were significant, correlation analysis data shown in appendix). Results indicated that Polyethylene (PE) based plastic material supported the highest bacterial biomass in biofilms developed in all test and control reactors exhibiting maximum density at highest concentration of $Fe(OH)_3$ whereas Fe and PVC showed reduced bacterial density with increasing concentration of Fe^{3+}.

4.2.1. Effect of Different Concentrations of Fe (III) on Microbial Profile in Biofilms

In aerobic batch mode biofilm reactor (ABBRI) without any exogenous Fe(III) supplementation, decreasing order of CFU/ml cm^2 recorded was; PE(9.434E+10)>Iron (5.206E+10)>PVC(5.024E+10)>TR(2.122E+10)>SS(2.009E+10).

In ABBRII, fed with 2.5 mg/l Fe(III), as the figure shows, CFU/ml cm^2 varied in the range of $9.4X10^{10}$/ml cm^2, the highest on plastic based material PE, to $3.6X10^9$/ml cm^2 the lowest on tire rubber (TR). Stainless steel supported more bacteria at 2.5 mg/l Fe(III) concentration as compared to the stainless steel in control reactor. This difference in cell count could be assigned to the absence of iron in control. Bacterial densities on PVC were measured significantly less than on PE yet slightly higher than on iron.

At 6.5 mg/l Fe(III) supplementation in ABBRII, stainless steel showed consistency in accumulation of more bacterial cell counts than control and even from ABBR1 with lower Fe(III) quantities. Cell count in ABBRII on stainless steel exceeded $3.7X10^0$/ml/cm^2 and $2.927X10^0$ /ml cm^2 than in ABBRI and control reactors, respectively. There was no significant difference between the enumerated bacterial counts on iron and PVC materials at Fe-6.5 mg/l. PVC showed improved CFU/ml cm^2 than at Fe_3^+ 2.5 mg/l while iron demonstrated a reduced cellular count at 6.5 mg/l of ferric iron supplement. PE again dominated in accretion of bacterial biomass. Tire rubber showed lowest CFU/ml cm^2 ($3.02X10^9$).

In case of ABBRIV, with highest fraction of augmented ferric iron i.e. 8.5 mg/l, average CFU/ml cm^2 of substrates lied in the range of $1.171X10^{11}$/cm^2 highest count repeatedly from PE to $2.24X10^8$/cm^2, the least count from iron. Stainless steel accumulated highest densities ($5.393X10^{10}$/cm^2) at 8.5 mg/l iron concentration than at other concentrations, comparatively.

Figure 4.8 An aerobic batch biofilm reactor (ABBR) after biofilm development on different support materials with supplementation of Fe-2.5 mg/l.

4.2.2. Effect of Support Materials — Substratum VS. Fe (III) Concentration

Statistical analysis revealed a significant positive as well as a negative correlation among the types of biofilm support materials and densities of attached bacteria.

PE based plastic material showed significantly improved bacterial densities at highest concentration of ferric iron with $1.7713X10^{11}$ CFU/ml cm^2. There was no significant difference between CFU/ml cm^2 at 0 mg/l and 2.5 mg/l Fe whereas biofilm grown at Fe_3^+-6.5 mg/l gave intermediate level of cell counts.

Iron showed atypical behavior towards Fe(III) additions. Contrary to some previous studies, it showed an inverse relationship between ferric iron concentrations and plate counts. Strange to our observations, ferric iron supplements lead to reduction in bacterial densities from lower to higher Fe concentrations as shown in figure 6. The least average count $2.24X10^8$ CFU/ml cm^2 was figured at highest 8.5 mg/l Fe concentration while control showed much higher count.

Stainless steel exhibited a significant linear relationship between iron quantities and biofilm density with an increasing tendency of CFU/ml cm^2 with increasing amounts of Fe(III). Cell counts at Fe-2.5 and control approximate each other i.e. $1.163X10^{10}$ and $2.009X10^{10}$ cells/cm^2. The highest count $5.393X10^{10}$ per cm^2 was found in ABR3 with Fe-8.5 mg/l, with $4.936X10^{10}$/cm^2 cells at Fe-6.5 mg/l.

Tire rubber also indicated a positive linear correlation between biomass densities and addition of various iron concentrations. Reactors with no (control) or very low (Fe-

2.5mg/l) amounts of Fe supported $2.959X10^9$ and $3.65X10^9$ CFU/cm^2 whereas Fe-8.5 mg/l fixed the highest magnitude of CFU/ml i.e. $4.73X10^{10}$ per cm^2 indicating that TR is also a candidate material that enhanced biofilm density with increasing iron concentration(s).

Polyvinyl chloride **(**PVC) did not show any promising indication of favoring biofilm development in relation to iron concentrations. CFU was found highest from biofilm on PVC in the reactor with lowest Fe(III) concentration revealing an inverse relation between both factors. An average CFU/ml $cm^2$was reduced to 3.01X109 and to 8.835X108 with increased iron concentrations of Fe-6.5mg/l and Fe-8.5 mg/l, respectively.

The results indicated that PE outnumbered other materials as a most suitable biofilm carrier with highest magnitude of $1.7713X10^{11}$ CFU/ml cm^2. Next to PE, stainless steel improved biofilm density as a function of Fe(III) concentration with maximum plate count of $5.39X10^{10}$. TR was also found a good candidate for biofilm stability that worked in relation to iron quantities (average CFU/ml/cm^2; $4.73X\ 10^{10}$). Neither PVC nor iron on the other hand, divulged themselves as a means of increasing microbial biomass in biofilms. Very low fixed biomass was supported by PVC and iron in relation to Fe concentrations as compared to PE, stainless steel and TR.

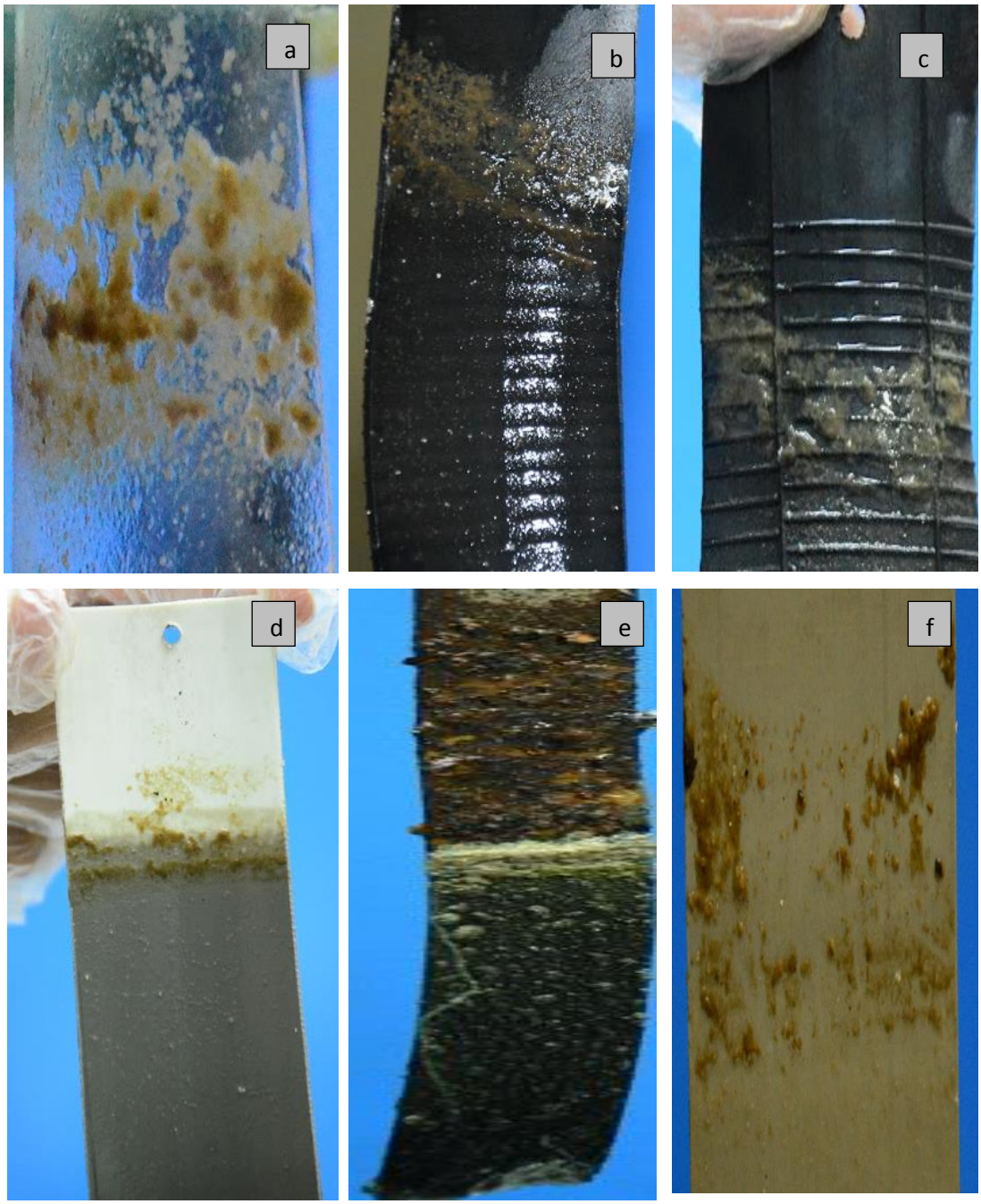

Figure 4.9. Representative biofilms developed on different support materials in aerobic batch biofilm reactors at different Fe(III) concentrations at the end of experiment. (a; Polyethylene (PE), b-c; Tire rubber (TR), d; Polyvinyl chloride PVC based pipe material, e; Iron, f; Stainless steel (SS).

4.3. Microbiological Profile of Activated Sludge and Biofilms Developed on Different Support Materials under Varying Concentrations of Fe(III) in Aerobic Batch Biofilm Reactors (ABBR)

4.3.1. Bacteria Isolated from Activated Sludge

Bacteria were isolated from activated sludge and subjected to light microscopy for their Gram's reaction. 31.58% of total (19) bacteria were found as Gram positive, 63.16% as Gram negative whereas only 5.26% were observed as Gram variable in reaction.

4.3.2. Identification of Bacteria Isolated from Biofilms Based on Morphological, Microscopic and Biochemical Characteristics

Utility of ferric iron in relation to different properties of support materials led to significant differences in microbial populations of biofilms in treated and untreated reactors. 30 bacterial isolates out of total isolated from different biofilms developed on different carrier materials under a range of $Fe(OH)_3$ concentrations were selected based on their characteristic properties i.e. morphology, color, mucoid, slime production and string forming capabilities. 40.9% of total bacteria were observed and recorded as Gram positive. 59.0% gave Gram negative reaction with 0% of Gram variable ones. Prominent bacterial species identified on the basis of their morphological and Gram's staining properties, biochemical characterization and growth on different media included *Pseudomonas spp., Vibrio spp., Shewanella spp., Providencia spp., Serratia spp., Klebsiella spp., Bacillus spp.* and *Staphylococcus spp.* as shown in table 1.

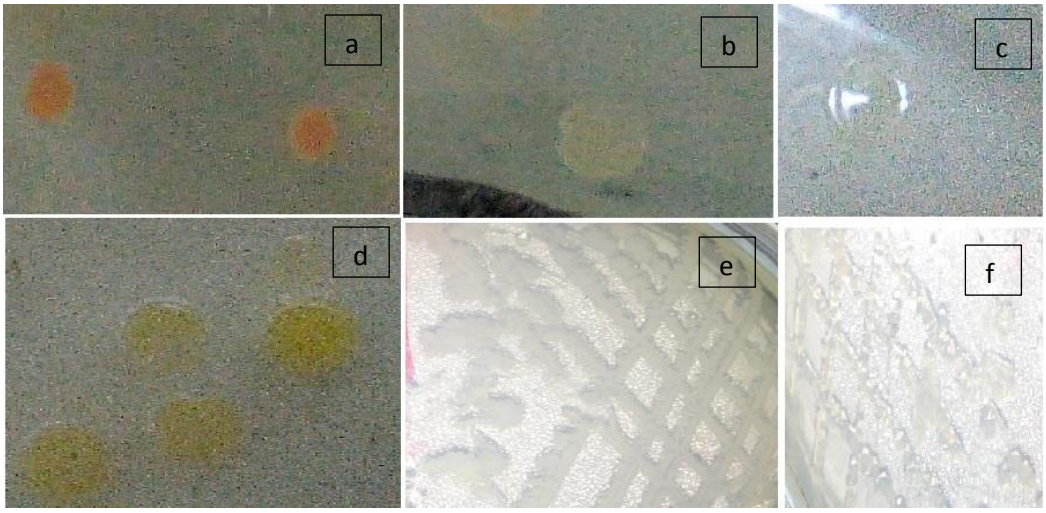

Figure 4.10. Characteristic morphologies of bacterial strains isolated from activated sludge and different biofilms under light microscope at X100. (a; orange colored medium sized colonies, b; large off white, c; transparent, round and large sized colony, , d; large egg yolk like colonies, e; white fluffy mesh-like growth, f; shiny, string forming growth).

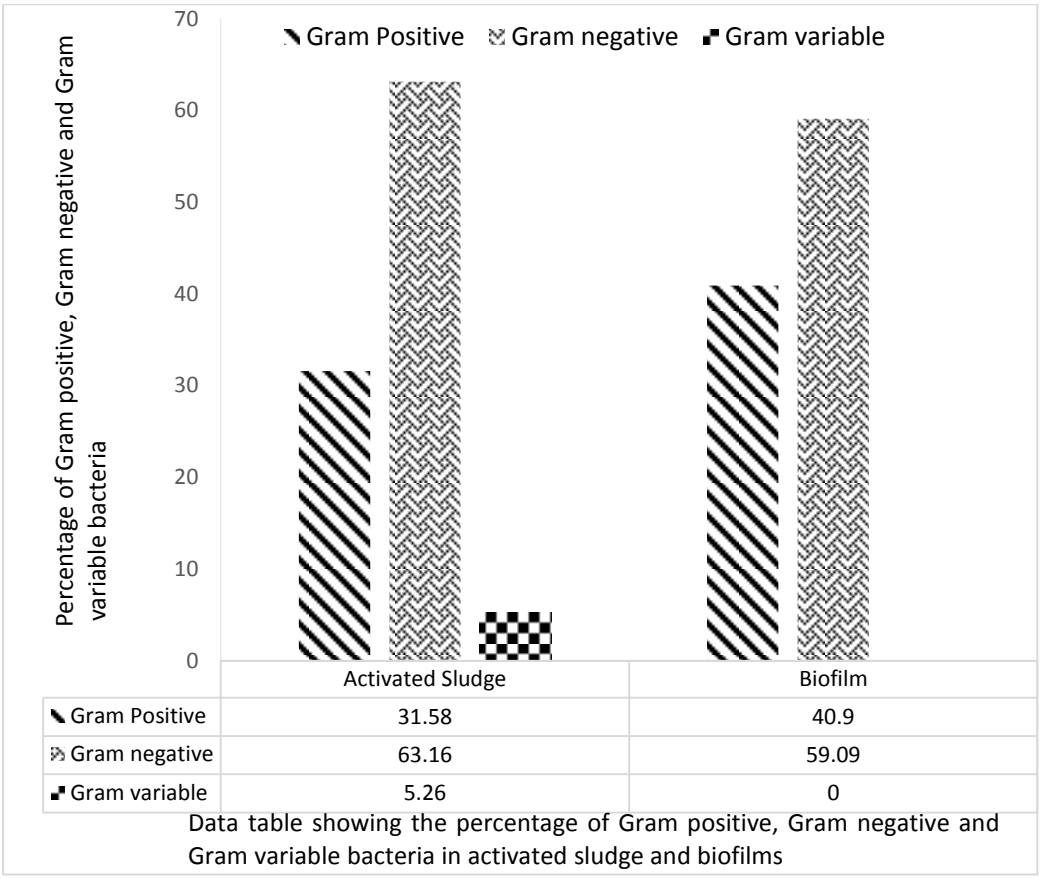

Figure 4.11. Figure 5: Percentage of Gram positive, Gram negative and Gram variable cells isolated from activated sludge and different biofilms developed on diverse support materials under varying Fe(III) concentrations.

Table 3 Morphological and biochemical characterization of bacterial isolates isolated from biofilms developed on different support materials in aerobic batch biofilm reactors (ABBR)

Fe(III)-mg/l	Material	Dilution (10^{-n})	Isolate No.	Morphology	TSI (A; acidic, K; basic)			SC	MR	VP	SIM		U	C	O	N	Mac. agar	Sp.
					S/B	G	H_2S				M	K						
2.5	SS	1	11	Greenish, circular, large, thin margins, thick bulging in middle.	K/A	-	-	-	-	+	-	-	-	+	+	+	NLF	*Pseudomonas mesophilica*
		3	12	Yellow, wavy margins, large, dry, rhizoid, mat.														
		3	13	Greenish, circular, large, thin margins, thick bulging in middle.														
		2	14	Small, courage, round (like egg yolk).														
		2	15	Round.	A/A	-	-	-	-	+	+	-	-	+	-	+	NLF	*Pseudomonas pseudoalcaligenes*
		4	16	Small, white, round, raised.														
		6	17	Pinkish, circular, large, flat.														
		6	18	Pure white, round, bulging, medium.														
		7	19	Yellow, raised, wavy pores inside the mesh.														
		7	20	Light pink, circular, large, flat	A/K	-	-	-	-	-	+	-	-	+	+	+	no	*Serratia ficaria*
2.5	TR	7	89	spreading rhizoidal growth, off white, flat	K/A	-	-	-	-	+	+	-	-	+	+	+	neg.	*Vibrio costicola*
		7	90	green, round, thick, pseudomonas like smell														
		8	91	round, greenish, medium sized														
2.5	PVC	2	52	waxy margins, off white, large, granular														
		3	53	Pink, round, shiny, medium, bright, moist.														
		3	54	Light pink, small, and moist.	A/A	-	-		-	+	+	-	-		+	+	LF	Indeterminate
		3	55	pale yellow, dry, medium sized														
		3	56	large, off white, flat, wavy wings														
		6	57	Off white small, round, raised.														
2.5	Iron	2	27	Round, large, off white, flat, swarming.														
		3	28	Wavy, leafy margins, white, shiny.														
		3	29	Yellow, small, round.	K/K	-	+	+	-	-	+	-	-	+	+	+	NLF	*Alteromonas putrefaciens*
		4	30	greenish, irregular margins, large														

		5	50	Round, off white, greenish, double ringed (thin margins, thick inside).	A/A	-	-	-	-	-	-	-	-		+	+	NLF	*Bacillus subtilis*
		8	57	Yellow, flat, medium sized.															
2.5	PE	8	94	wrinkled, irregular margins, opaque, shiny, medium, moist, flat															
		8	95	String forming, opaque margins.															
		5	96	Round margins, thick, mucoid, medium sized, opaque															
6.5	PVC	3	21	round, flat, clear, medium to large															
		6	22	white, round, raised															
		7	23	large, flat ,raised ,thin, thick inside															
		7	24	wavy, leafy margins, greenish, dry															
		8	25	tiny, clear, round, raised															
		7	26	Small, round, clear.	K/K	-	-	+	-	-	+	-	-	+	+	+	NLF	
6.5	SS	6	87	large, round, off white, moist															
		5	88	small to medium sized, round,(off white shiny)appearance															
6.5	TR	8	104	Off white, shiny, thick, round.															
		8	105	Round, circular, clear.															
		5	106	Round. moist, mucoid, in middle with white colored hollows from growth out ward	A/K	-	-	-	-	-	+	-	-	+	+	+	LF	*Vibrio mediterranei*
		7	107	Yellow, small, round.															
6.5	PE	7	92	round, pseudo smell, pigmentation															
		6	93	Round with swarming, greenish, pseudo smell.	K/A	-	-	+	-	-	+	-	-	+	+	+	NLF	*Vibrio fluvialis*
6.5	Iron	7	84	Round, small to medium, off white, raised from center.															
		7	85	star shaped, off white, large, thick in middle	A/K	-	-	-	-	-	+	-	+	+	+	+	NLF	*Comamonas acidovorans*
		7	86	Rhizoidal, large, greenish.															
8.5	PVC	7	81	Off white, thick, flat, wavy margins.															
		6	82	round(little greenish),double ringed, margins thin, thick in center	A/K	-	-	-	-	-	+	-	+	+	-	+	LF	*Providencia heimbachae*
		6	83	Flat, greenish, large spreading.															
8.5	SS	5	108	clear transparent, mucoid, medium to large, irregular shaped	A/A	-	-	-	-	-	-	-	-	+	+	+	pos. NLF	*Pseudomonas mesophilica*
		7	109	transparent, small ,round, moist,	A/K	-	-	+	-	+	+	-	-	+	+	+	pos.	*Pseudomonas alcaligenes*
		7	110	transparent, round, round, small															
8.5	TR	7	111	Yellowish, opaque, large, circular, mucoid, shiny.															

		8	112	Round, concentric, thick center, thin margins, opaque.														
		4	113	Transparent, round, large spreading, with swarming.														
		4	114	Tiny, transparent, round.														
		5	115	Round, medium sized, turbid off white, moist mucoid.														
8.5	Iron	2	1	Round, transparent, bulging, shiny, medium sized	K/K	-	-	+	-	-	+	-	-	+			NLF	*Pseudomonas stutzeri*
		7	7	Yellow, round, small, bulging growth	A/K	-	-	+	-	-	+	-	+	+	-	+	NLF	*Serratia ficaria*
Control	PVC	5	98	Round, swarming, greenish, pseudo like smell, medium sized.	K/K	+	+	+	-	-	+	-	-	+	+	+	NLF	*Shewanella putrefaciens*
		5	99	Small, round, transparent.	K/K	-	-	-	-	-	+	-	-	+	+	+	NLF	*Pseudomonas pseudoalcaligenes*
Control	SS	4	100 (i)	Round, off white, medium sized, thick mucoid.														
		7	100 (ii)	Round, large, greenish, moist, swarming.														
Control	TR	4	101	String forming, opaque and translucent.	K/A	-	-	+	-	+	-	-	-	+	+	+	pos.	*Klebseilla spp.*
		4	102	Thick, moist, irregular, margins.	+	-		-	+	+	-	-				NLF	+	*Klebsiella terrigena*
		6	103	Off white, round, medium sized.														
Control	Iron	8	116	small, round, transparent,														
		3	117	Clear transparent, mucoid, string forming, large.														
		4	118	medium, transparent, round														
Control	PE	7	119	Round with granular margins, shiny, moist, light creamy.														
		2	120	Round, moist, off white.	A/A	-	-	-	+	-	+	-	-	+	+	+	neg.	*Pseudomonas pseudoalcaligenes*
		7	121	Small pin head sized, clear transparent, round, raised.	K/K	-	-	-	-	+	+	-	-	+	+	+	LF	*Staphylococcus sp.*

(SC: Simmon's citrate, U: Urease, C: Catalase, O: Oxidase, N: Nitrate, Mac. Agar: Growth on MacConkey agar, S/B: slant/butt, G: Gas, M: Motility, K: Reaction after Kovac's reagent addition)

4.4. Bacterial Density and Diversity in Activated Sludge Using Various Techniques

The heterotrophic colony forming count (CFU/ml) data revealed facts about the effect of sludge processing before plating and colony counting. The results showed comparable differences between the bacterial density and diversity when the supernatant was used side by side to the sludge for heterotrophic plate count (HPC/ml). The sludge supernatant displayed more cell density in all serially diluted plates with a difference of 3.373×10^2 CFU/ml as compared to CFU/ml from sludge that was inoculated directly on the media plates. Microbial diversity, on the other hand was found poor in plates spread with supernatant from processes sludge.

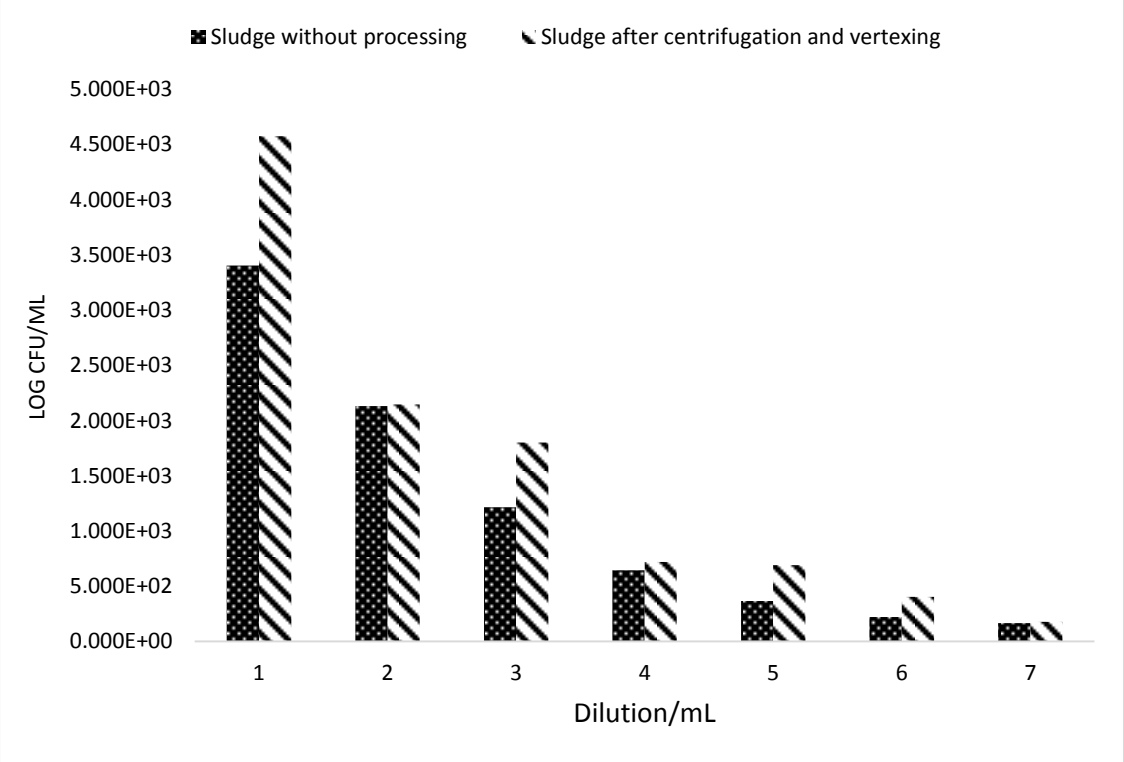

Figure 4.12. Enumeration of bacteria isolated from activated sludge with and without prior processing by centrifugation and vertexing.

4.5. Molecular Profiling of Microbial Community of Nitrifying and Denitrifying Bacteria in Biofilms Developed on Different support Materials under Varying Concentrations of Fe(III)

Identification of bacterial isolates taking part in microbial community structure is usually based on microscopic and macroscopic characteristics, however, analysis of DNA at the sequence level serves as a powerful tool not only for rapid identification of cultivable and uncultivable microorganisms at the genus and strain level but also for assessing the microbial diversity. Activated sludge along with five biofilm samples developed from activated sludge were processed for their whole DNA extraction. DNA from activated sludge was successfully extracted by the protocol of Singka et al. (2012). DNA extraction from biofilm samples was attempted by three methods out of which only commercial kit extracted DNA of satisfactory concentration. Short fragments of bases in the range of 232-328 were amplified by primers specific for all ammonia oxidizing bacteria (Nso190F), Nitrospira species (Nspra-675),nitrobacter species (Nitro-1198F) and for subunit A of amo gene i.e. ammonium monooxygenase A (amoA) (Table 4).

Table 4.2. Primers and their specificities used for the amplification of target genes from whole genome of activated sludge and biofilm samples

No	Sample	Primer	No. of bases of amplified fragment	Specificity	Accession No.
1	Fe-6.5 (mg/l)-TR	Nso190f	328	AOB, 16S rDNA	Awaited
2	Fe-6.5 (mg/l)-PE	Nspra-675f	312	Nitrospira 16S rDNA	Awaited
3	Fe-8.5 (mg/l)-TR	Nitro-1198F	308	All Nitrobacter spp.	Awaited
4	Fe-8.5(mg/l)-PE	Nspra-675f	276	Nitrospira 16S rDNA	Awaited
5	Control-TR	Nitro-1198f	232	All Nitrobacter spp.	Awaited
6	Activated sludge	amoA 1F	287	amoA	Awaited

4.5.1. Sequence Analysis of the Genes

Sequence similarity analysis of primary DNA sequences confirmed that polymerase chain reaction (PCR) products of the expected sizes from the DNA of biofilm samples and activated sludge were indeed amoA fragments and fragments of the respective target sites. All the generated sequences gave a perfect match with the available sequence(s) of related species. The phylogenetic relationship based on amo genes offers a finer level resolution (to the strain level) than 16S rDNA sequences for both the γ- and the β-subdivision of ammonia-oxidizing bacteria. Phylogenetic trees were constructed based on the amplified sequences by Mega6.The obtained sequence(s) were deposited in NCBI database (http://www.ncbi.nlm.nih.gov/nucleotide/).

Phylogenetic sequencing analysis indicated the relationship and presence of several species of nitrifying and denitrifying bacteria in biofilm established on tire rubber without any exogenous addition of ferric iron. Significant species included *Nitrobacter hamburgensis* X14 with lowest E value of 0.15 indicating significant match of the sequence within the database. Probability of presence of other related species in the specimen is indicated in phylogenetic tree that included *Nitrobacter winogradskyi* Nb-255, *Nitrobacter hamburgensis* X14, *Bradyrhizobium oligotrophicum* S58, *Rhodopseudomonas palustris* TIE-1, *Rhodopseudomonas palustris* BisB5 and *Rhodopseudomonas palustris* CGA009.

Based on ammonium monooxygenase gene subunit A (amoA), sequencing analysis revealed the presence of several species of ammonia oxidizing bacteria (AOBs) in activated sludge. Phylogenetic tree shows relationships among *Nitrosomonas europaea*, *Nitrosomonas eutropha* and *Nitrosospira multiformis* strains in activated sludge. Nitrosomonas europaea has been a long-standing model strain that provided foundational knowledge of AOB physiology, biochemistry, and genetics. *Nitrosomonas eutropha* strain, a close taxonomic relative of *N. europaea* that is apparently restricted to environments with very high ammonium loads like waste water treatment plants. Similarly, *Nitrosospira multiformis* strain is a representative of the most common AOB genus found in soils (11).

Molecular sequence based analysis of biofilm grown on PE based plastic material with the addition of 6.5 mg/l concentration of $Fe(OH)_3$ exhibited mainly the presence and abundance of *Candidatus Nitrospira defulvii* sp., *Nitrosomoas europeae* strains, *Leptospirillum ferriphilum* YSK and *Leptospirillum ferriphylum* ML04. Biofilm on

the same material (PE), under same environmental and nutritional conditions, with the only exception of higher concentration of $Fe(OH)_3$ in ABBR, on the other hand, showed greater diversity of bacterial sp. related to the target group of nitrifying bacteria. In addition to the sp. present at Fe-6.5 mg/l i.e; *Candidatus Nitrospira defulvii* sp., *Leptospirillum ferriphilum* YSK and *Leptospirillum ferriphylum* ML04, it also demonstrated significant homology with *Bradyrhizobium diazoefficiens* NK6, *Bradyrhizobium* japonicum USDA 110, *Nitrobacter hamburgensis* sp. and *Rhodopseudomonas palustris* BisB5. *Nitrosomoas europeae* strains present at 6.5 mg/l concentration of ferric iron was found absent at 8.5 mg/l of ferric iron.

Evolutionary relationships of taxa in case of biofilm developed on tire rubber (TR) based material at Fe-6.5 mg/l showed a great diversity of AOB. These included three different strains of Nitrosomonas sp. i.e; *Nitrosomonas sp. Is79A3, Nitrosomonas sp. AL212* and *Nitrosomonas europaea ATCC 19718*, five different Uncultured *Nitrosomonadales* bacterium clones, Nitrosospira multiformis ATCC 25196 and Thermodesulfovibrio yellowstonii *DSM 11347*. Amplified nucleotide sequence for genus Nitrobacter showed the presence of *Nitrobacter hamburgensis* X14, *Nitrobacter winogradskyi* Nb-255 sp. in biofilm microbial community grown on TR in ABBR under 8.5 mg/l concentration of $Fe(OH)_3$ that match to the corresponding species of genus Nitrobacter in biofilm on TR from control ABBR. But at higher concentration of $Fe(OH)_3$, TR supported the growth of some additional species of genus Nitrobacter i.e; *Nitrobacter* sp. clone NA20, *Nitrobacter* sp. clone NA14, Nitrobacter sp. strain R6 and some uncultured *Nitrobacter* sp. which were not found in biofilm on TR developed in ABBR without exogenous supplementation of ferric iron. E values of all respective bacterial species are shown in table 8. It decreases exponentially as the Score (S) of the match increases within the database.

4.5.2. Evolutionary Relationships and Presence of Nitrifying Bacteria in Biofilm Developed on Tire Rubber from Untreated Aerobic Batch Biofilm Reactor (ABBR)

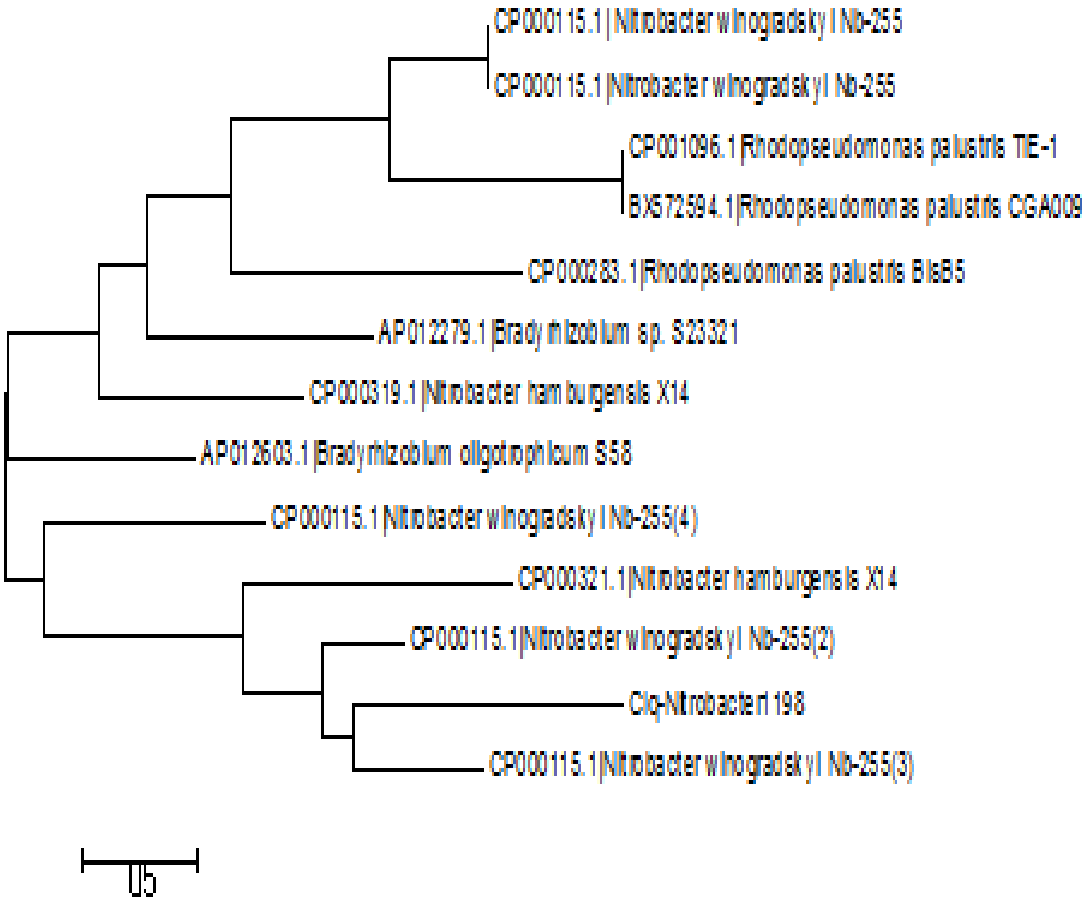

Figure 4.13. Evolutionary relationships of taxa found in biofilm developed on tire rubber from control membranous batch reactor. The primer used was Nitro-1198F specific for all Nitrobacter species. The evolutionary history was inferred using the Neighbor-Joining method. The optimal tree with the sum of branch length = 12.99795644 is shown. The tree is drawn to scale, with branch lengths in the same units as those of the evolutionary distances used to infer the phylogenetic tree. The evolutionary distances were computed using the Maximum Composite Likelihood method and are in the units of the number of base substitutions per site. The analysis involved 13 nucleotide sequences. All positions containing gaps and missing data were eliminated. There were a total of 15 positions in the final dataset. Evolutionary analyses were conducted in MEGA6

4.5.3. Evolutionary Relationships and Presence of Nitrifying Bacteria in Activated Sludge

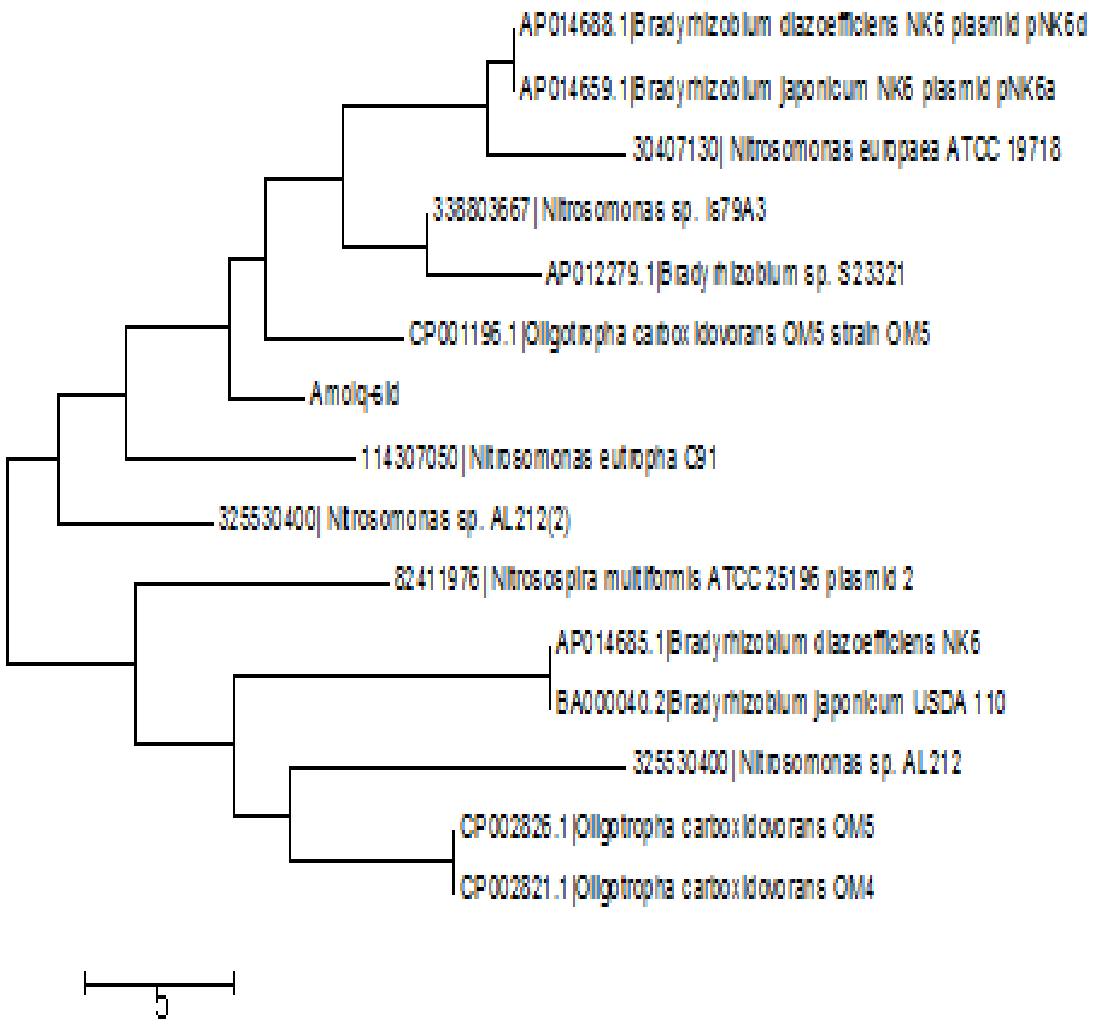

Figure 4.14. Evolutionary relationships of taxa. The primer used was AmoA specific for ammonium monooxygenase gene (subunit A) of all AOB. The evolutionary history was inferred using the Neighbor-Joining method. The optimal tree with the sum of branch length = 93.65915937 is shown. The tree is drawn to scale, with branch lengths in the same units as those of the evolutionary distances used to infer the phylogenetic tree. The evolutionary distances were computed using the Maximum Composite Likelihood method and are in the units of the number of base substitutions per site. The analysis involved 15 nucleotide sequences. All positions containing gaps and missing data were eliminated. There were a total of 17 positions in the final dataset. Evolutionary analyses were conducted in MEGA6

4.5.4. Evolutionary Relationships and Presence of Nitrifying Bacteria in Biofilm Developed on Polyethylene (PE) at Fe-6.5 mg/l in Aerobic Batch Biofilm Reactor (ABBR)

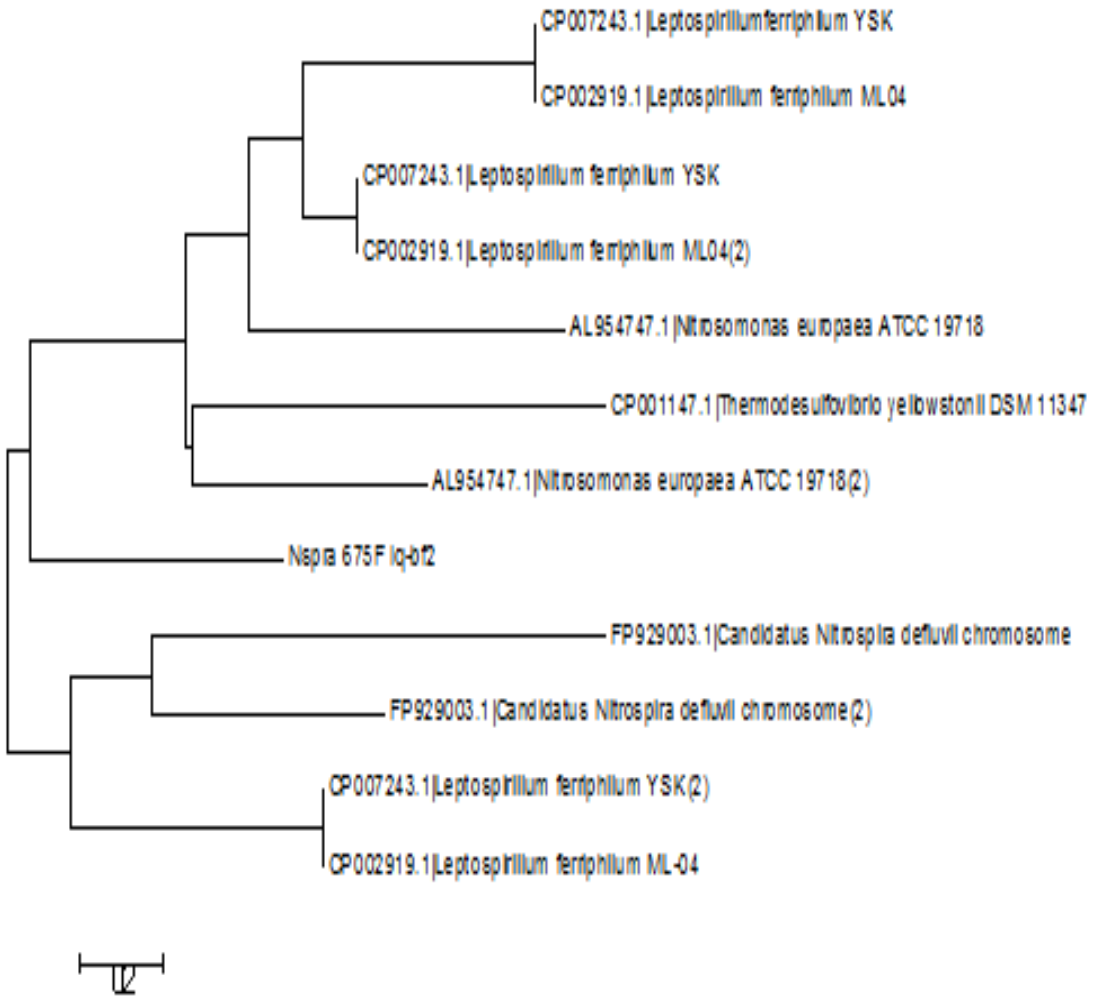

Figure 4.15. Evolutionry relationships of taxa. The evolutionary history was inferred using the Neighbor-Joining method. Primer Nspra-675 is specific for genus Nitrospira . The optimal tree with the sum of branch length = 14.80824332 is shown. The tree is drawn to scale, with branch lengths in the same units as those of the evolutionary distances used to infer the phylogenetic tree. The evolutionary distances were computed using the Maximum Composite Likelihood method and are in the units of the number of base substitutions per site. The analysis involved 20 nucleotide sequences. All positions containing gaps and missing data were eliminated. There were a total of 16 positions in the final dataset. Evolutionary analyses were conducted in MEGA6

4.5.5. Evolutionary Relationships and Presence of Nitrifying Bacteria in Biofilm Developed on Polyethylene (PE) at Fe-8.5 mg/l in Aerobic Batch Biofilm Reactor (ABBR)

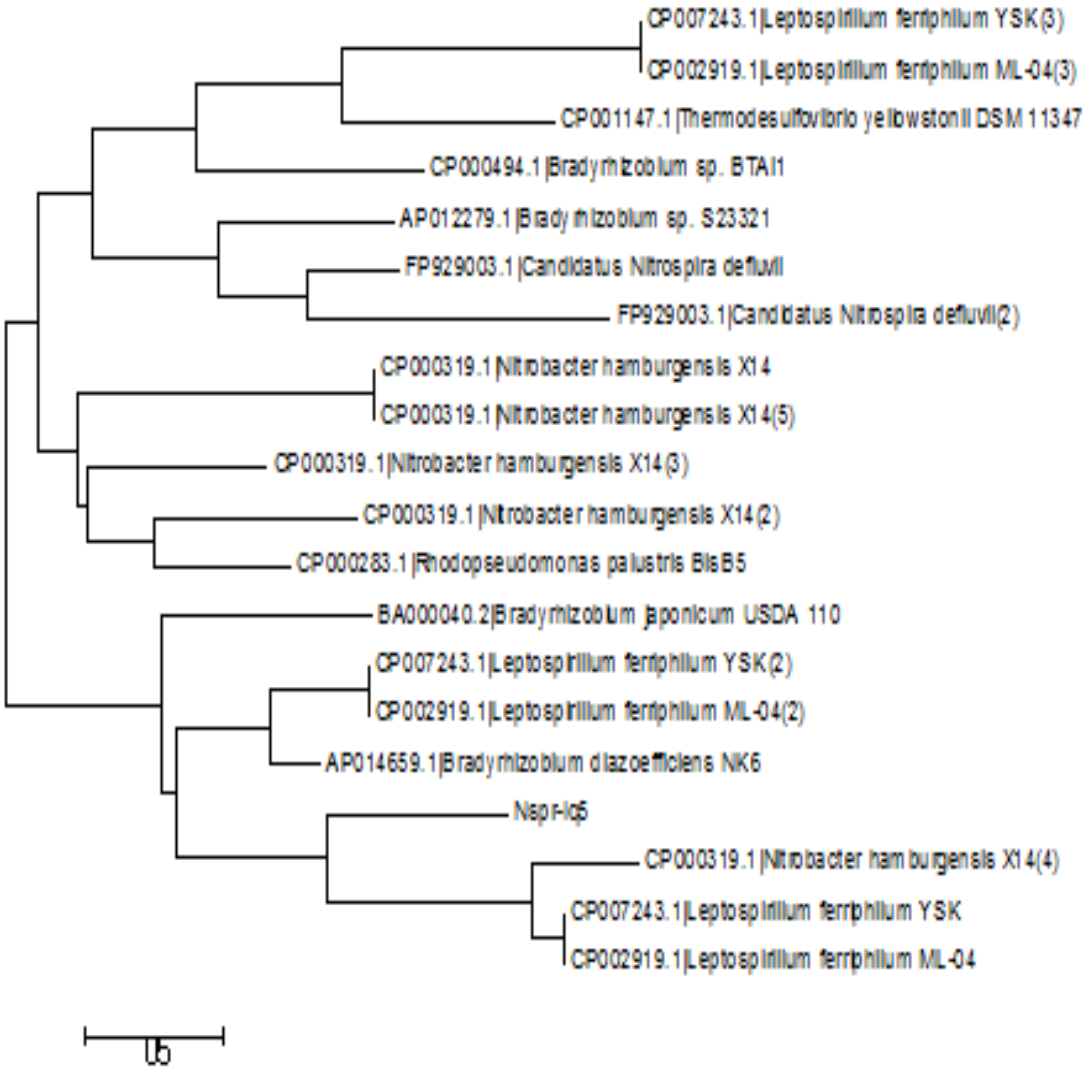

Figure 4.16. Evolutionary relationships of taxa. Phylogenetic tree shows the presence of Nitrospira and related species in biofilm developed on polyethylene (PE) based plastic material at 8.5 mg/l concentration of ferric iron. The evolutionary history was inferred using the Neighbor-Joining method. The primer used was Nspra-675F specific for all Nitrospira species. The evolutionary history was inferred using the Neighbor-Joining method. The optimal tree with the sum of branch length = 7.08669103 is shown. The tree is drawn to scale, with branch lengths in the same units as those of the evolutionary distances used to infer the phylogenetic tree. The evolutionary distances were computed using the Maximum Composite Likelihood method and are in the units of the number of base substitutions per site. The analysis involved 12 nucleotide sequences. All positions containing gaps and missing data were eliminated. There were a total of 16 positions in the final dataset. Evolutionary analyses were conducted in MEGA6.

4.5.7. Evolutianary Relationships and Presence of Nitrifying Bacteria in Biofilm Developed on Tire Rubber (TR) at Fe-6.5 mg/l in Aerobic Batch Biofilm Reactor (ABBR)

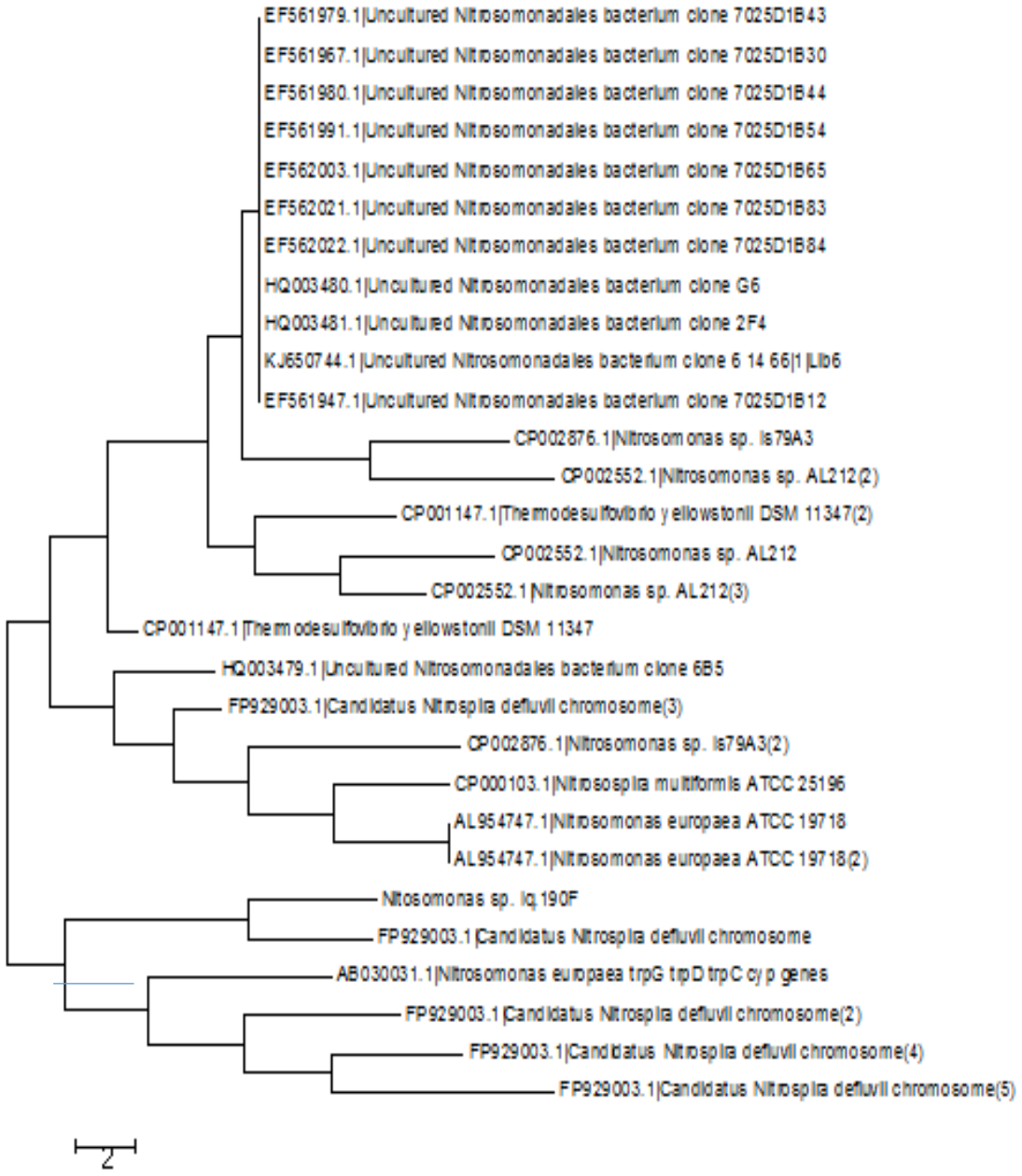

Figure 4.17. Evolutionary relationships of taxa. The primer used was Nso190f specific for ammonia oxidizing bacteria. The evolutionary history was inferred using the Neighbor-Joining method. The optimal tree with the sum of branch length = 119.53383398 is shown. The tree is drawn to scale, with branch lengths in the same units as those of the evolutionary distances used to infer the phylogenetic tree. The evolutionary distances were computed using the Maximum Composite Likelihood method and are in the units of the number of base substitutions per site. The analysis involved 29 nucleotide sequences. All positions containing gaps and missing data were eliminated. There were a total of 12 positions in the final dataset. Evolutionary analyses were conducted in MEGA6.

4.5.8. Evolutionary Relationships and Presence of Nitrifying Bacteria in Biofilm Developed on Tire Rubber (TR) at Fe-8.5 mg/l in Aerobic Batch Biofilm Reactor (ABBR)

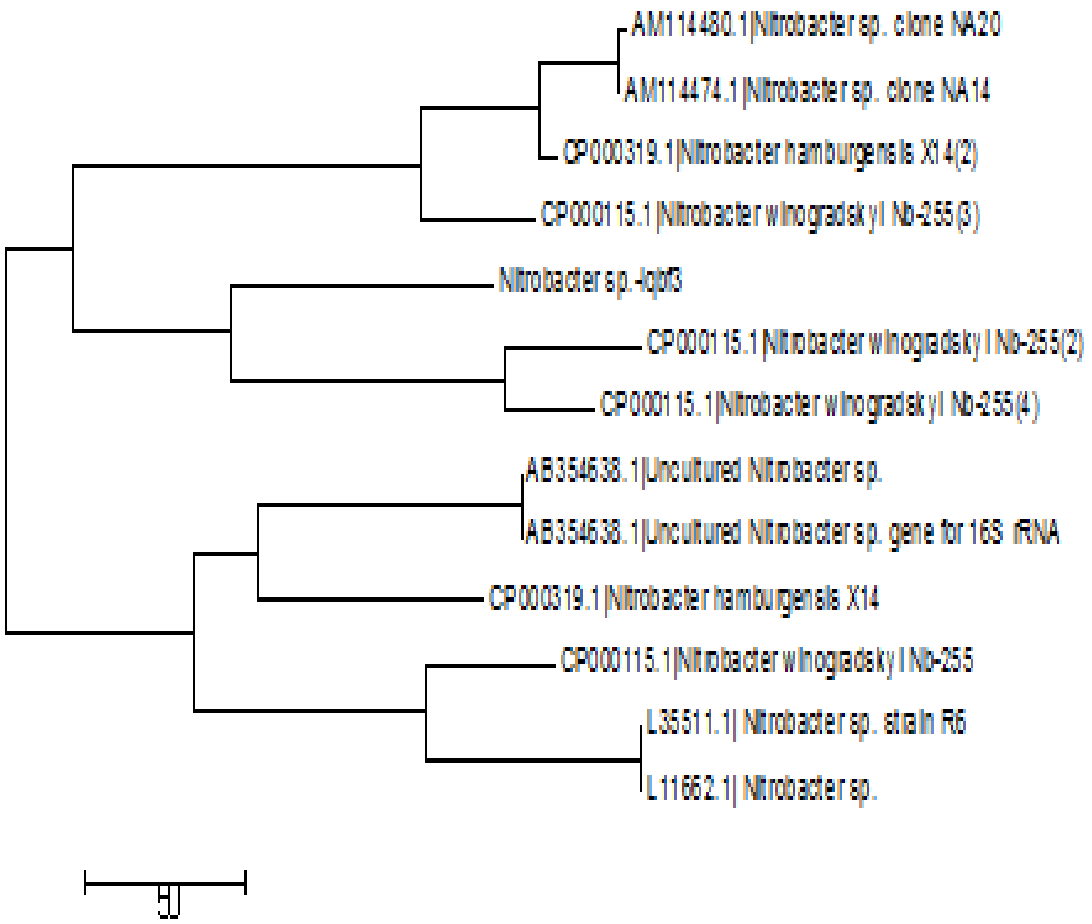

Figure 4.18. Evolutionary relationships of taxa. The evolutionary history was inferred using the Neighbor-Joining method. The primer used was Nitro-1198F specific for all Nitrobacter species. Divergence times for all branching points in the topology were calculated with the RelTime method using the branch lengths contained in the inferred tree. The analysis involved 15 nucleotide sequences. All positions containing gaps and missing data were eliminated. There were a total of 15 positions in the final dataset. Evolutionary analyses were conducted in MEGA6.

Table 4.3. E-values of bacterial strains retrieved from database

Sample	Species	E	Sample	Species	E	Sample	Species	E
Control-TR	Rhodopseudomonas palustris BisB5	7.6	Fe-8.5mg/l-PE	Leptospirillum ferriphilum YSK	0.084	Fe-8.5-TR	Nitrobacter sp. clone NA20	6.3
	Nitrobacter hamburgensis X14	4.8		Leptospirillum ferriphilum ML-04	0.084		Nitrobacter sp. clone NA14	6.3
	Nitrobacter winogradskyi Nb-255	4.8		Candidatus Nitrospira defluvii	0.29		Nitrobacter sp. strain R6	6.3
	Nitrobacter winogradskyi Nb-255	1.9		Thermodesulfovibrio yellowstonii DSM 11347	3.0		Nitrobacter sp. |L11662.1|	6.3
	Nitrobacter hamburgensis X14	O.15		Nitrobacter hamburgensis X14	0.46		Uncultured Nitrobacter sp.	0.52
	Bradyrhizobium oligotrophicum S58	6.6		Bradyrhizobium diazoefficiens NK6	0.18		Nitrobacter hamburgensis X14	0.52
	Bradyrhizobium sp. S23321	6.6		Bradyrhizobium sp. S23321	2.3		Nitrobacter winogradskyi Nb-255	0.52
	Rhodopseudomonas palustris TIE-1	6.6		Rhodopseudomonas palustris BisB5	2.3		Nitrobacter sp. clone NA20	6.3
	Rhodopseudomonas palustris BisB5	6.6		Bradyrhizobium japonicum USDA 110	2.3		Nitrobacter sp. clone NA14	6.3
	Rhodopseudomonas palustris CGA009	6.6		Bradyrhizobium sp. BTAi1	8.0		Nitrobacter sp. strain R6	6.3
				Nitrobacter hamburgensis X14	8.0		Nitrobacter sp. |L11662.1|	6.3
Activated Sludge	*Nitrosomonas europaea* |AL954747.1|	4.0	Fe-6.5mg/l-PE	*Candidatus Nitrospira defulvii* sp.	0.29	Fe-6.5mg/l-TR	*Nitrosomonas sp. Is79A3*	2.0
	Nitrosospira multiformis ATCC 25196 |CP000105.1|	4.0		Nitrosomonas europaea ATCC 19718	3.0		*Nitrosomonas sp. AL212*	4.0
	Bradyrhizobium diazoefficiens |AP014688.1|	9.6		*Leptospirillum ferriphilum* YSK	0.46		*Nitrosomonas europaea ATCC 19718*	0.46
	Bradyrhizobium japonicum|AP014659.1|	9.6		*Leptospirillum ferriphylum* ML04	0.18		Nitrosospira multiformis ATCC 25196	6.0
	Bradyrhizobium sp. S23321 |AP012279.1|	9.6		Thermodesulfovibrio yellow	0.29		*Thermodesulfovibrio yellowstonii DSM 11347*	3.5
	Oligotropha carboxidovorans |CP002826.1|	9.6						
	Oligotropha carboxidovorans |CP002821.1|	9.6						
	Oligotropha	9.6						

	carboxidovorans |CP001196.1|							
	Bradyrhizobium japonicum |BA000040.2|	9.6						

4.6. Screening Bacterial Isolates for their Biofilm Forming Ability by Biofilm Development Assays

Bacteria isolated from several all biofilms developed on different substrata at a range of Fe(III) concentrations in ABBRs were quantified for their biofilm formation abilities by biofilm assays i.e. Congo red agar (CRA) assay, tube method (TM) and tissue culture plate (TCP) assay, the gold standard method for this purpose, and the data was compared. Results revealed that all the bacterial strains seem to have dissimilar biofilm formation tendencies as is evident from the figure below.

By TM detection assay, 67.08 % of total 79 bacterial isolates were found as strong biofilm formers, 26.58 % moderate and only 5.0% weak or non-biofilm formers. Result of 1.26% bacteria remained indeterminate by TM. The Congo red agar method detected 34.18% isolates as strong, 8.87% intermediate and 40% weak/none biofilm formers. By contrast, TCP assay, the gold standard screening assay indicated very different results. By this method, 96.20% isolates seemed to have strong biofilming tendency with only 3.79% as moderate biofilm formers and none as weak or non-biofilm former.

Statistically, the non-biofilm formers by all methods were considered as true negatives, whereas, non-biofilm forming by CRA and TM but not by TCP were taken as false negatives. Similarly, biofilm producers by all three assays were true positives yet biofilm formers by CRA and TM but nor by micro titer method were recorded as false positives.

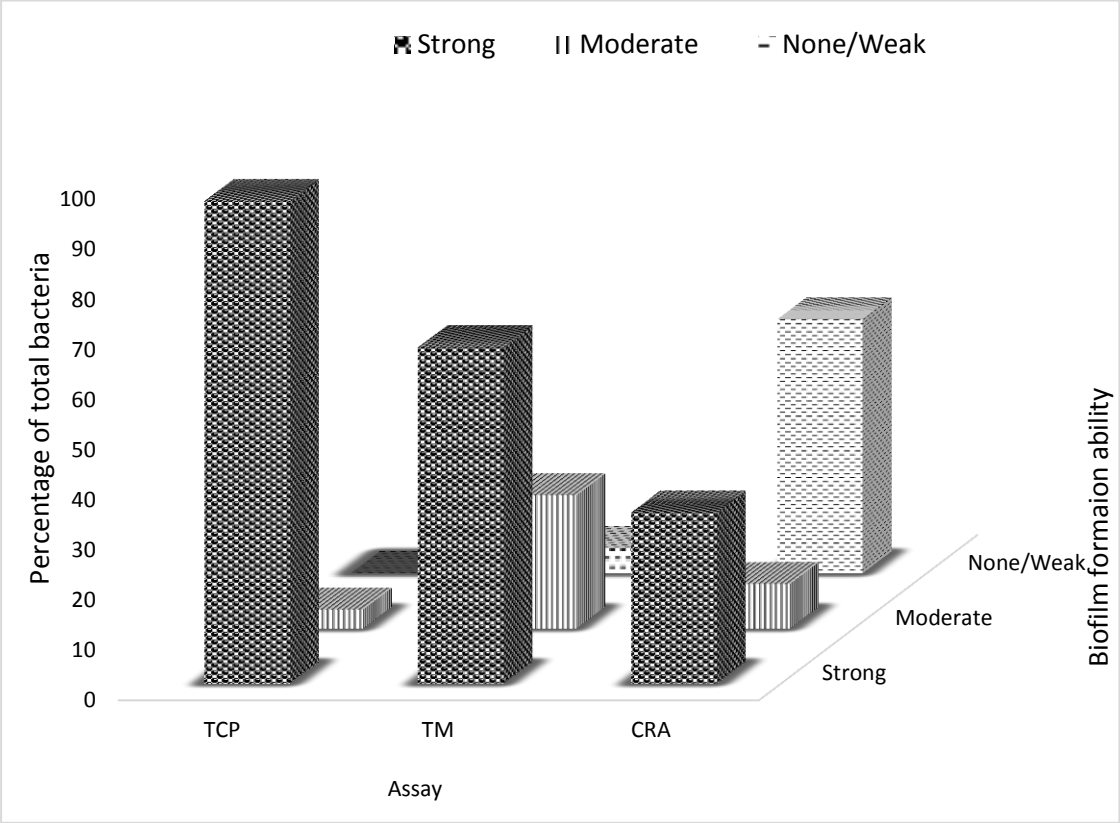

Figure 4.19. Biofilm forming ability of bacteria (weak, moderate, strong) isolated from biofilms developed on different carrier materials under varying concentrations of Fe(III) using; tissue culture plate (TCP), tube method (TM) and congo red agar (CRA) method

Table 4.5. Screening of bacteria isolated from different biofilms developed on different carrier materials under varying Fe(III) concentrations for their biofilm formation ability by TCP, TM and CRA method

Biofilm Formation	TCPn(%)	TMn(%)	CRAn(%)
Strong	76(96.20)	53(67.08)	27(34.18)
Moderate	3(3.79)	21(26.58)	7(8.87)
None/Weak	0(0)	4(5.06)	40(50.63)

(Total Isolates: 79, Indeterminate results in CRA: 5, Indeterminate results in tube method: 1)

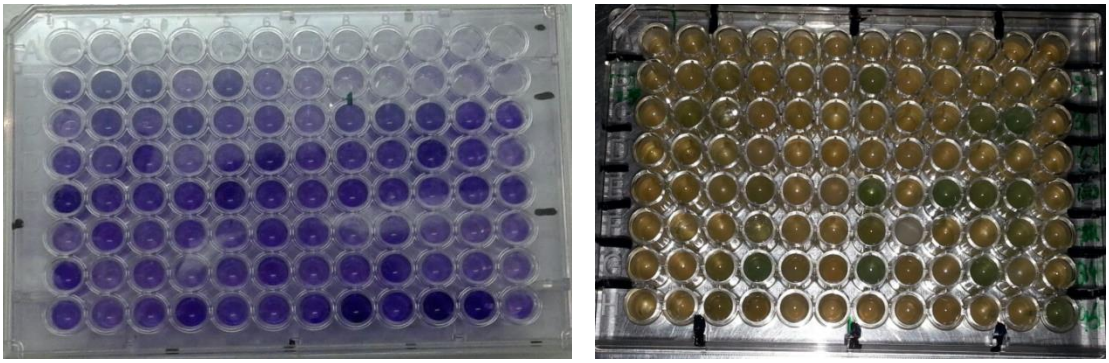

Figure 4.20. Biofilm forming ability of bacteria isolated from biofilms developed under various concentration of Fe(III) on different support materials using tissue culture plate (TCP) method (from left to right; micro titer plates before and after staining with crystal violet)

Figure 4.21. Congo red agar (CRA) palte assay for biofilm detection of bacteria isolated from biofilm. (left; positive CRA test, right; negative CRA test)

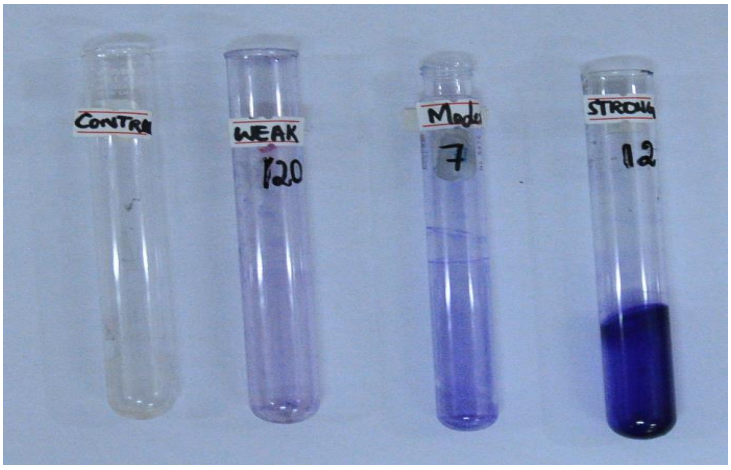

Figure 4.22. Biofilm formation ability of different bacteria isolated from biofilms developed on different support materials in tube method (left to right: control, weak, moderate and strong biofilm formers)

4.7. Nitrification Rate of Biofilms Developed on Different Support Materials under varying Concentrations of Fe(III)

Previously, nitrogen removal efficiencies of several systems and planktonic cultures have been investigated, however, very little is known about nitrogen removal performance of their biofilms. In order to investigate the nitrification and denitrification potential of nitrifying and denitrifying bacteria among multispecies biofilms developed on selected attached growth materials under the effect of varying ferric iron concentrations, support materials per cm^{-2} of their area along with biofilms were fed with ammonium enriched medium and $Fe(OH)_3$ (0 mg/l, 2.5 mg/l, 6.5 mg/l, 8.5 mg/l) and finally incubated in dark on shaker under agitated conditions. Relative effects of substratum with respect to Fe(III) concentrations on nitrification rate were monitored for a period of one month over different intervals and data was compared. The results obtained showed three support materials out of five had an improved nitrification tendency over others.

4.7.1. Nitrification Rate in Biofilms Developed on Stainless Steel

Results indicated that within the biofilm established on stainless steel at Fe-2.5 concentration, there was an obvious build up in NO_2^- -N as well as NO_3^--N values from 0.0501 to 0.3 mg/l and 0 to 3.12 mg/l over a period of 30 days, with 0.170 and 1.6 mg/l concentration at 15^{th} day, respectively. The percentage increase in NO_2^- -N concentration, during first 15 days and last 15 days was 70.5% and 82.5%, respectively. Very similar trend was observed in biofilms incubated with Fe-6.5 mg/l and Fe-8.5 mg/l quantities where values ranged from 0.083-0.25 mg/l and 0.04-0.2 mg/l in case of nitrite and 0-2.78 mg/l and 0-3.6 mg/l in case of nitrate, respectively. On the contrary, control NO_2^- showed inverse correlation between ferric and nitrite concentration indicating that presence of iron improved NH_4^+-N oxidation.

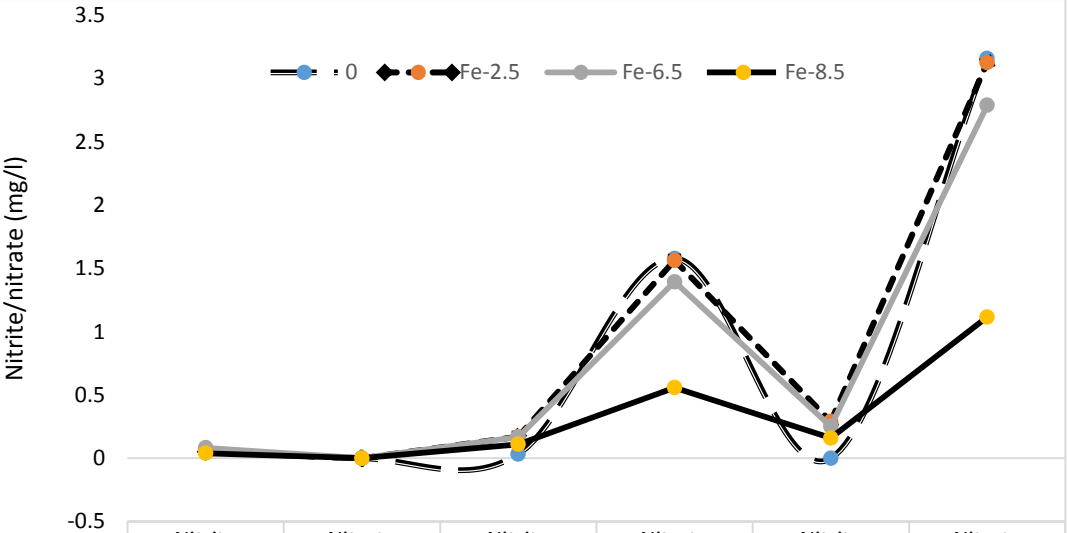

	Nitrite	Nitrate	Nitrite	Nitrate	Nitrite	Nitrate
	0		15		30	
	Days					
0	0.0668	0	0.0334	1.5789	0	3.1581
Fe-2.5	0.0501	0	0.17025	1.56312	0.2904	3.126407
Fe-6.5	0.083	0	0.1667	1.3944	0.2505	2.7889
Fe-8.5	0.0401	0	0.1101	0.5579	0.1603	1.1155

Interval (days), data table presenting nitrite and nitriate concentrations at different Fe(III) supplements (mg/l)

Figure 4.23. Nitrite-nitrogen and nitrate-nitrogen production and transformation rate (mg/l) in biofilms developed on Stainless steel (SS) at different concentrations of Fe(III)

4.7.2. Nitrification Rate in Biofilms Developed on Polyvinyl Chloride (PVC)

In biofilms grown on PVC, there was a slight increase in NO_2^- -N at Fe-2.5 mg/l from 0.083-0.1 mg/l in first 15 days that persisted for the next whole period that accounts to the low activity of ammonia oxidizing bacteria (AOB). Although there was an increase in NO_2^- -N in all cases of biofilms from PVC except control biofilm with time, yet there was no significant difference between the accumulated concentrations. Control biofilm showed complete oxidation of nitrite into other N compounds with time as shown in figure below. In contrast to nitrite, with the same time lapses, there was significant amassing of NO_3^- -N in all biofilms including control. NO_3^- -N concentrations were found mottled from 0.0835, 0.00, 0.00 and 0.00 mg/l at 0 day (at Fe-2.5 mg/l, F3-6.5 mg/l, Fe-8.5 mg/l and control) to 2.79, 0.30, 1.70 and 2.79 mg/l at 30^{th} day with their intermediate values at mid-15^{th} day.

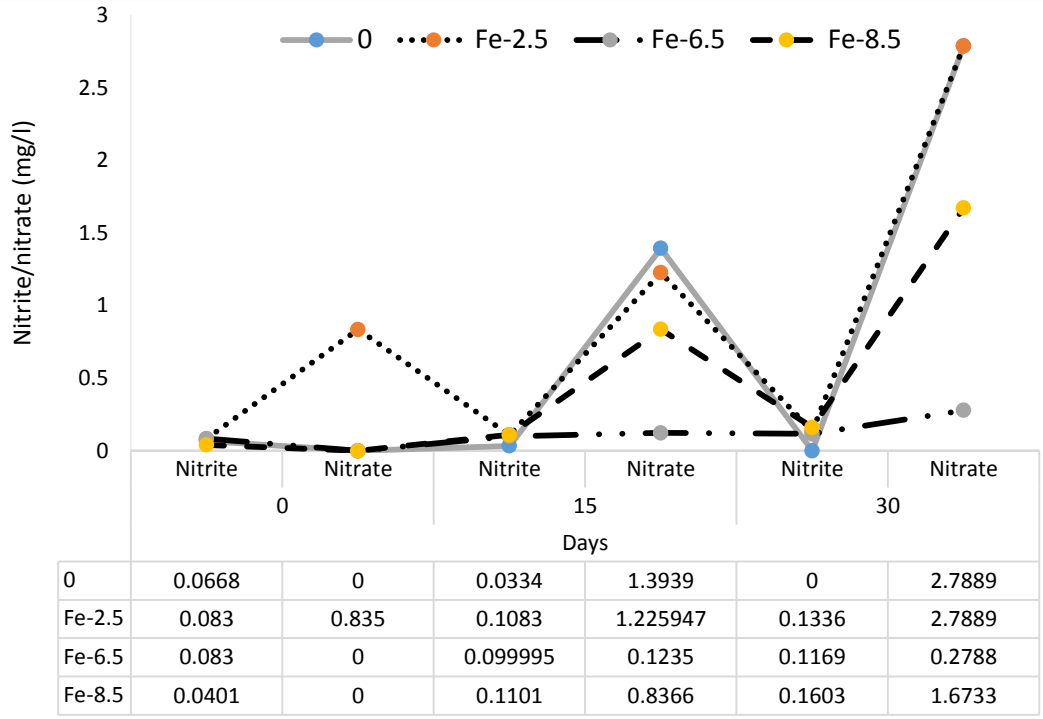

0	0.0668	0	0.0334	1.3939	0	2.7889
Fe-2.5	0.083	0.835	0.1083	1.225947	0.1336	2.7889
Fe-6.5	0.083	0	0.099995	0.1235	0.1169	0.2788
Fe-8.5	0.0401	0	0.1101	0.8366	0.1603	1.6733

Interval (days), data table presenting nitrite and nitriate concentrations at different Fe(III) supplements (mg/l)

Figure 4.24. Nitrite and nitrate accumulation and transformation rate (mg/l) in biofilm developed on Polyvinyl chloride (PVC) at different concentrations of Fe(III)

4.7.3. Nitrification Rate in Biofilms Developed on Iron

Biofilms developed on iron as a carrier material showed a marked AOB activity resulting in gradual accumulation of NO_2^- -N from 0.584 mg/l to 1.002 mg/l at 15th day of incubation and then to 1.42 mg/l at 30th day along with its further conversion into NO_3^- -N by the activity of NOB in the same duration with a rise from 0 mg/l to 1.4 mg/l at the end of experiment as shown in figures. The same trend was observed in other biofilm samples incubated with 6.5 and 8.5 mg/l Fe (III) indicating a positive impact of ferric iron on nitrification/denitrification activity within autotrophic biofilms developed on iron.

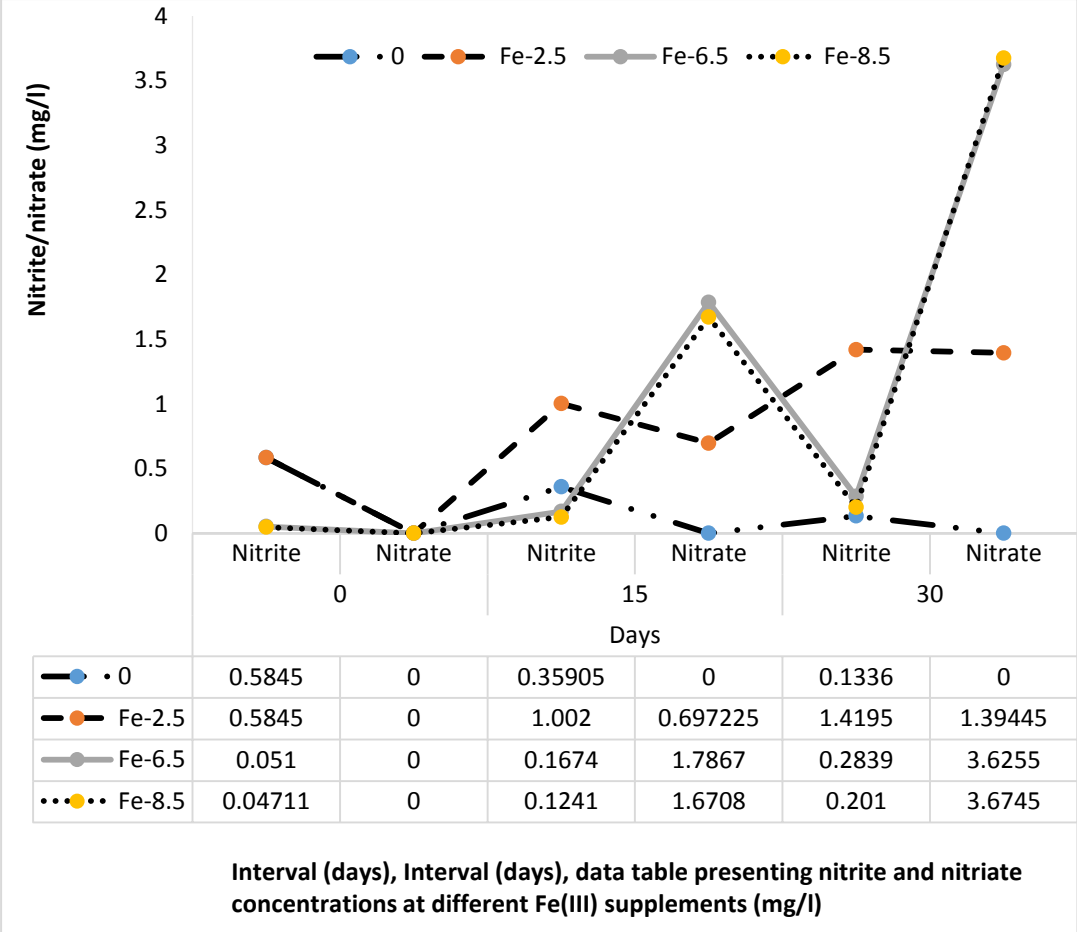

0	0.5845	0	0.35905	0	0.1336	0
Fe-2.5	0.5845	0	1.002	0.697225	1.4195	1.39445
Fe-6.5	0.051	0	0.1674	1.7867	0.2839	3.6255
Fe-8.5	0.04711	0	0.1241	1.6708	0.201	3.6745

Interval (days), Interval (days), data table presenting nitrite and nitriate concentrations at different Fe(III) supplements (mg/l)

Figure 4.25. Nitrite-nitrogen and nitrate-nitrogen production and transformation rate (mg/l) in biofilm developed on Iron at different concentrations of Fe(III)

4.7.4. Nitrification Rate in Biofilms Developed on Polyethylene (PE)

Biofilms from Polyethylene showed slight increase in NO_2^- -N concentration over time including control biofilm as shown above, indicting low AOB activity. There was successive increase in NO_3^- -N concentration like the case of PVC, at the same time from 0-0.223 mg/l at Fe-2.5 mg/l, 0-1.116 mg/l at Fe-6.5 mg/l and 0-2.79 mg/l at Fe-8.5 mg/l concentration of ferric iron over the period of experiment.

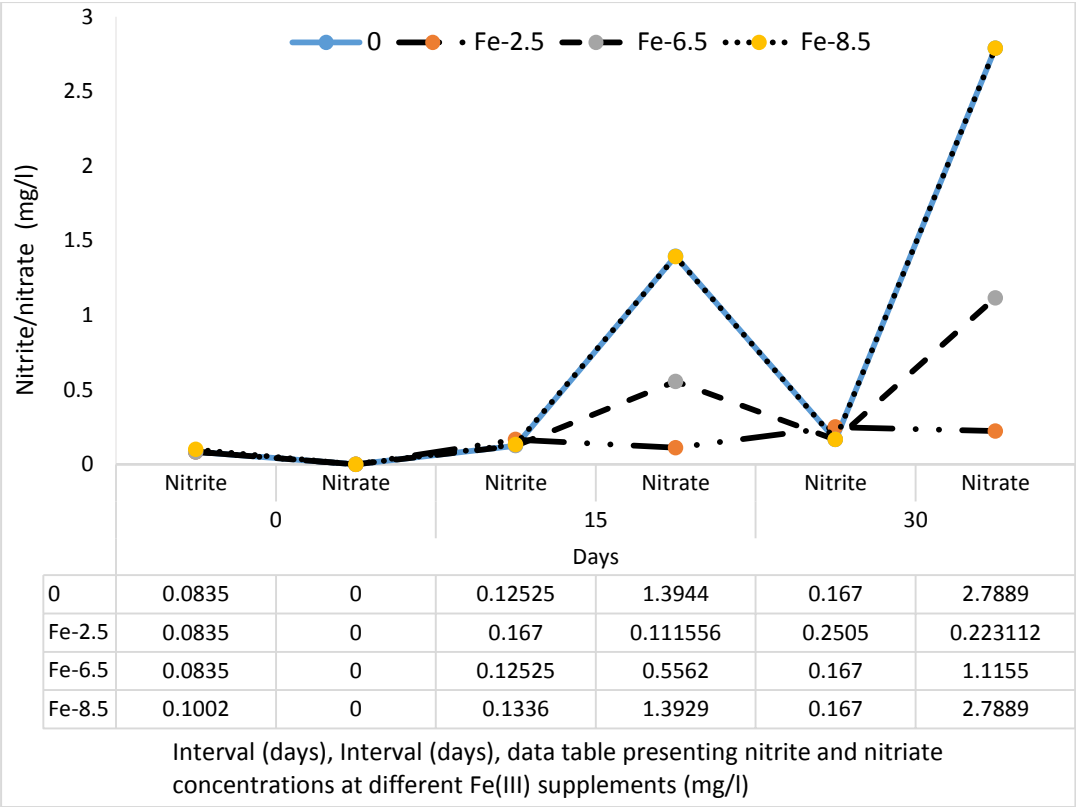

0	0.0835	0	0.12525	1.3944	0.167	2.7889
Fe-2.5	0.0835	0	0.167	0.111556	0.2505	0.223112
Fe-6.5	0.0835	0	0.12525	0.5562	0.167	1.1155
Fe-8.5	0.1002	0	0.1336	1.3929	0.167	2.7889

Interval (days), Interval (days), data table presenting nitrite and nitriate concentrations at different Fe(III) supplements (mg/l)

Figure 4.26. Nitrite and nitrate production and transformation rate (mg/l) in biofilm developed on Polyethylene (PE) at different concentrations of Fe(III)

4.7.5. Nitrification Rate in Biofilms Developed on Tire Rubber (TR)

In TR biofilms, maximum accumulation of NO_2^- -N occurred at Fe-6.5 mg/l concentration with a value of 3.19 mg/l after 30th days that declined at Fe-8.5 mg/l indicating that the highest concentration of ferric iron was inhibitory to the AOB activity. There was an increase in NO_3^- -N from undetectable range - 2.6 mg/l, undetectable - 3.62 mg/l, undetectable - 2.789 mg/l and undetectable - 2.788 mg/l at 2.5, 6.5, 8.5 mg/l concentrations of ferric iron and control, respectively. Yet, there was no prominent difference among values across the concentrations as indicated in figure below.

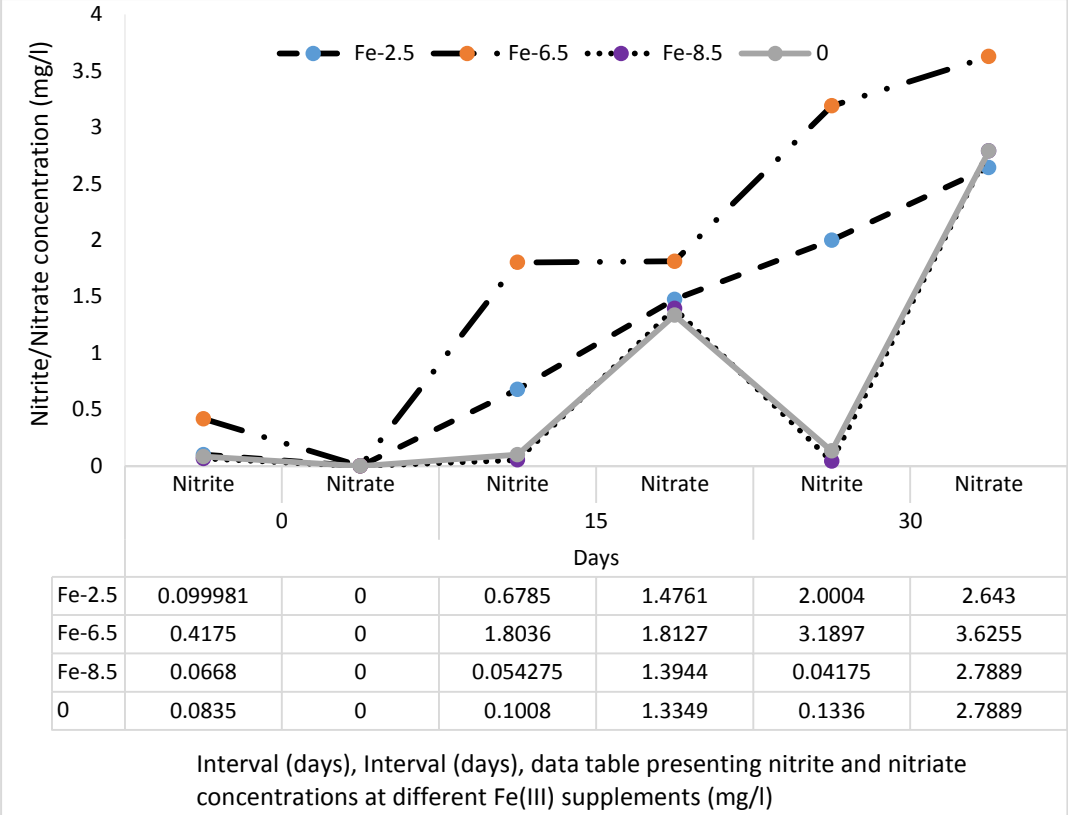

Fe-2.5	0.099981	0	0.6785	1.4761	2.0004	2.643
Fe-6.5	0.4175	0	1.8036	1.8127	3.1897	3.6255
Fe-8.5	0.0668	0	0.054275	1.3944	0.04175	2.7889
0	0.0835	0	0.1008	1.3349	0.1336	2.7889

Interval (days), Interval (days), data table presenting nitrite and nitriate concentrations at different Fe(III) supplements (mg/l)

Figure 4.27. Nitrite and nitrate accumulation and transformation rate (mg/l) in biofilm developed on Tire rubber (TR) at different concentrations of Fe(III)

4.8. Biofilm Structural Characterization

4.8.1. Characterization of Extracellular Polymeric Substance (EPS) of Biofilms Developed on Different Support Materials under varying Fe(III) Concentrations by Fourier Transform Infrared Spectroscopy (FTIR)

The biofilms developed on various substrata with varying Fe^{3+} concentrations were characterized by fourier transform infrared spectroscopy (FTIR) to determine the presence or absence of specific molecular fragments (functional groups) in the EPS and the spectra were compared as shown below.

Figure 4.28. *TENSOR 27* Fourier Transform Infra-red Spectroscope used for characterization of extracellular polymeric substances (EPS) of biofilms developed on different support materials under varying concentrations of Fe(III)

4.8.1.1. Extracellular Polymeric Substance (EPS) of Biofilms on Polyethylene (PE)

In case of biofilms developing on Polyethylene (PE) material supplemented with 2.5 mg/l $Fe(OH)_2$, bands at 3113.70 cm^-, 1624.86 cm^- wavenumber and a medium sized stretching band at the left end of spectrum at 3465.50 cm^- with single spike corresponded to the presence of carboxylic acid radicals, sp^2 hybridized alkenes (-C=C-) and N-H bond representing primary amines. Stretches in the fingerprint area at 970.27 cm- and 839.2 cm- instructed C-C, C-N and C-O bonds. Fe-6.5 mg/l concentration led to the expression of characteristic bands of carboxylic acids, stretching and bending vibration of sp3 hybridized C-H/OH bond (methyne or alcohol), alkenes and C-C, C-N, C-C at 3274.24 cm^-, 2927.7 cm^-, 1632 and 1002.81 cm^- respectively. A broad band at Fe(III) 8.5 mg/l yet lesser than in Fe(III) 6.5 mg/l reflected carboxylic radicals with slight difference in transmittance. The results conveyed that with increasing Fe_3^+ quantities, there was a decrease in % transmittance of carboxylic acid radicals from 97% at its 2.5 mg/l concentration to 88% at 6.5 mg/l and <90% at 8.5 mg/l concentration.

Spectrum of EPS of biofilm from control ABBR showed a wide band, scissoring and bending vibrations of carboxylic residues and alkanes (C-H) at 3272.1 cm^-, 2922.13 cm^- and medium to weak skewed bands of amines ($-NH_2$) at 1644.37 cm^-, 1536.43 cm^- and 1420.35 cm^- wavenumbers, respectively. Some peaks disappeared in control

spectrum present in tests indicating differences in the structure of biofilms grown at different Fe^{3+} concentrations.

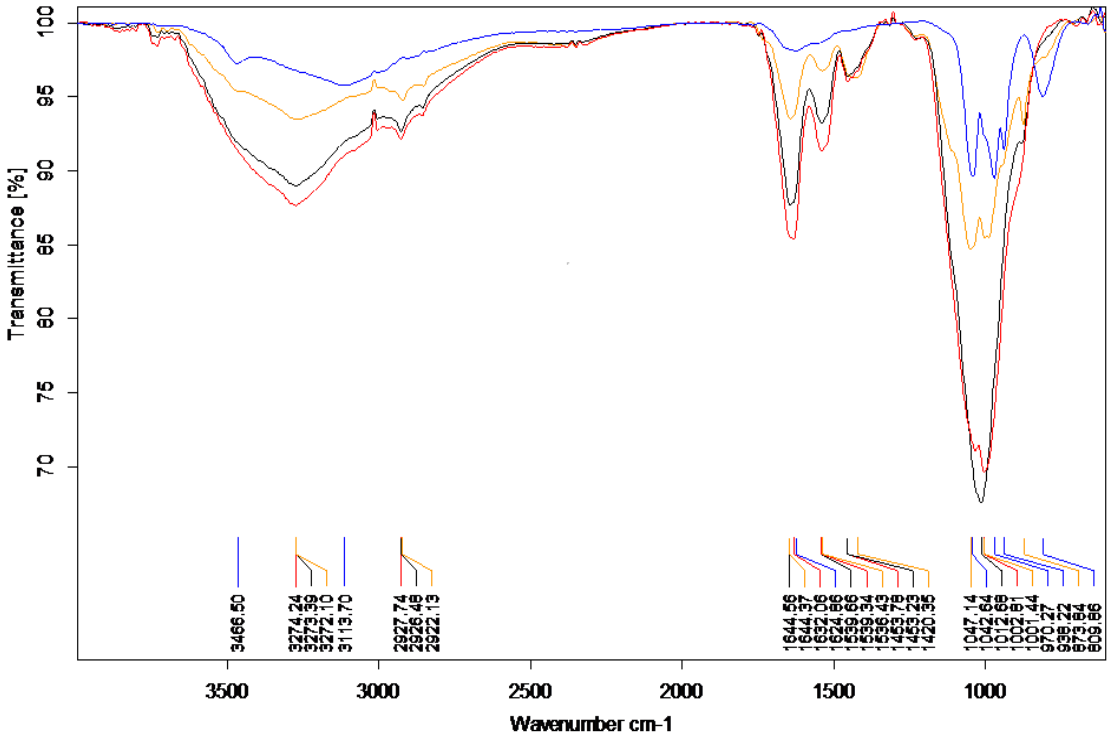

Figure 4.29. FTIR spectra of extracellular polymeric substance (EPS) from biofilms developed on Polyethylene (PE) at different Fe(III) concentrations (Blue: Fe-2.5, Red: Fe-6.5, Black: Fe-8.5, Yellow: Control)

4.8.1.2. Extracellular Polymeric Substance (EPS) of Biofilms on Tire Rubber (TR)

The IR spectrum of TR biofilm with Fe-2.5 mg/l generated a stretch for carboxylic acids with a spike at 3271.94 cm^- with 97% transmittance. It also exhibited bends of alkenes and C-H bonding at 1629 cm^- and 1531.03 cm^- and medium to small scissoring bends of NH_2 bonding with corresponding percentage transmittance in the range of 94% to 100%. This biofilm incubated with Fe^{3+} demonstrated more production of proteinaceous components in its spectrum.

The spectrum of Fe-6.5 mg/l test was observed with thin pointed bend in the left of spectrum region with 90% transmittance indicating carboxylic acid production at 3237.38 cm^-. Narrowly pointed transmittance bends at 1644.38 cm^- and 1636.49 cm^- referred to $–NH_2$ group whereas 1452.19 was indicator of alkane (C-H) bonding along with increasing transmittance from 87% to 93%. The weakest transmittance less than

80% was observed at 1113.73 cm^- linked to C-N, C-C and C-O types of bonding. As compared to the former biofilm, there was predominance of acid, amines and alcoholic functional groups.

At Fe-8.5 mg/l, a wide sharply pointed band at 3272.61 cm^- and a deepest strong, peaked band at 1035.03 cm^- (81% transmittance) were attributed to carboxylic acid and C-O-C bonding of ethers and esters.

In comparison to Fe supplemented biofilms, very different IR spectra patterns were developed from control biofilm. The peaks appeared at 3276.45 cm^-, 1452.90 cm^- and 1049.94 cm^- that were ascribed to C=O-OH, (sp^3) C-H bonding of alkanes and C-O-C groups of ethers and esters. The upshots were an indicative of great variation in biofilm structural components on TR material under varying ferric hydroxide concentrations.

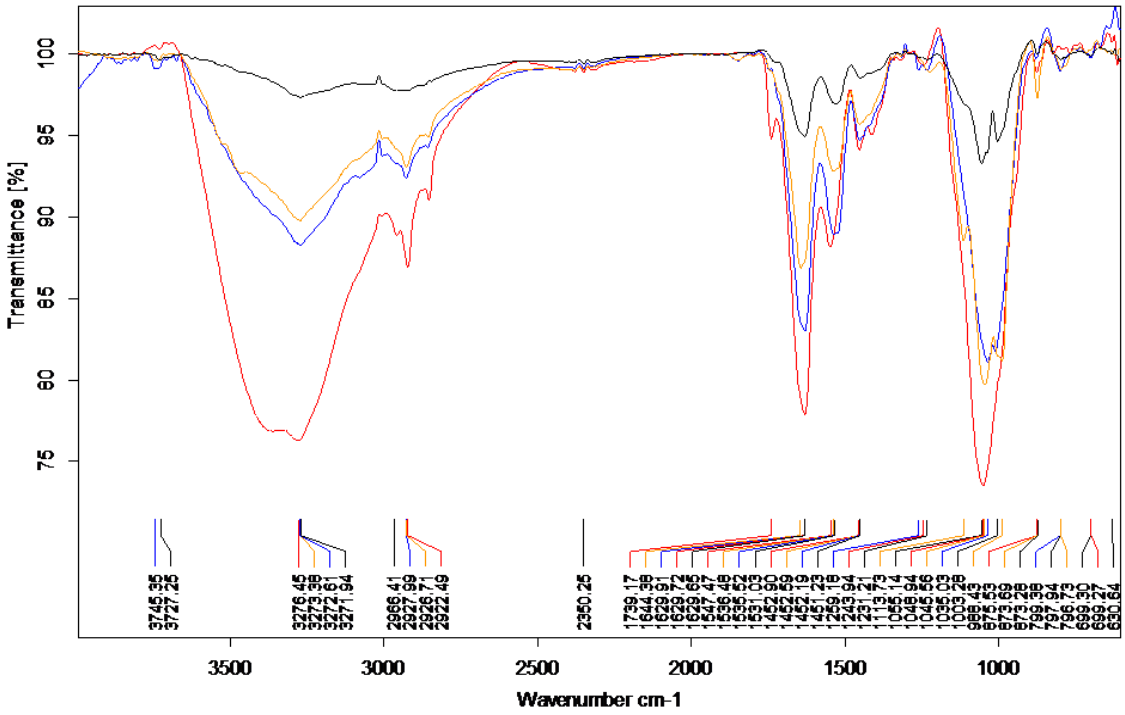

Figure 4.30. FTIR spectra of extracellular polymeric substance (EPS) from biofilms developed on Tire Rubber (TR) at different Fe(III) concentrations. (Black: Fe-2.5 mg/l, Yellow: Fe-6.5, Blue: Fe-8.5, Red: Control)

4.8.1.3. Extracellular Polymeric Substance (EPS) of Biofilms on Stainless Steel (SS)

The biofilm on stainless steel from control reactor displayed small tethering bends at the left upper portion of spectrum revealing the presence of amines with 98%

transmittance whereas medium to small sized vibrational stretches at the right side of IR spectrum specified C-C and C-O groups at 1057.08 cm^{-}. Average percentage transmittance of Fe^{3+} 2.5 test biofilm was greater according to the spectrum than in control. Almost all bends appeared at the same locations as they were found in control biofilm IR spectrum.

The spectrum of Fe-6.5 mg/l biofilm showed one strong and wide bend at 3271.47 cm^{-} wavenumber for the existence of carboxylic acid radicals with scissoring bends in the range of 1645.68 cm^{-}-1452.26 cm^{-} related to aliphatic unsaturated and saturated groups i.e. alkenes (C=C) and alkanes (C-H).The spectrum of Fe-8.5 mg/l biofilm was very similar to the spectrum at lower Fe^{3+} 6.5 mg/l concentration except the difference of % transmittance that was 3-5% higher at 6.5 mg/l than at 8.5 mg/l. The % transmittance reached to the lowest at 6.5 mg/l Fe^{3+} concentration in stainless steel biofilm indicating the highest saturation in biofilm incubated with Fe^{3+} 6.5 mg/l content in the reactor is due to excessive production of alkanes, alkenes and carboxylic acids.

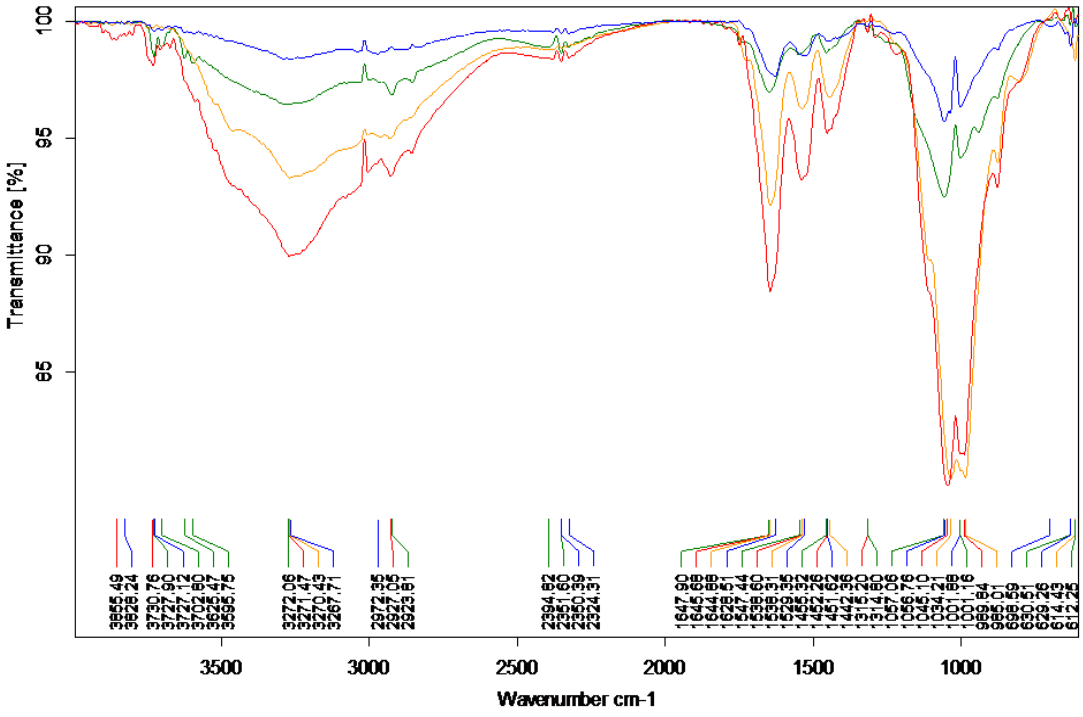

Figure 4.31. FTIR spectra of extracellular polymeric substance (EPS) from biofilms developed on Stainless steel at different Fe(III) concentrations. (Blue: Fe 2.5 mg/l, Red: Fe 6.5 mg/l, Yellow: Fe-8.5 mg/l, Green: control)

4.8.1.4. Extracellular Polymeric Substance (EPS) of Biofilms on Iron

The presence of alcoholic groups, carboxylic groups, alkenes and alkanes was predicted from the spectra of all biofilms scrapped from iron as a support material. All IR spectra were alike except the difference of % transmittance that was found highest (91-100%) at the lowest added Fe^{3+} concentration.

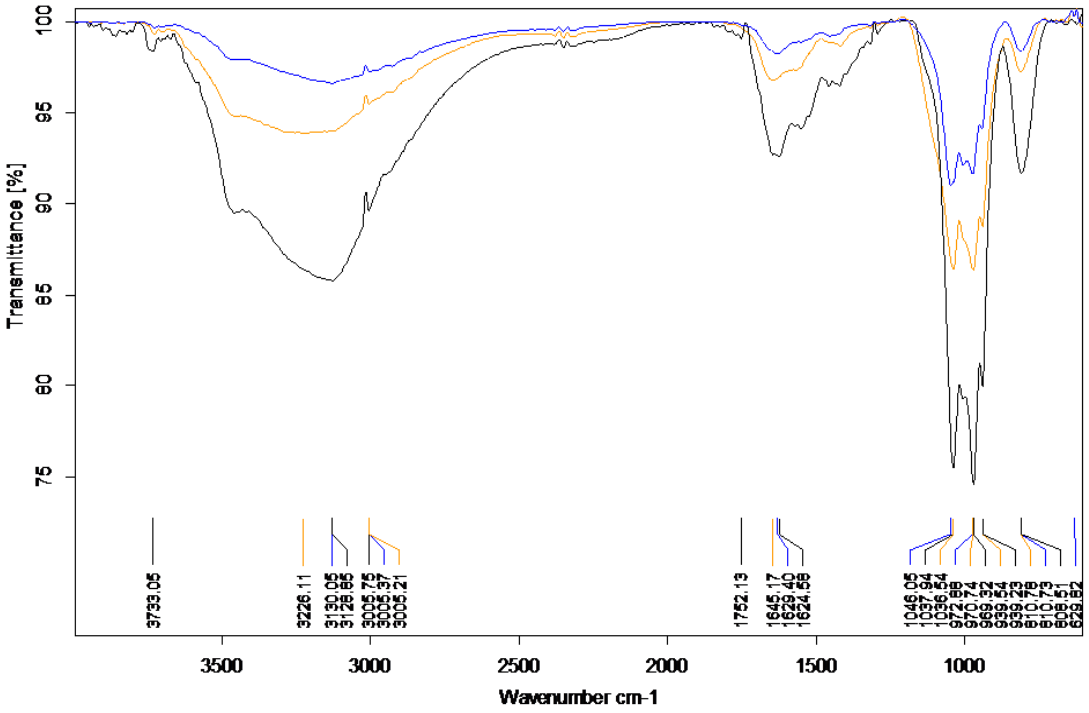

Figure 4.32. FTIR spectra of extracellular polymeric substance (EPS) from biofilms developed on iron at different Fe(III) concentrations. (Blue: Fe-2.5, Black: Fe-6.5, Yellow: Control)

4.8.1.5. Extracellular Polymeric Substance (EPS) of Biofilms on Polyvinyl Chloride (PVC)

EPS of all biofilms developed on a range of Fe^{3+} concentrations including the control, showed a broad and strong band in an area ranging from 3384.2 cm^{-}-3270.49 cm^{-} wavenumber presenting the carboxylic acid production with different levels of transmittance percentage. The maximum % transmission was observed at Fe-6.5 mg/l concentration. Small to medium scissoring, stretching and sharp vibrational bends in the rest of spectrum demonstrated presence of C=O (aldehydes), C-O-C (ethers and esters) and C-H (alkanes).

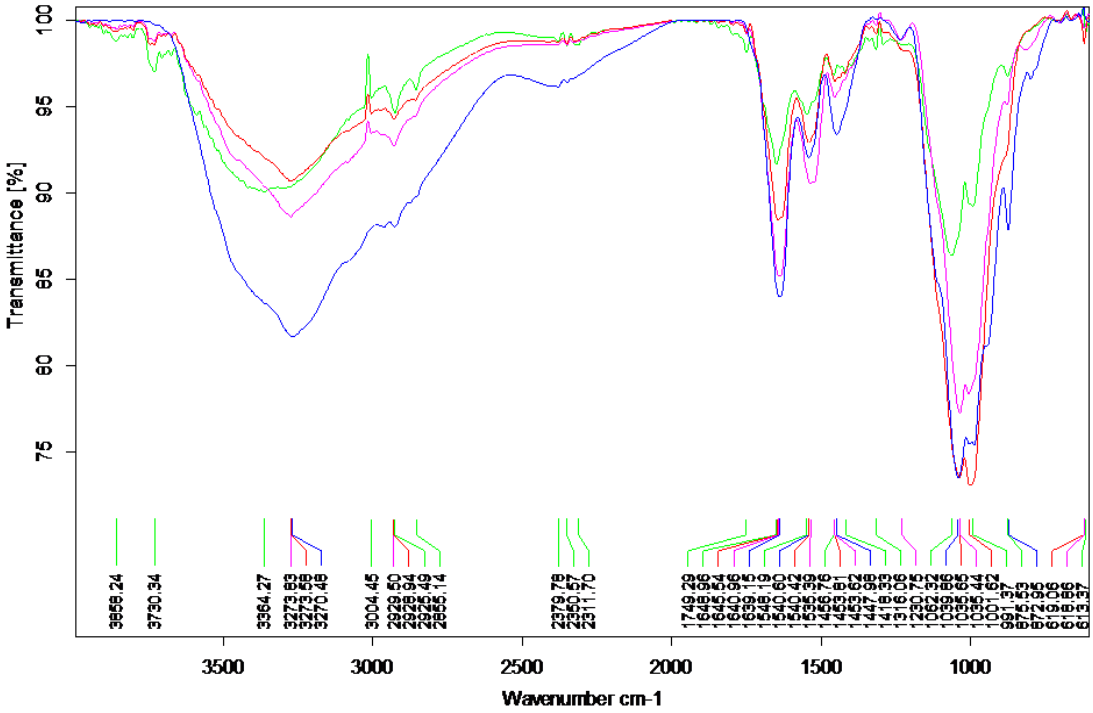

Figure 4.33. FTIR spectra of extracellular polymeric substance (EPS) from biofilms developed on PVC at different Fe(III) concentrations. (Blue: Fe-2.5 mg/l, Red: Fe-6.5 mg/l, Purple: Fe-8.5 mg/l, Green: Control)

FTIR finding revealed the molecular scale impact of growing biofilms on different support materials and supplementing with ferric iron as a nutrient and electron acceptor on their structural and architectural components of EPS of biofilms grown on different attachment surfaces. Abundance of functional groups in varying fractions in EPS of different biofilms gives also a clue to varying contents of their respective cellular moieties e.g. lipids, proteins, saccharides and glycerol.

4.9. Surface Characterization of Biofilms Developed on Various Support Materials under Varying Fe(III) Concentrations in Aerobic Batch Biofilm Reactors (ABBR) by Scanning Electron Microscope (SEM)

To estimate the impact of ferric iron supplementation with respect to substratum on biofilms, scanning electron microscope (SEM) images of biofilms developed on Polyvinyl chloride (PVC) and Tire rubber (TR) incubated with Fe-8.5 mg/l concentrations and without supplementation of ferric iron (control) scanned by JEOL (JSM-6490A) SEM are shown below.

4.9.1. Surface Morphology of Biofilms Developed on Polyvinyl Chloride (PVC) without Treatment and Treatment with Fe-8.5 mg/l

Figure 4.34. Biofilms on Polyvinyl chloride (PVC) and tire rubber (TR) (left; before scanning electron microscopy on stud, right; biofilm samples inside ion sputtering device for gold deposition on the surface of biofilms

The biofilm covered whole surface of PVC plastic material incubated at Fe-8.5 mg/l concentration with irregular thick and thin areas (X100). PVC control biofilm also covered whole surface but was found comparatively smoother than biofilm cover at Fe-8.5 mg/l further confirming heterogeneous nature of biofilms. Voids and channels were clearly obvious in both Fe-8.5 mg/l PVC and PVC control biofilms at X1,000. At Fe-8.5 mg/l, small and large rod shaped bacteria, diatoms, chains and clusters of cocci, coccobacilli, spiral shaped bacteria, yeasts and filamentous bacteria attached to the plastic surface individually and in clusters associated with microcolonies were observed at X10,000 and X20,000. In control, cocci and rod shaped bacilli were also present but bacilli predominated. One bacterium seemed Gallionella, an iron oxidizing bacterium, based on its typical stalked structure and morphology and previous reports yet this identification may be poor.

4.9.1.1. Biofilm on Polyvinyl chloride (PVC) Treated with Fe-8.5 mg/l

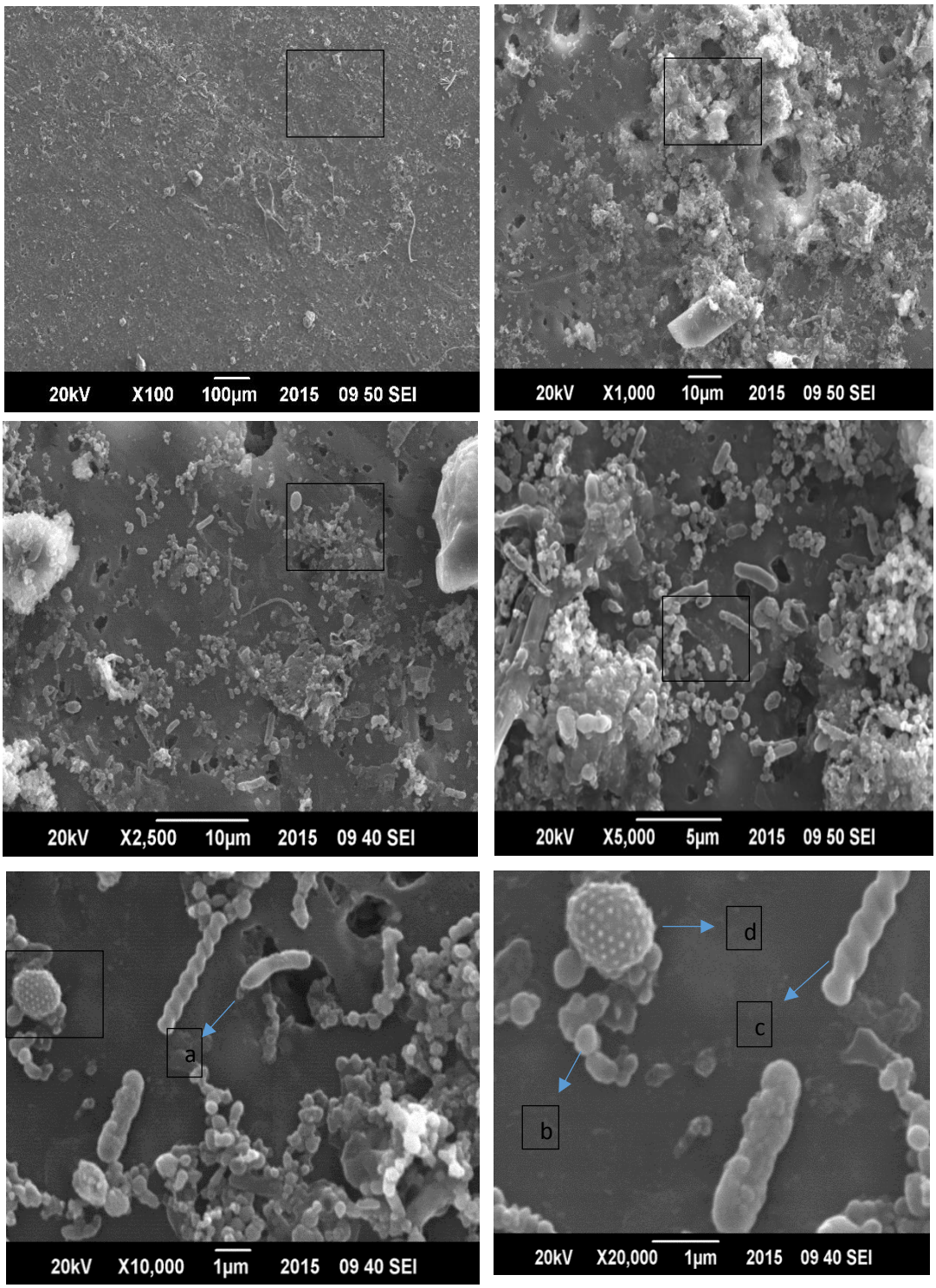

Figure 4.35. Scanning electron micrographs of biofilms developed on Polyvinyl chloride (PVC) in aerobic batch biofilm reactor (ABBR) supplemented with Fe-8.5 mg/l at X100, X1,000, X25,00, X5,000, X10,000 and X20,000. Blank squares indicate the area magnified at next higher resolution. a; rod, b; coccus, c; spiral, d; may be a diatom

4.9.1.2. Biofilm on Polyvinyl chloride (PVC) without Treatment

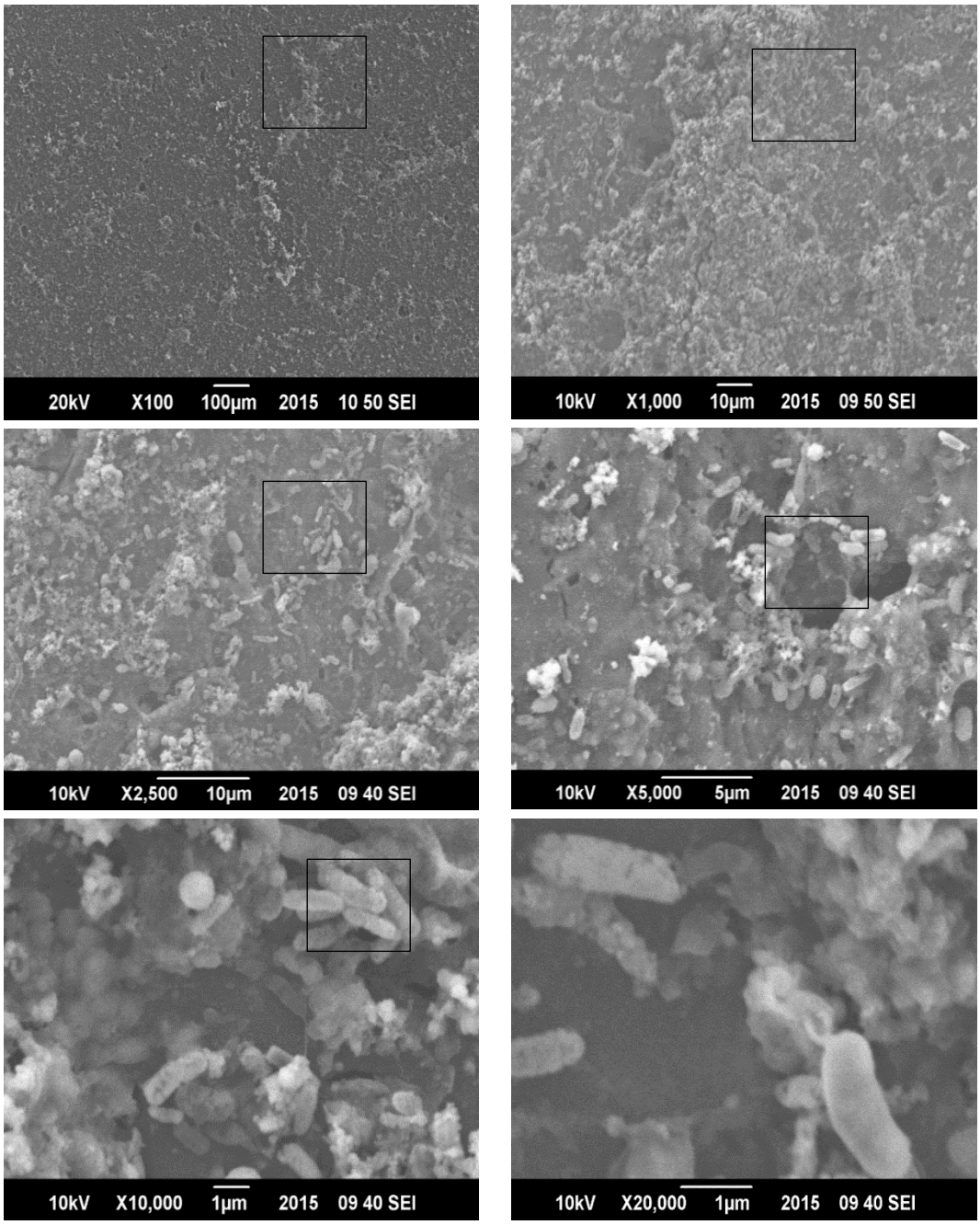

Figure 4.36. Scanning electron micrographs of biofilms developed on polyvinyl chloride (PVC) in control aerobic batch biofilm reactor (ABBR) with no addition of Fe(III) at X100, X1,000, X25,00, X5,000, X10,000 and X20,000. Blank squares indicate the area magnified at next higher resolution.

4.9.2. Surface Morphology of Biofilms Developed on Tire Rubber (TR) without Treatment and Treatment with Fe-8.5 mg/l

At X100, surface morphology of biofilm was visualized as irregular, uneven covering over whole areas with crevices, furrows, grooves and small flocs on it in Fe-8.5 tire rubber (TR) biofilm. Biofilm cover on TR in untreated reactor, on the other hand, was found patchy and irregular with several small and large granules over its surface. Rod shaped bacteria were found attached on rubber surface and associated with microcolonies that ranged in cellular diameter from 1.36 µm to 1.93 µm while size of cocci bacteria was in the range of 80.62 nm to 139.28 nm at X20,000 magnification. Control TR biofilm contained several rosette shaped filamentous organisms and innumerable rods and cocci. Size of bacilli was found upto 730.62 nm in diameter and 1.84 nm in length. Characteristic bacteria with tufts of flagella around their all sides (peritrichous) were detected. Cells were embedded within abundant extra polymeric matrix evident at X25,00, X5,000 and X10,000 in both types of biofilms. Electron micrographs showed greater microbial diversity in control biofilm on TR compared to at 8.5 mg/l yet there was no significant difference of EPS contents between the two biofilms.

The analysis of electron micrographs revealed the heterogeneous nature of biofilm surfaces. Biofilm morphology and texture was related to the prevailing conditions employed during biofilm establishment such as nutrients, type of attachment material, pH and temperature.

4.9.2.1. Biofilm on Tire Rubber (TR) Treated with Fe-8.5 mg/l

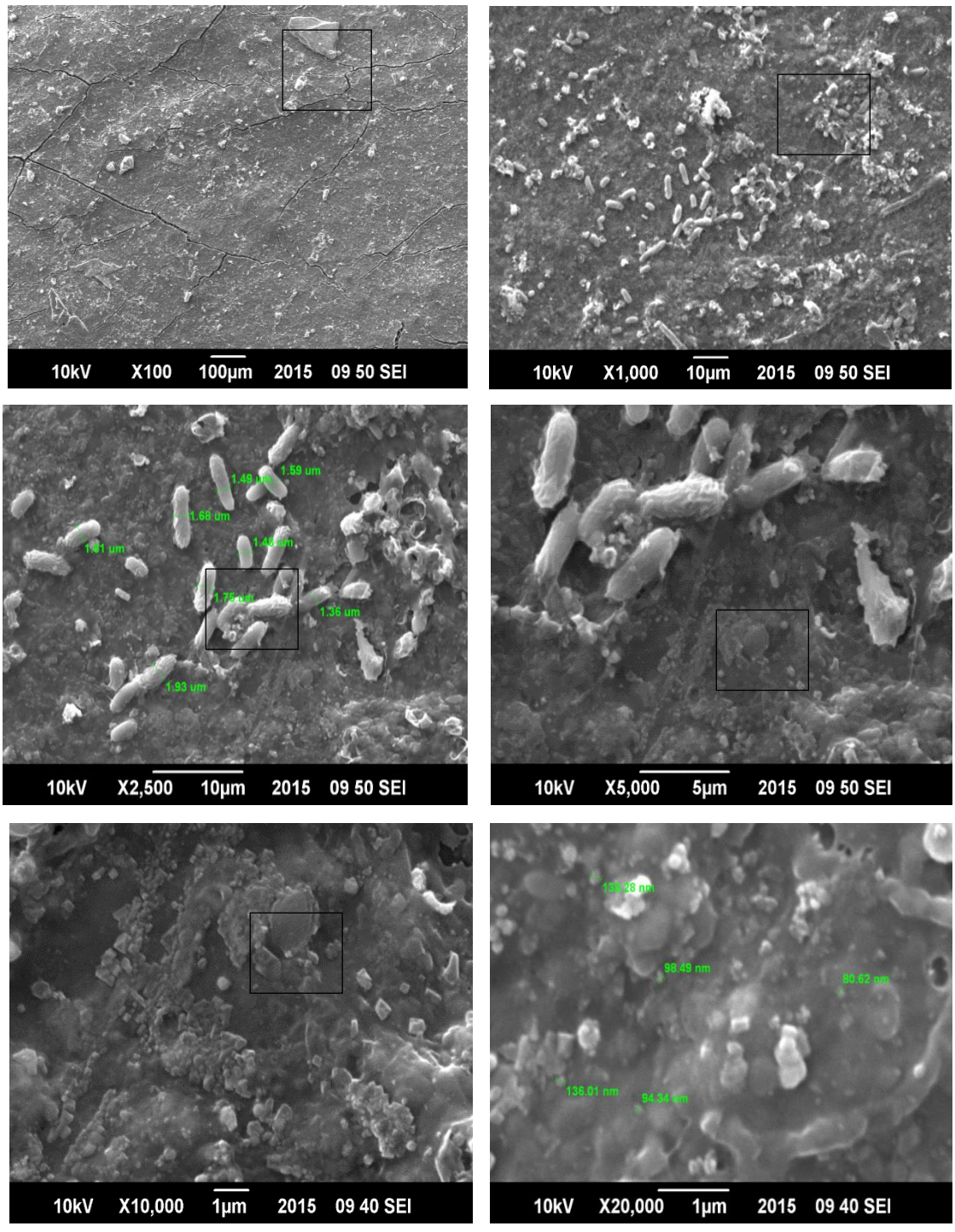

Figure 4.37. Scanning electron micrographs of biofilms developed on tire rubber (TR) in aerobic batch biofilm reactor (ABBR) supplemented with Fe-8.5 mg/l at X100, X1,000, X25,00, X5,000, X10,000 and X20,000. Blank squares indicate the area magnified at next higher resolution

4.9.2.2. Biofilm on Tire Rubber (TR) without Treatment

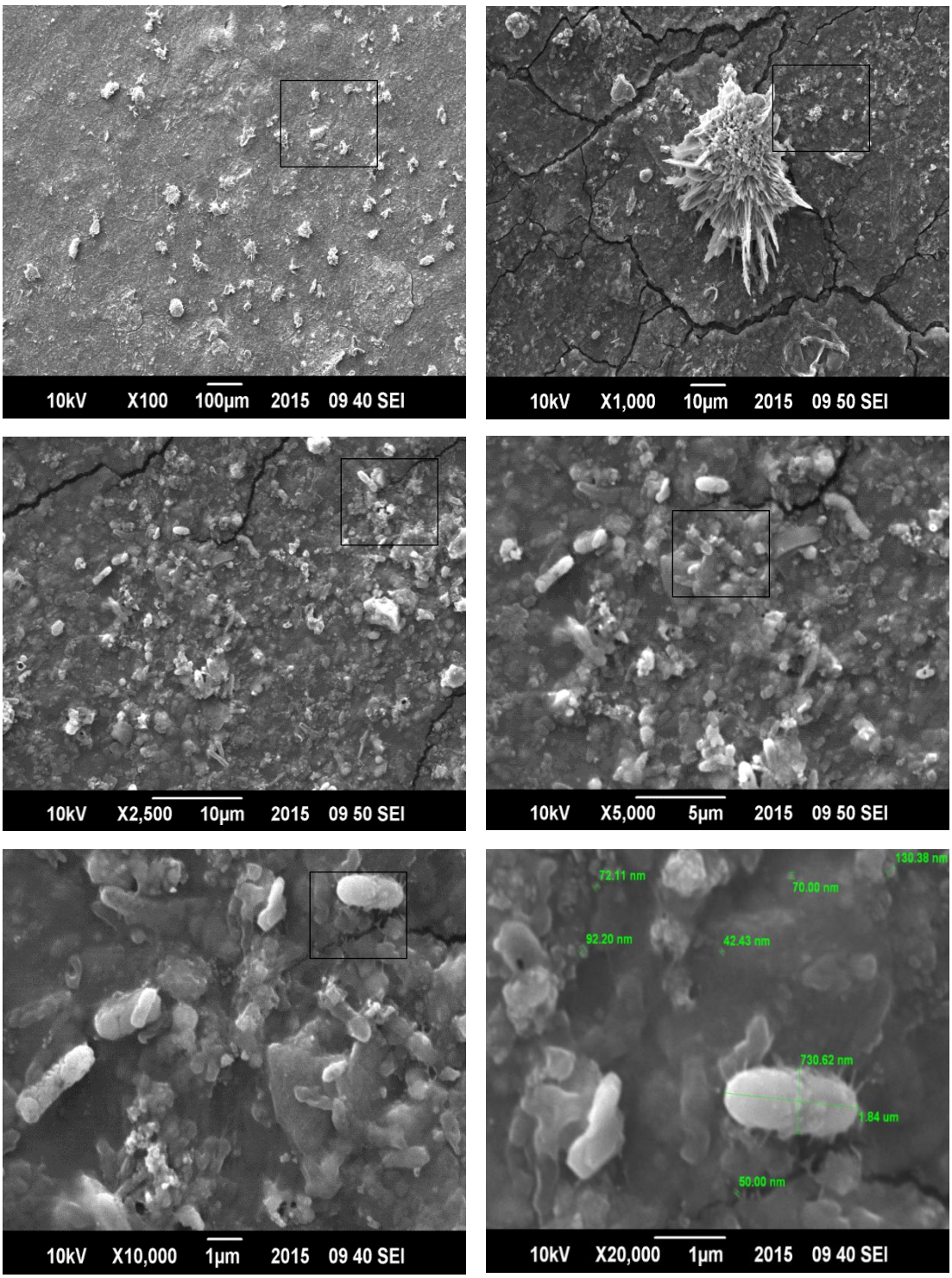

Figure 4.38. Scanning electron micrographs of biofilms developed on tire rubber (TR) in control aerobic batch biofilm reactor (ABBR) with no supplementation of Fe(III) at X100, X1,000, X25,00, X5,000, X10,000 and X20,000. Blank squares indicate the area magnified at next higher resolution.

4.10. Fluorescence *in situ* Hybridization (FISH) and Confocal Laser Scanning Microscopy (CSLM) of Surface Attached Bacteria in Biofilms

Conventional cultivation-based methods to measure microbial abundance are unsuitable for quantifying uncultured microorganisms that constitute the majority of microbial life in most environmental or medical samples. This problem is solved by the quantification approach applied here, which combines fluorescence *in situ* hybridization (FISH) with rRNA-targeted oligonucleotide probes and digital image analysis.

The presence, cellular counts per cm^2 of the attachment surface, spatial organization, stratification patterns of the target bacteria, bio volume fraction, spatial arrangement analysis and structure of biofilms were investigated by FISH with 5' end (5, 6-fluorescein isothiocyanate, FLUOS) fluorescently labelled phylogenetic oligonucleotide probes EUBI, EUBII, EUBIII, Bet42 and Gam42 specific for all eubacteria, β and γ proteobacteria, respectively**,** according to previously described protocols. (8), (9)

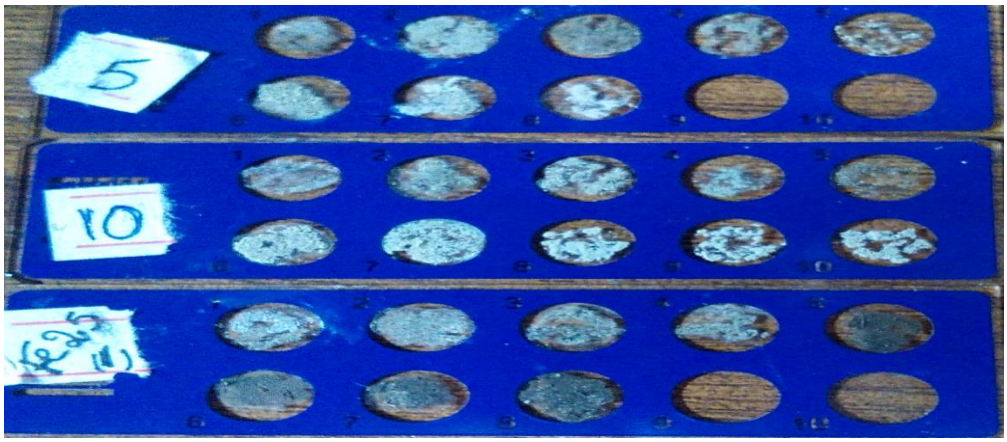

Figure 4.39. Teflon coated ten well glass slides after fixation of biofilms developed on different support materials under varying Fe(III) concentrations.

4.10.1. Automated Slicing, Identification, Quantification and Spatial Distribution Analysis of Biofilms by Digital Image Analysis

Systematic collection of high resolution, two dimensional optical sections of biofilms scanned with Confocal laser scanning microscope (CLSM) equipped with multi Argon filters, at a distance of 1.14 µm and their digital analysis demonstrated the efficiency of fluorescently labelled oligonucleotide probes and that they were permeable to target groups of bacteria (eubacteria, β and ϒ) (8).

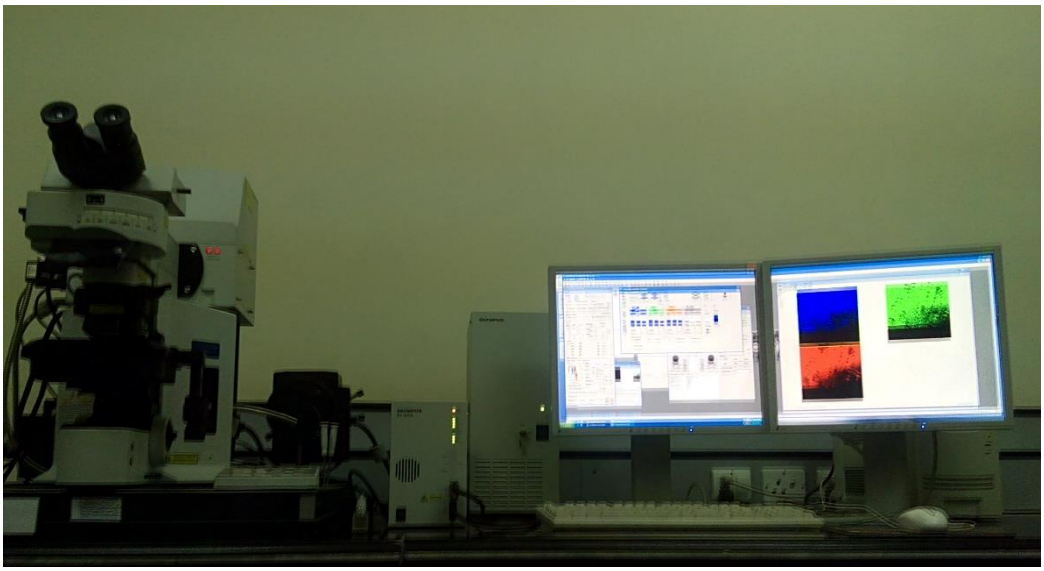

Figure 4.40. Fluo *View*™ (*Fv*1000) Confocal laser scanning microscope (CLSM) used for optical sectioning of biofilms for eubacteria, beta and gamma proteobacteria developed on different carrier materials under varying Fe(III) concentrations

4.10.2. Use of Reference Cells and FISH Optimization

In order to carry out the optimization of the FISH technique, *Pseudomonas aeruginosa* (ATCC ® 9027™) and pure *Bacillus subtilis* (accession number: KJ600795) strains were deposited as negative and positive internal controls for ϒ and β populations of bacteria on the starting wells of ten well glass slides that gave FISH results accordingly. Negative control gave no signal when scanned with CLSM whereas pure cultures of *Pseudomonas aeruginosa* and *Bacillus subtilis* strains when applied with EUB probe(s) individually and in combination with β and ϒ probes gave strong fluorescence signals indicating the functionality of the phylogenetic probes. All

biofilm samples demonstrated positive hybridization results with the probe EUB-338 (I, II,III), Bet42 and Gam42.The results were considered as positive that gave good signals with target cells. The results revealed the potential of this technique as a rapid screening method for bacterial identification and quantification. In the conventional identification of bacteria, time consuming series of physiological and biochemical tests are necessary, the identification of isolated bacteria using FISH and molecular phylogenetic probes targeting 16S- or 23S-rRNA is rapid (Bhavanath *et al.*, 2009).

4.10.3. Biofilms Developed on Tire Rubber (TR) at Different Concentrations of Fe(III) in Aerobic Batch Biofilm Reactors (ABBRs)

The structure and porosity of test biofilms differed considerably than the biofilms developed on tire rubber (TR) in untreated aerobic batch biofilm reactor (ABBR) depending on substrate gradient within the biofilms. It was not easy to distinguish growth from attachment of cells. However, it may be possible that dark areas in the images representing voids with rough surfaces were filled with deposited cells. Optical sections of biofilms from control reactor showed higher cell counts in the sections from upper biofilm yet comparatively lesser than in test biofilm. Images from lower parts of biofilms showed more porosity. The presence of different cell densities was an indication of different growth rates of microorganisms on the surface under varied Fe^{3+} concentration. Such differences in the biofilm structures shed information about their development along axis. There were more surface irregularities in test biofilms than in control indicating their structural heterogeneity. Hybridization experiments with FLUOS labelled phylogenetic probes showed the presence of small and large bacterial rods and cocci in isolated as well as in aggregates and microcolonies.

In compact portions of biofilms where porosity was low, the target bacteria were found restricted to the surface areas of biofilm. In contrast, when the microstructure of biofilm was loose, they were located in the interior of biofilm indicating the ecological interactions of bacteria as an integral part of their survival mechanism. Higher substrate_concentration results in higher fluxes for biofilm growth. Ample nutrients availability lead to less porous microstructure of biofilm with higher cellular density and low substrate availability made it highly porous with retarded growth.

Visual observations of biofilms were in agreement with predictive models of Rittmann and Loosdrecht et al.

4.10.3.1. In situ Detection of Total Eubacteria

CLSM imaging coupled with quantification of TR biofilms statistically by the application of digital image analysis in microbial ecology (DAIME) software indicated an increasing trend of eubacterial population with rise in Fe^{3+} concentration. At a magnification of X10, there was a difference of 7.5E+02 cm^{-2} cells from the lowest concentration of Fe^{3+} to the highest concentration with 3.00E+01, 4.40E+01 and 1.05E+02 cells at Fe-2.5 mg/l, Fe-6.5 mg/l and Fe-8.5 mg/l, respectively. Again at 100X, a similar pattern of increase in cellular content was observed with the highest number of eubacteria at Fe-8.5 mg/l i.e. 8.80E+01 cm^{-2} whereas the lowest (4.90E+01 cm^{-2}) was found from control biofilm with no addition of $Fe(OH)_3$ (Table 4.4).

4.10.3.2. In situ Detection of Beta Proteobacteria

FISH combined with CLSM imaging quantification showed the presence of β group of bacteria within the microbial community structure of TR biofilm. At 10X, maximum β proteobacteria cells calculated were found to be 1.42E+02 cm^{-2} of the biofilm surface area at the highest Fe^{3+} concentration with minimum count as 8.10E+01 cm^{-2} with no supplementation of Fe^{3+}. Likewise, at 100X, there was highest number of cells at Fe-8.5 mg/l i.e. 1.80E+02 cm^{-2} of biofilm surface area indicating a linear relationship between the cell density and Ferric iron concentration from 2.5 mg/l to 8.5 mg/l.

4.10.3.3. In situ Detection of Gamma Proteobacteria

In contrary to the total eubacteria and β proteobacteria, ϒ population demonstrated an inverse relationship between the ferric iron concentration and their cell density. The highest ϒ cells were calculated from the biofilm developed at Fe (III)-2.5 mg/l with a measure of cell count as 7.30E+01 cm^{-2} and 2.91E+02 cm^{-2} at 10X and 100X, respectively.

4.10.3.4. Biovolume Fraction

By measuring the areas of probe-labeled biomass in randomly recorded image pairs, an unbiased estimate of the relative biovolume of the population of interest can be obtained. This approach expresses abundance as "biovolume fraction" (relative to the total biovolume of the whole microbial community). This value equals the share of biochemical reaction space occupied by the quantified population and thus can be

more relevant ecologically than absolute cell numbers (e.g. a few large cells can contain the same biovolume as many small cells). Another advantage lies in the complete independence of this method from the morphology of the quantified organisms.

In this study, biovolume fraction as measured by DAIME was found to be 100% in nearly all cases except in case of control reactor biofilm for β population on TR where it was observed to be 101.7% at 10X and 84.9% at 100X magnification. In case of negative control, it was observed as 0%.

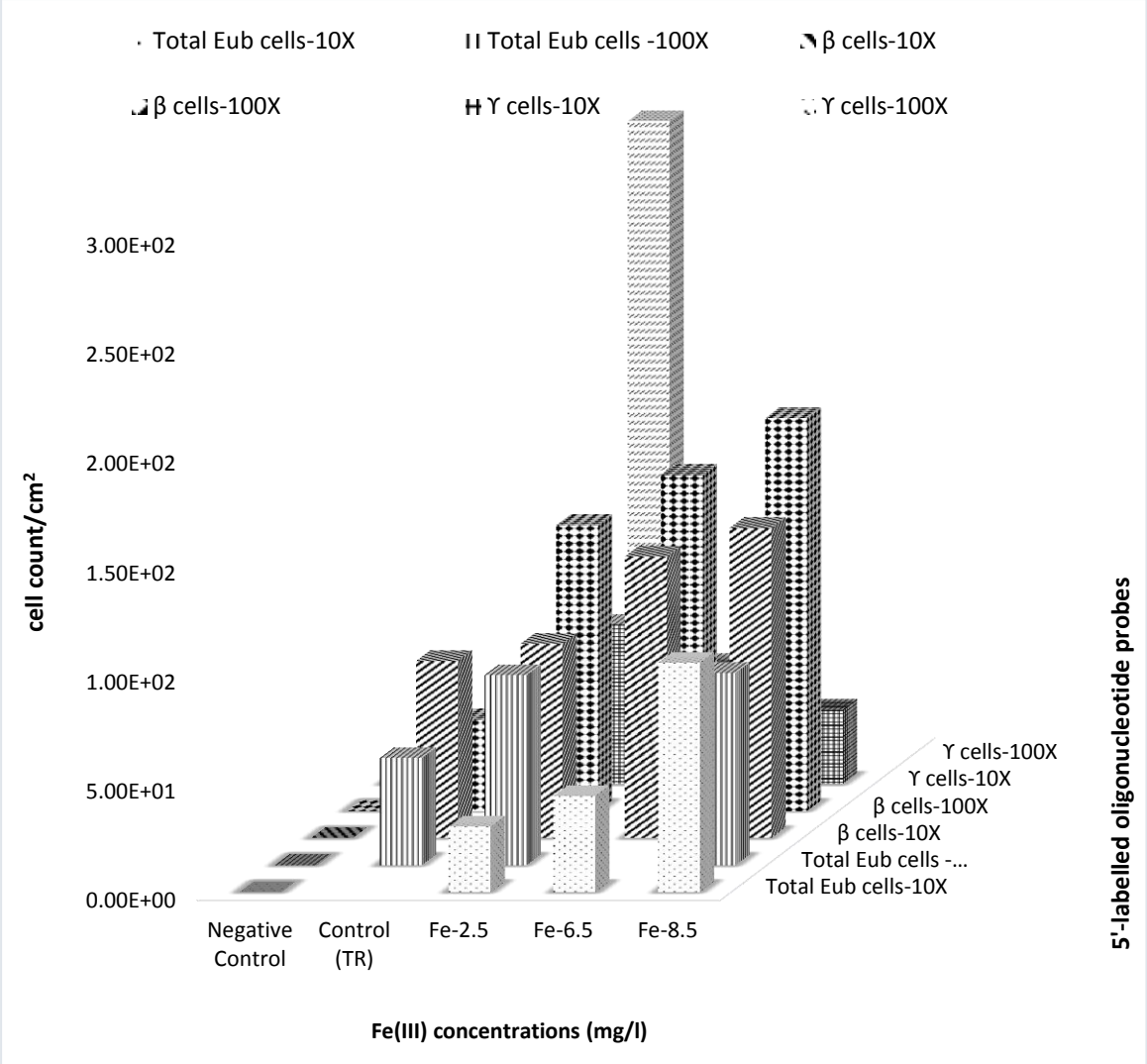

Figure 4.41. Eubacterial, Beta and Gamma proteobacteria cellular count per cm^2 of biofilm developed on tire rubber under various concentrations of Fe(III).

Table 4.4. Quantification of Eubacterial, Beta and Gamma proteobacteria per cm^2 of biofilm developed on tire rubber under various concentrations of Fe(III)

	Total Eub cells-10X	Total Eub cells -100X	β cells-10X	β cells-100X	ϒ cells-10X	ϒ cells-100X
Negative Control	0.00E+00	0.00E+00	0.00E+00	0.00E+00	0.00E+00	0.00E+00
Control (TR)		4.90E+01	8.10E+01	4.20E+01		
Fe-2.5	3.00E+01	8.70E+01	8.90E+01	1.31E+02	**7.30E+01**	**2.91E+02**
Fe-6.5	4.40E+01		1.29E+02	1.54E+02	5.50E+01	3.30E+01
Fe-8.5	**1.05E+02**	**8.80E+01**	**1.42E+02**	**1.80E+02**	3.40E+01	

4.10.3.5. Confocal Laser Scanning Microscopy (CLSM) of in situ Hybridized Biofilms

4.10.3.5.1. CLSM of Negative Control and Reference Bacterial Strain

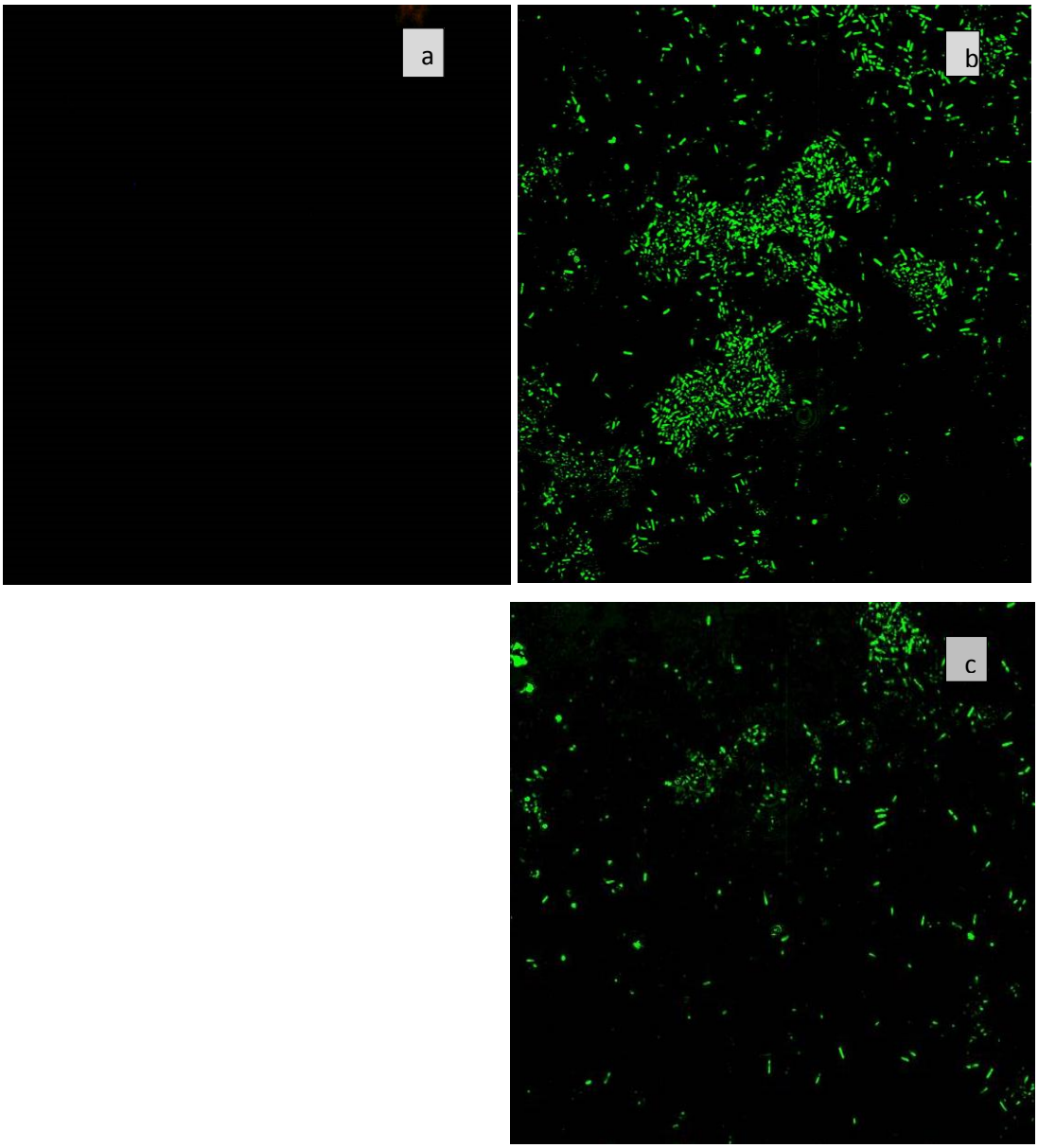

Figure 4.42. CLSM projections of negative control and reference strains after hybridization with 5' end labelled 5, 6- fluorescein isothiocyanate (FLUOS) phylogenetic oligonucleotide probes. (a; negative control showing no binding with mixture of fluorescent probes, b; ATCC 9027 *Pseudomonas aeruginosa* strain exhibiting green fluorescence with mixture of eubacterial probes (EUB I, EUB II, EUB III) at X10, c; ATCC 9027 *Pseudomonas aeruginosa* strain exhibiting green fluorescence with mixture of eubacterial probes (EUB I, EUB II, EUB III) at X100)

4.10.3.5.2. CLSM of Reference Bacterial Strain

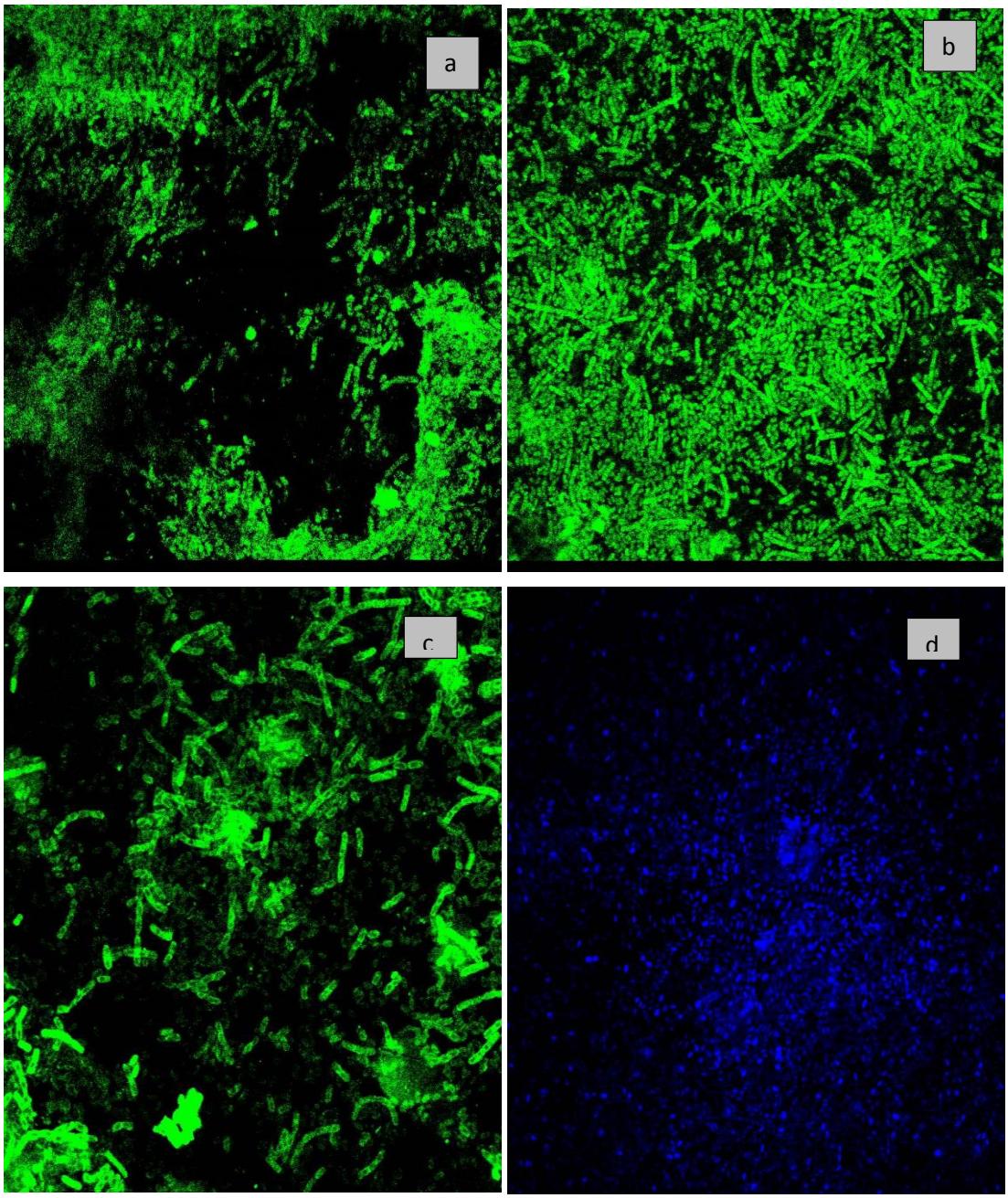

Figure 4.43. CLSM projections of pure *Bacillus subtilis* strain after hybridization with 5' end labelled 5, 6- fluorescein isothiocyanate (FLUOS derivative) phylogenetic oligonucleotide probes at X100. (a; EUB mixture (EUB I, EUB II, EUB III), b; Bet42, c; EUB mixture + Bet42, d; Gam42 scanned using different channels of CLSM)

4.10.3.5.3. CLSM of Biofilm on Tire Rubber (TR) from Control Aerobic Batch Biofilm Reactor (ABBR)

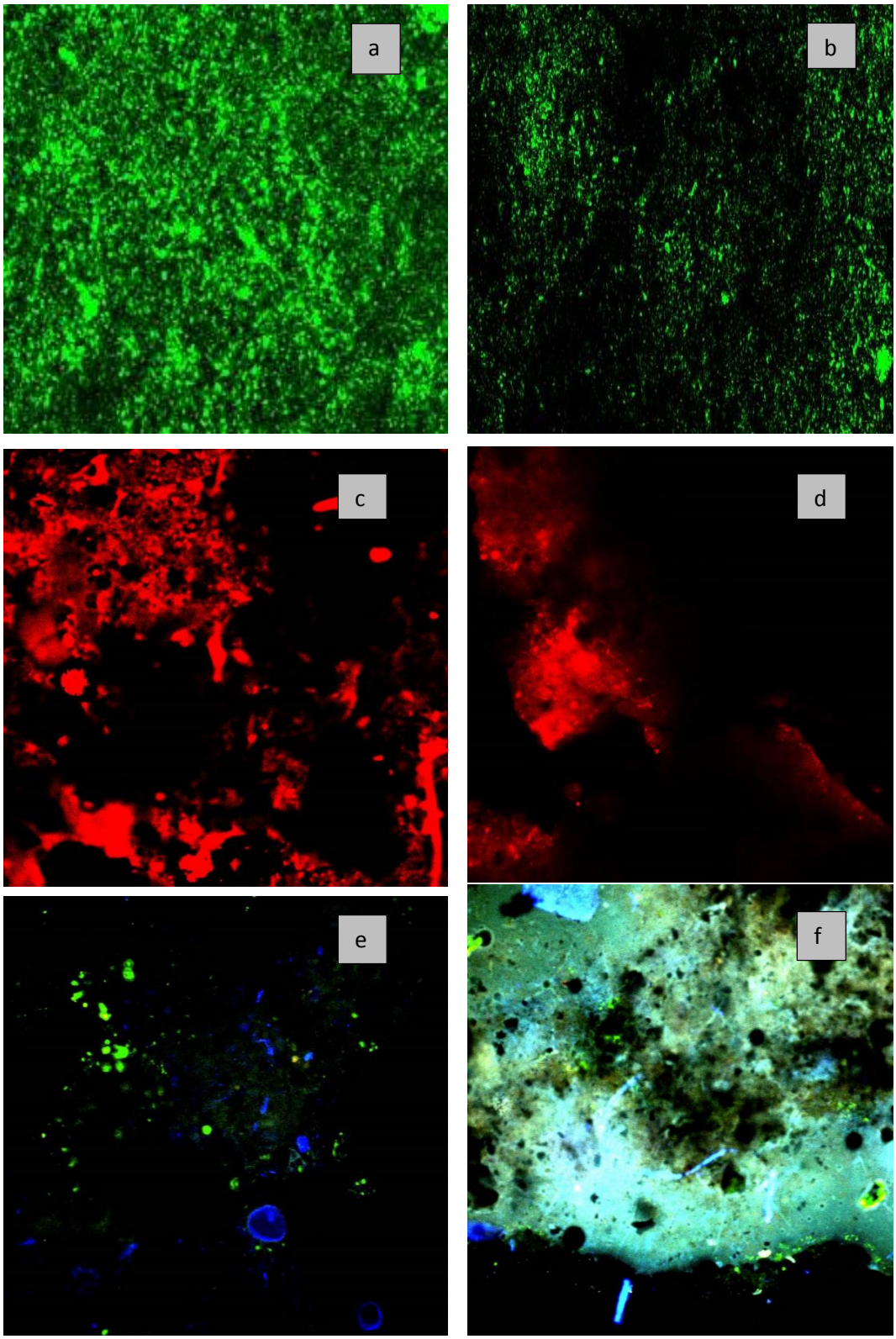

Figure 4.44. CLSM images of biofilm developed on tire rubber (TR) in control aerobic batch biofilm reactor (ABBR) (a-b; EUB mix at 100X from upper and lower depth of biofilm, c-d; Bet42 at 10X and 100X respectively, e-f; Mixed channels at 10x and 100x respectively, yellow signals do not yield from binding of

probes but are the result of overlaying red and green) Background fluorescence was reduced by CLSM technique.

4.10.3.5.4. CLSM of Biofilm on Tire Rubber (TR) at Fe(III)-2.5 mg/l

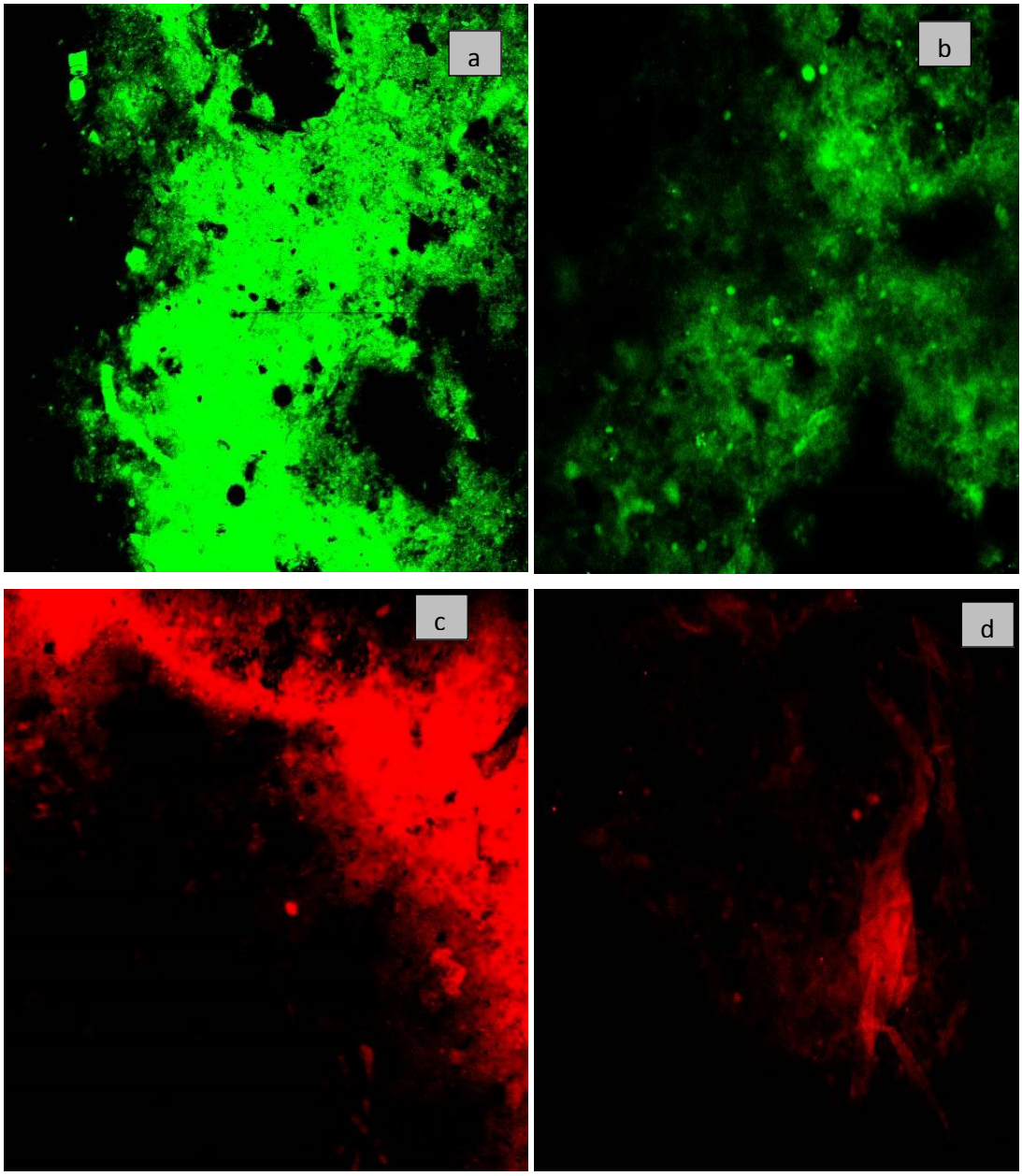

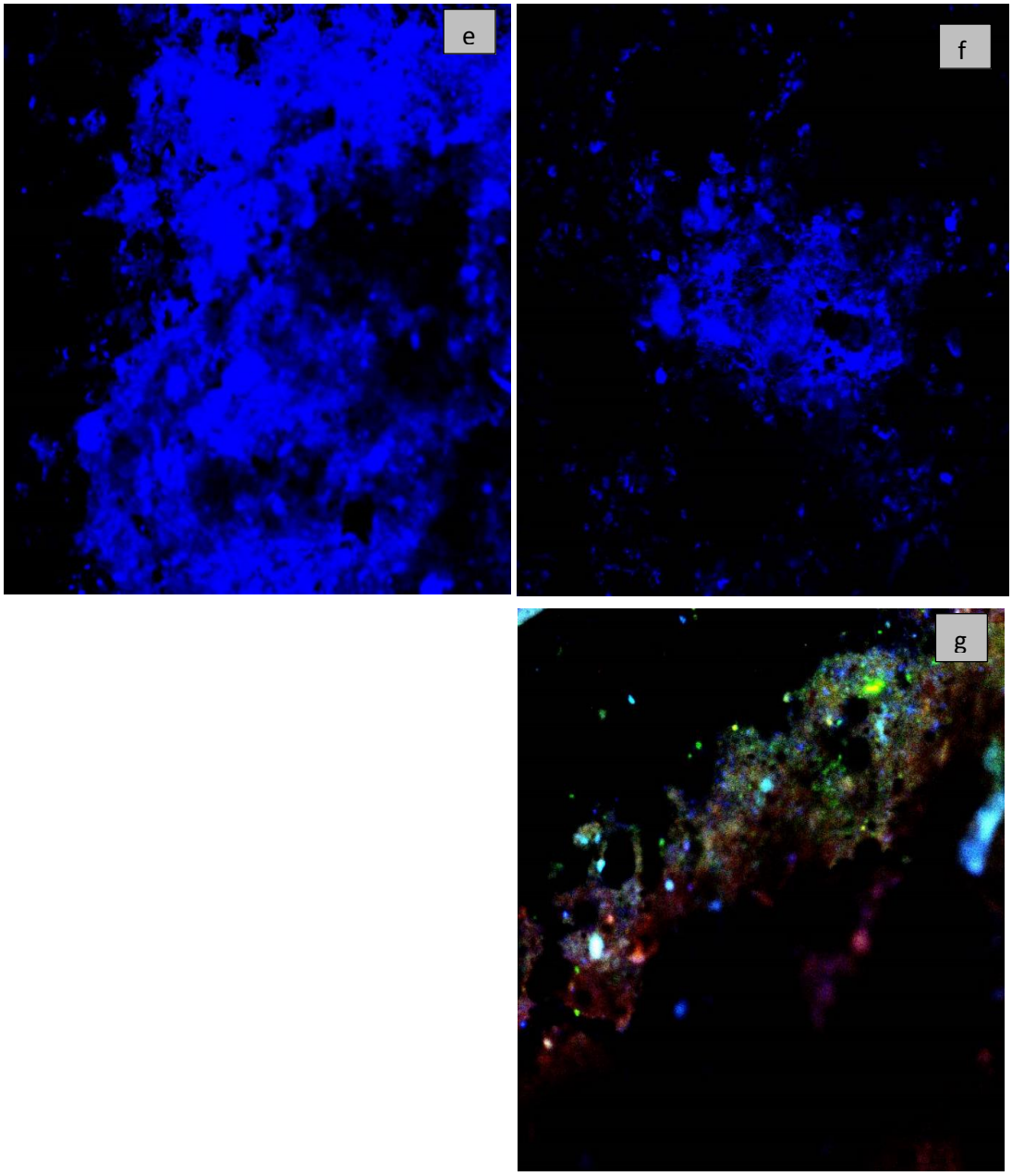

Figure 4.45. CLSM images of biofilm developed on tire rubber (TR) in aerobic batch biofilm reactor (ABBR) at Fe-2.5 mg/l (a-b; with Eubacterial mixture of probes (EUB I, EUB II, EUB III) at10X and 100X respectively , c-d; Bet42 at 10X and 100X respectively, e-f; Gam42 at 10X and 100X respectively, g; Mixed channels at 10X), yellow and pink signals do not yield from binding of probes but are the result of overlaying of images i.e. red and green give yellow, red and white give pink) Background fluorescence was reduced by CLSM technique.

4.10.3.5.5. CLSM of Biofilm on Tire Rubber (TR) at Fe(III)-6.5 mg/l

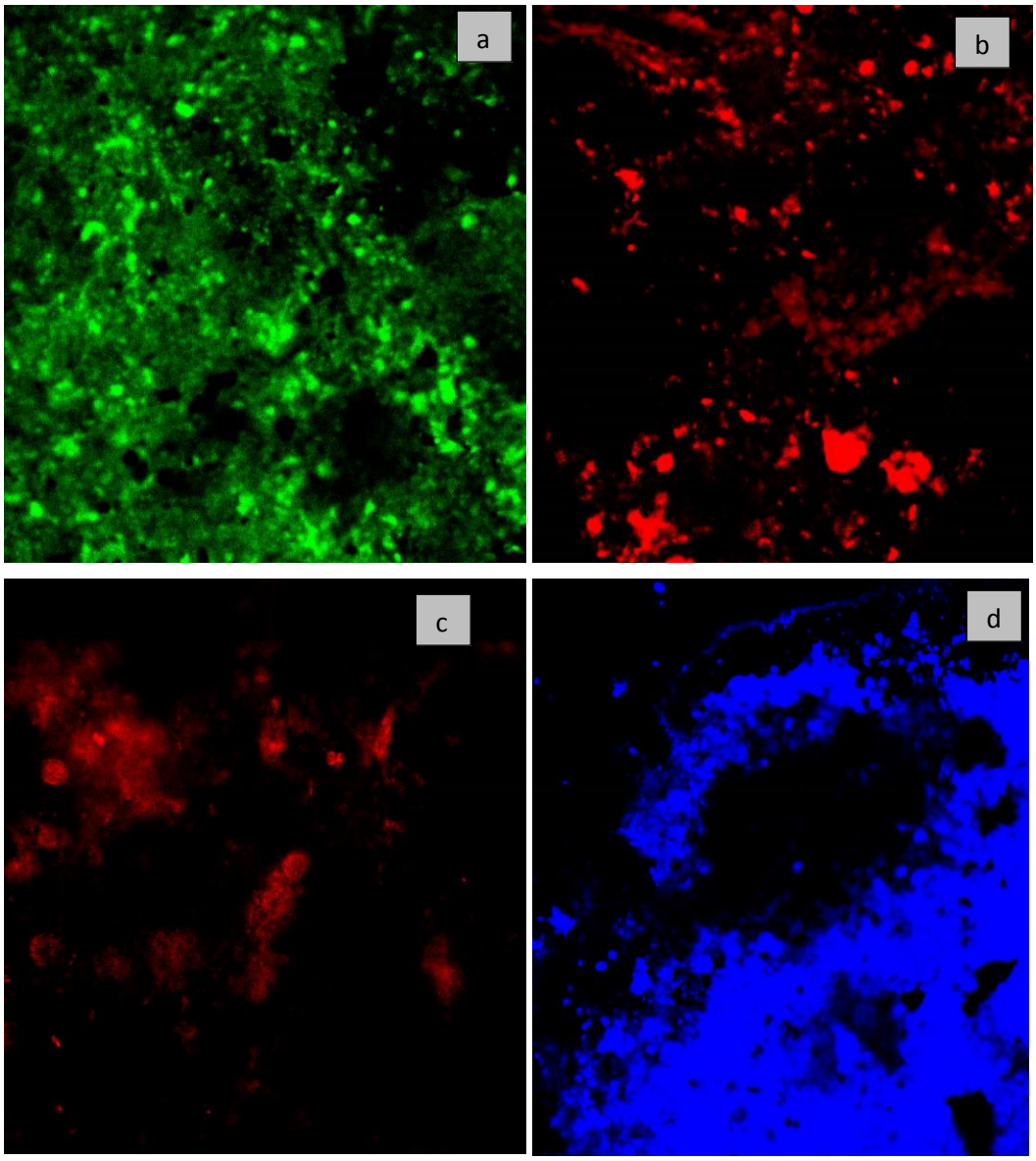

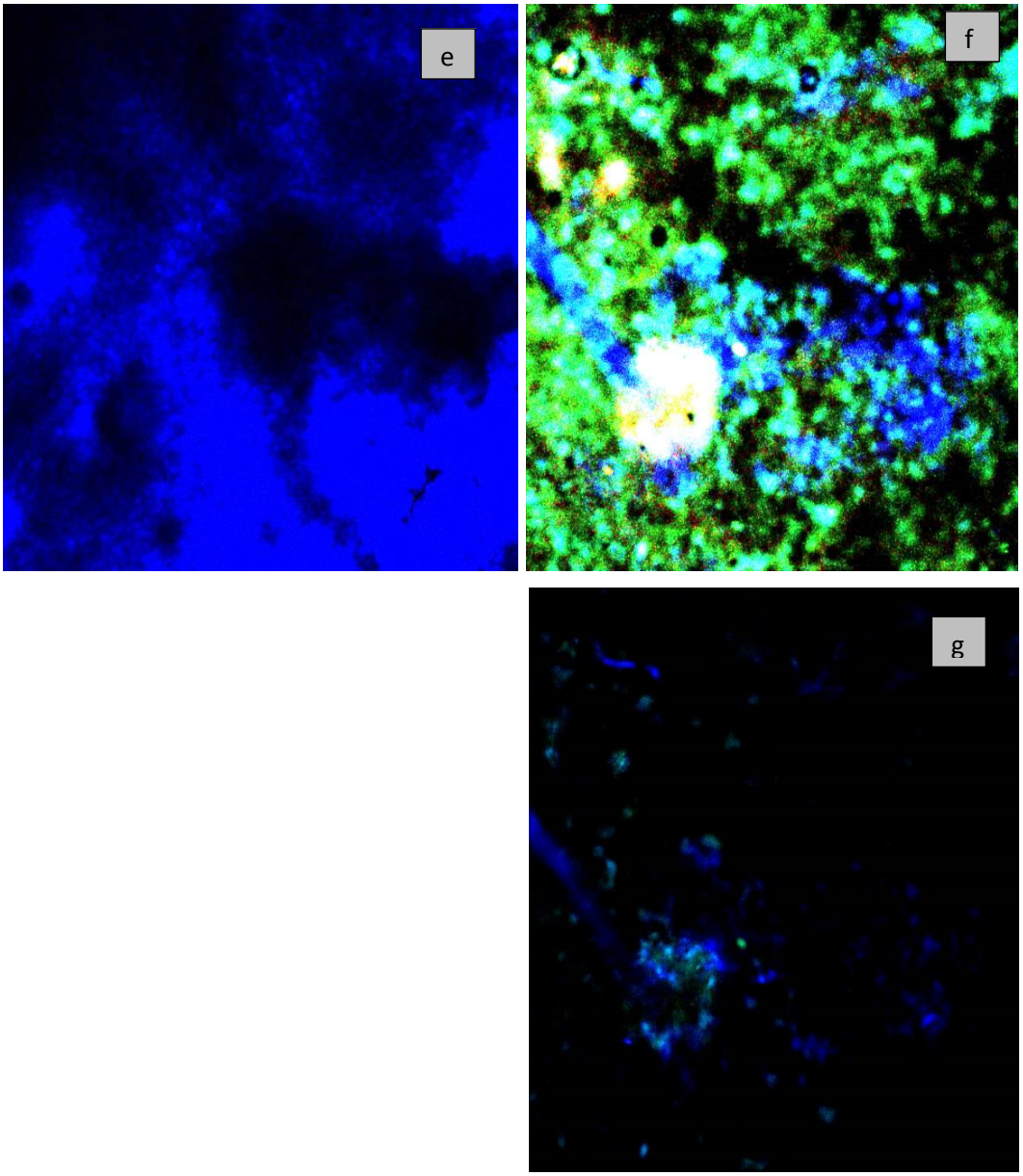

Figure 4.46. CLSM images of biofilm developed on tire rubber (TR) in aerobic batch biofilm reactor (ABBR) at Fe-6.5 mg/l (a; with Eubacterial mixture of probes (EUB I, EUB II, EUB III) at X10, b-c; Bet42 at X10 and X100, respectively, d-e; Gam42 at 1X0 and X100, respectively, f- g; Mixed populations at 10X and 100x, respectively), yellow signals do not yield from binding of probes but are the result of overlaying red and green. Background fluorescence was reduced by CLSM technique.

4.10.3.5.6. CLSM of Biofilm on Tire Rubber (TR) at Fe(III)-8.5 mg/l

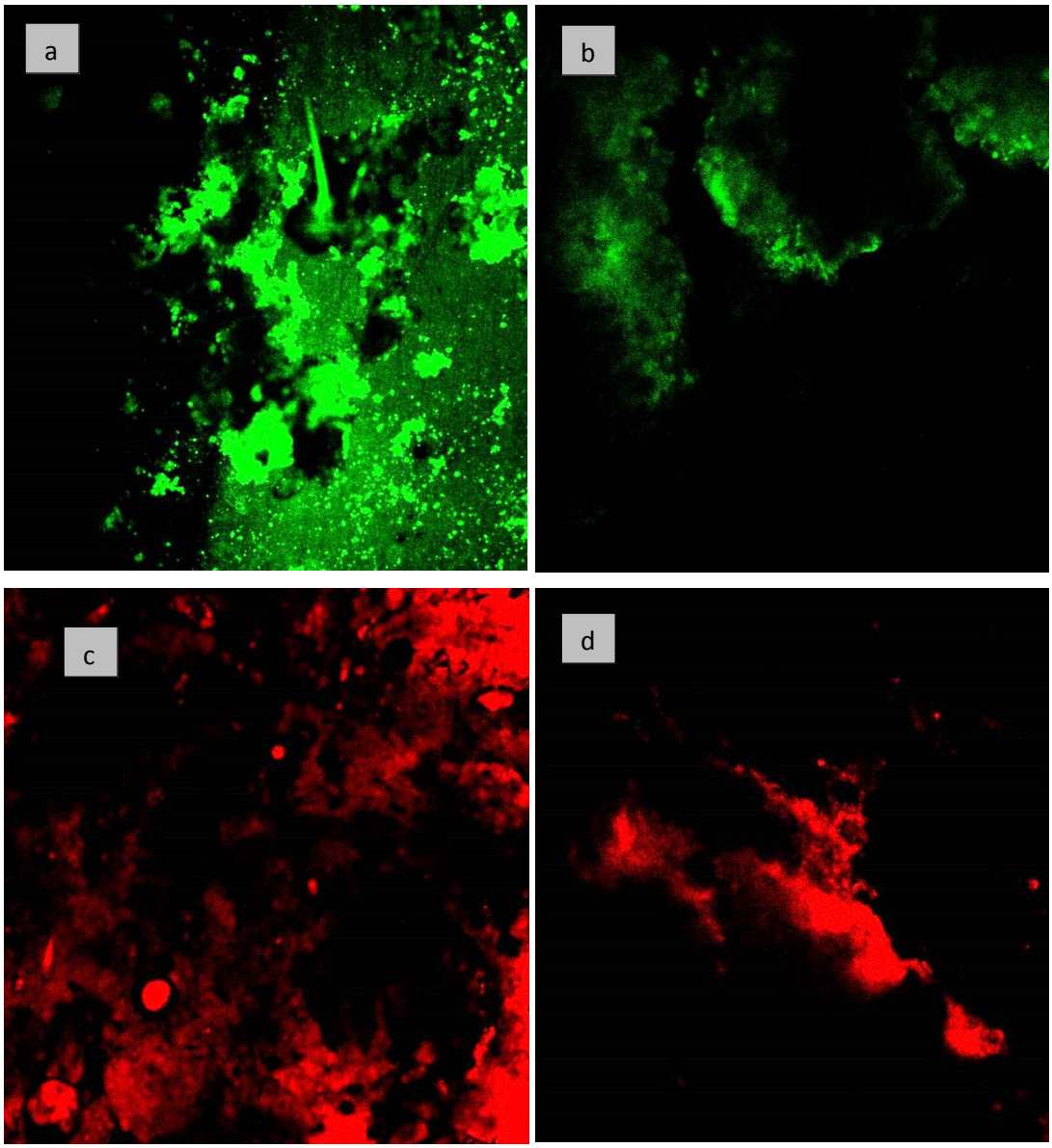

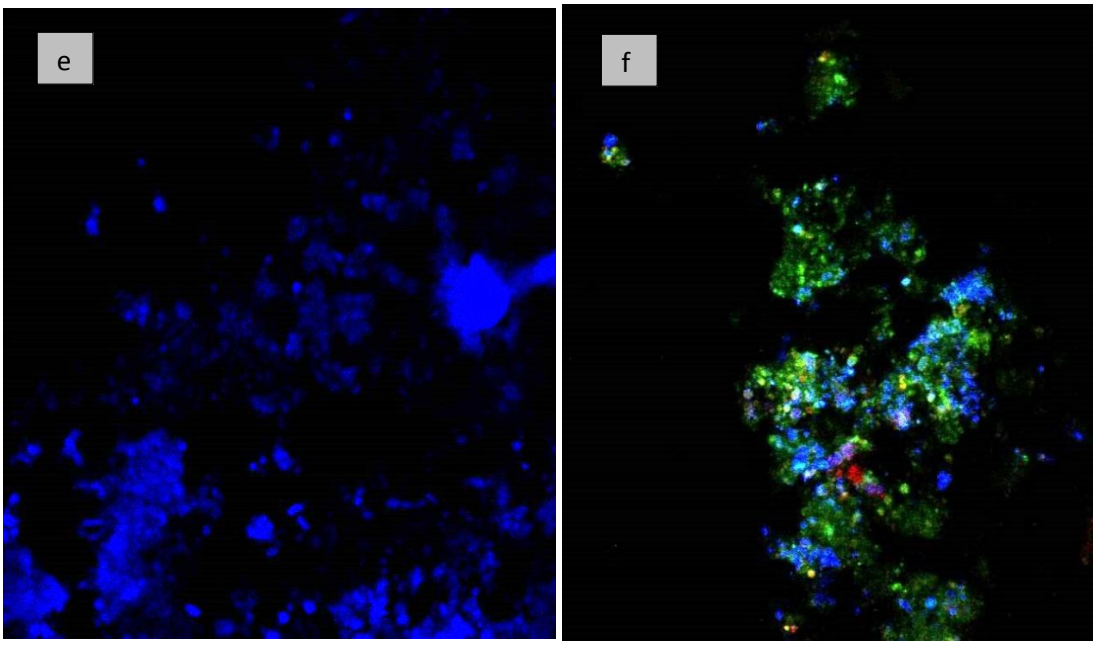

Figure 4.47. CLSM images of biofilm developed on tire rubber (TR) in aerobic batch biofilm reactor (ABBR) at Fe-8.5 mg/l (a-b; with Eubacterial mixture of probes (EUB I, EUB II, EUB III) at X10 and X100 respectively, c-d; Bet42 at X10 and X100, respectively, e; Gam42 at X10, f; Mixed channels at X100), Beta and gamma probes were applied along with their competitor probes. yellow and pink signals do not yield from binding of probes but are the result of overlaying of images i.e. red and green give yellow, red and white give pink) Background fluorescence was reduced by CLSM technique.

4.10.4. Biofilms Developed on Polyethylene (PE) at 8.5 mg/l of Fe(III) in Aerobic Batch Biofilm Reactors (ABBRs)

FISH was performed on biofilm of PE developed at Fe^{3+}-8.5 mg/l in aerobic batch biofilm reactor (ABBR) using mixture of EUB probes and EUB in combination with beta, gamma and their competitor probes for enhanced specificity, to determine their abundance, spatial distribution and coaggregation patterns. Total eubacterial population enumerated was found to be 1.08E+02 cells per cm^2 of PE biofilm which were found to be 2.00E+01 cells more than found at 8.5 mg/l concentration of Fe^{3+} on TR. Biovolume fraction recorded was 100 percent.

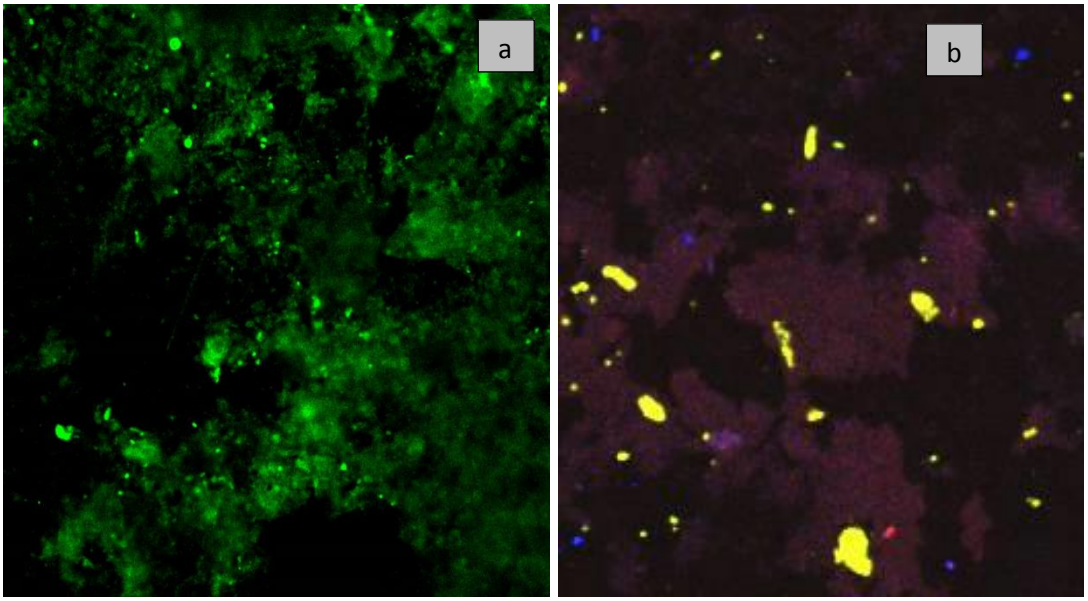

Figure 4.47. CLSM images of biofilm developed on Polyethylene (PE) in aerobic batch biofilm reactor (ABBR) at Fe-8.5 mg/l (a) with Eubacterial mixture of probes (EUB I, EUB II, EUB III) at X100 (b) with mixed channels at X100. Yellow and pink signals do not yield from binding of probes but are the result of overlaying of images i.e. red and green give yellow, red and white give pink) Background fluorescence was reduced by CLSM technique.

It has been postulated previously that surface attached bacteria i.e. biofilms are more active within their defined spatial distribution due to nutritional enrichment at the surfaces. Biofilms are usually described as microbial populations embedded within extracellular polymeric slime (EPS), concentrated at the interfaces. However, as the biofilms in activated sludge membrane processes is comprised of microorganisms and flocs as well (1). So in this present study, both microorganisms and microbial flocs have been included in the domain of biofilm description. The study proved positive as well as negative effects of increasing concentration of Fe^{3+} used as a nutrient, electron acceptor and flocculating agent and different surface properties of bio carriers on the structure and function of biofilms in aerobic batch biofilm reactors (ABBR).

When the reactors were run with different concentrations of Fe^{3+}, there was observed a 38% more reduction in COD and BOD_5 of the sludge at 8.5 mg/l compared to the untreated reactor (chap 4, fig.1). Higher removal in COD of sludge may be attributed to the activities of both autotrophic and heterotrophic bacteria. The results were comparable with those of previous studies as Rehman et al., (2012) reported a 93 % decrease in BOD5 and COD on plastic media trickling filter system (2). Similarly, Ghaniyari-Benis et al., (2009) carried out a study on the remediation of medium-strength wastewater in fixed bed biofilm reactor using Pall rings as a media to support the formation of biofilm that resulted in 83.4% COD removal efficiency. As penetration depth of different substrates in biofilms depends on the level of biofilm porosity, substrate concentration and rate of mass transfer at the liquid-biofilm interface in the biofilm. Random checks for dissolved oxygen (DO) measurement showed the presence of an average DO within a range of 0.25 mg/l to 2.12 mg/l (chap.4, table 1) contributing towards greater removal of COD in test reactors compared to control.

Volatile fatty acids profile exhibited an increase from 147.5 in control reactor to 475 mg/l with increasing concentration of ferric iron in (ABBR) (chap. 4, fig. 3) that were in agreement with previous work of Park et al (2007). Park et al. (2007) revealed that probably Fe reduction in sludge leads to deflocculation and reduction in volatile residues (3). Like COD in various studies applied as a limiting substrate, volatile acids have also been used as limiting substrate because volatile acids conversion into methane is generally considered as a rate limiting step (4). Wang et al.(2010) also

reported an increase in VFA content (640 ± 220 mg/l) after 46-60 days of operation of anaerobic sludge digestion system (5). Periodical monitoring of pH inside the reactors indicated average pH remained in the range of 7.1 to 7.32 (chap. 4, table 2) at different phases of experiment. Addition of Fe^{3+} and ammonium metabolism results in lowering of media pH (6). But in this study, variation of pH within a limited range may be subjected to the buffering effect of K_2HPO_4 and KH_2PO_4, the ingredients of Minimal Salt Media (MSM) added in the ABBR at the initial phase of experiment. Several reports exist describing the role of K_2HPO_4, NH_4PO_4, $CaHPO_4$ and $MgHPO_4$ for the purpose of maintaining the pH of media. Visual observation indicated that at higher Fe^{3+} concentration i.e. 8.5 mg/l, sludge settled more rapidly to the bottom of mechanically stirred aerated batch reactors due to formation of larger flocs. At lower Fe_3^{+} concentrations, the sludge settled slowly. These observations could be explicated by the previous work of Higgins and Novak, and Phong et al. (2008) (7). Trivalent ferric iron cations become incorporated within microbe-EPS network that resulted in denser flocs (7).

In the present investigation, biological nitrification was found responsible for the removal of NH_4^+ and NO_2^- suggesting that Fe^{3+} possibly enhanced nitrification by affecting the activity of ammonium oxidizing bacteria (AOB) and nitrite oxidizing bacteria (NOB) (chap.4, fig. 4, 5).Transformation rate of ammonium (NH_4^+-N) into NO_2^--N and NO_3^--N within the aerobic batch reactors indicated NO_2^--N build up after second week of reactors set up. It showed that presence of Fe^{3+} in all systems promoted activity of NOB during the initial period (higher NO_3^--N) and when Fe^{3+} was consumed and become limiting, their growth and activity also declined resulting in reduced oxidation of NO_2^--N into NO_3^--N that lead to NO_2^--N build up during the subsequent period (third and fourth week). The findings were very different from the results of Woznica et al. (2010). They found constant activities of AOB and NOB immobilized on polyurethane. These differences are assumed to be due to the presence of Fe^{3+} and different biocarrier properties employed in this study.

One more possible explanation for such nitrification results might be that at higher carbon contents within highly loaded systems, activity of AOB was suppressed due to spatial competition between ammonium oxidizing bacteria and heterotrophs (8). Moreover, as AOB preferably grow at alkaline pH values (>7), however, NH_4^+-N

metabolism and lowered pH of the medium after Fe^{3+} addition might have contributed towards lowered AOB performance (6). Untreated ABBR at the same time showed anomalous pattern of NO_3^--N concentration with its increasing value in the middle of operation that declined again at the end. It may be that in the first week NOB activity was low that increased during the middle of operation due to low dissolved oxygen (DO) content as low DO favors denitrifiers. After second week, heterotrophic denitrification might also have took part in the conversion of nitrates into further nitrogen containing compounds.

In shake flask experiments, concentration of Fe^{3+} did not exert inhibitory effect on nitrification process of autotrophic biofilms in case of all materials. Yet, it demonstrated an influence on AOB and NOB populations indirectly by variation in rate of nitrification to varying extent. Similarly, difference in nitrite and nitrate production and transformation rate on different surfaces at single concentration refers to the effect of varying surface properties. Keeping in mind that microbial density and diversity is different in different biofilms as revealed by heterotrophic plate counts (HPC/ml cm^2), molecular sequencing analysis, scanning electron microscopy (SEM) and confocal laser scanning microscopy (CLSM) of biofilms so their activities would be too. Biofilms of Polyethylene (PE) and Polyvinyl chloride (PVC) (chap. 4, fig. 25, 23) in ammonium enriched media under dark incubation conditions bared low AOB activity with no significant accumulation of nitrite over time and with increasing Fe^{3+} concentrations yet there was prominent increase in nitrate concentration due to higher NOB activity. This is due to the fact that low dissolved oxygen (DO) has always negative impact on nitrification and favors denitrification. Dentrifiers are facultative bacteria that prefer nitrogen oxides in the absence of oxygen as terminal electron acceptors (9). Biofilms from Stainless steel (SS), Tire rubber (TR) and Iron (Fe) (chap. 4 fig. 22, 26, 24) indicated improved NH_4^+-N and NO_2^--N oxidation comparatively than control biofilms over the period of time. Iron showed higher nitrite and nitrate concentration at 6.5 mg/l of Fe^{3+} over the period of month (NO_2^-: 0.147, 1.803, 3.1897 mg/l at 0, 15^{th} and 30^{th} day, NO_3^-: 0, 1.8123, 3.63 mg/l at 0, 15^{th} and 30^{th} day) highlighting the effect of Fe^{3+} concentration on nitrification. Studies have reported Iron as a good candidate for improved nitrification as it provides attachment sites for bacteria. Lo et al. (2010) observed similar results and concluded that denitrifiers competition for the exploitation of nitrite and low DO level (biofilms

in this study were also incubated under anoxic conditions) limit NOB growth and backlog of NO_2^--N in the system (8). There was an inadequate evidence in opposition to some previous reports for improved NOB activities in biofilms due to low nitrite levels in that study. Lipponen et al. (2002) reported in their study nitrification and nitrifying bacteria as ubiquitous in drinking water distribution networks in Finland. The number of AOB varied from $4.2X10^4$ to $1.1X10^8$ g^-, with the corresponding range for NOB being between $1.8X10^3$ and $2.3X10^8$ g^- with their high number in boreal regions of pipelines (10). A study conducted by Andersson et al. (2008) confirmed good potential of LECA, pumice, wood chips and Kaldnes K1 in their FISH study for mono species biofilm formation of *Comamonas denitrificans* 110 and *Brachymonas denitrificans* B79 and denitrification, however, with strong weekly variations. Kaldnes K1 is a commercial carrier material that has been used for denitrification purposes. This variation could be due to slow initial surface attachment, interactions between a hydrophobic, negatively charged (at pH 6–9) high density polyethylene (HDPE) surface (11) and negatively charged bacteria might be obstructed by repulsion, impeding initial adherence. In addition, microorganisms generally attach more rapidly to rough surfaces (Denkhaus et al., 2006). According to authors, the smooth surface of the HDPE plastic was difficult for the bacteria to colonize but once initial attachment took place, the irreversible attachment and further maturation was fast, resulting in an unevenly distributed biofilm. Thus, depending on the colonization level of the individual carriers, randomly taken out for denitrification rate measurement, the result varied. As irregular surfaces with cavities offer protection against chafing to microorganisms so high denitrification rates on such materials indicated the presence of more population of denitrifiers in biofilms and subsequently, their activity.

As the values indicated presence of both nitrification and denitrification processes operating simultaneously in each vessel it gives an indication of utility of the setup in simultaneous nitrification-denitrification (SND) process. The SND process starts with a partial nitrification of NH_4^+ to nitrite and subsequently continues with a direct reduction of nitrite to N2 gas. Previously, Zhang et al. (2007) have introduced a flexible biofilm reactor for similar possibility of SND in the same reactor (12). It can be concluded here that ammonium feed strategies can be applied in biofilm based

reactors to optimize wastewater treatment performance at particular Fe^{3+} concentration and specific membrane.

Comparative statistical analysis (two-way ANOVA with replication) of heterotrophic plate count (CFU/ml cm^2) indicated that both factors, different surface properties and Fe^{3+} concentration, exerted influence on microbial density in biofilms ($p<0.05$) (chap. 4, fig. 6). Polyethylene (PE) supported more bacterial density with an increasing concentration of Fe^{3+} being highest at 8.5 mg/l (1.77131E+11 CFU/ml cm^2) whereas Fe and PVC, on the other hand, showed a significant decrease in bacterial count with an increase in concentration of $Fe3^{+}$ across the specified range (Fe; 2.241E+08 CFU/ml cm^2, PVC; 8.84E+08 CFU/ml cm^2). Present investigation validated the work of Novak et al (1997) and Park (2007) that Fe^{3+} plays role in flocculation and promotes biofilm (3). SS and TR showed intermediate cell counts yet again highest at 8.5 mg/l of Fe^{3+}.There was a linear positive correlation between the ferric iron concentration and cell counts within all materials except Fe and PVC where Fe^{3+} additions were found inhibitory to biofilm development on PVC and iron as a support material. Bacterial enumeration results of PVC match the previous studies yet the results of iron as a biofilm carrier were found contradictory to previous studies of Niquette et al (2000) and others. Niquette et al. (2000) reported highest bacterial densities on iron and the lowest counts were measured on PVC (13). SS is a relatively new plumbing system and few reports are available regarding its short term and long term performance in water environments. There is general shift all around the world from copper to SS due to corrosion problem in buildings and wet environments and failure of copper pipes. Percival et al (1998) presented results of their study where they found significantly different number of cells on SS 304 grade i.e.1.9X103 CFU/cm^2 compared to $3.2X10^2$ CFU/cm^2 of pipe. Metal ions were also detected in water (14). Andersson et al. (2008) recommended polyurethane foams, cell rubber and plastic as suitable biofilm formers based on the results of their study since they posses' large protected surface areas and low densities (15). Several reports have stated that iron supports biofilms by providing attachment sites to bacteria and promotes iron oxidizing/reducing bacteria by electron shuttling either directly or by the involvement of hydrogen (16). However very different behavior of iron as a biofilm carrier in this work may be subjected to the presence of exogenous Fe^{3+} concentrations and rusting compounds that proved noxious to the bacterial

populations. Biofilms in pipelines inside the buildings and water distribution systems (WDS) can represent reservoirs favoring the growth of some potentially pathogenic bacteria such as Legionella and Mycobacteria (17), are often a source of contamination and biofouling in membrane reactors thus posing serious threat to public health and environment. In this scenario, where biofilms become a nuisance and need their control by mitigation strategies, piping materials made up of PVC and Fe can be recommended as durable and cost effective if employed with specified supplementation of Fe^{3+} in WDS.

Accumulation of more biofilm on PE could be ascribed to its two dimensional rough surface , presence of large dimples and ridges that can store moisture for bacterial growth, surface charge, more hydrophobicity and biodegradability properties of PE (18), (19). Surface roughness helps biofilm development through the provision of nearby surfaces to which detached biofilm pieces can reattach and thus enhances bacterial adhesion and biomass retention while surface hydrophobicity can affect bacterial adhesion and subsequent biofilm growth. A polar surface allows interaction with water molecules and water soluble compounds, facilitating the accumulation of molecules at the surface. Also it has been argued that when the physical appendages of bacteria (flagella, fimbriae and pili) overcome the physical repulsive forces of the electrical double layer. Subsequently, the appendages make contact with the bulk lattice of the conditioning layer stimulating chemical reactions such as oxidation and hydration and consolidating the bacteria - surface bond (20). It is experimentally difficult to determine the contribution of individual surface properties to the observed biofilm microbial community change, primarily due to the technical difficulties in creating surfaces that differ only in one surface property. For example, surfaces varied in a study conducted by Kim et al. (2014) with regard to surface conductivity and potentially other surface physical and chemical characteristics which were not targeted for characterization in that particular study which may also have contributed to a change in the biofilm microbial community (19). Our results varied from the previous findings of Zacheus et al. (2000) that reported similar accumulation of bacterial biofilms on SS, PVC and PE surfaces (21). A related study was also carried out by Lahota et al. (2004) in order to compare the impact of PE and copper materials on biofilm density. The formation of biofilm was slower in copper pipes than in the PE pipes but after 200 days there was no difference in microbial numbers between the

pipe materials (22).Total number of bacteria reached steady state faster in PE pipes than in copper pipes suggestive of PE as an excellent material for biofilm development in areas where biofilm role can be exploited positively e.g. membrane bed biofilm reactors in waste water treatment processes to reduce the organic load of waste water prior to its disposal in environment, biofilteraion purposes, biotransformation processes and production of products.

Investigators have used various methods to quantify number of microorganisms adhering to surfaces. We tested 79 bacteria strains isolated from biofilms developed in different ABBR by three (quantitative tissue culture plate (TCP), semi quantitative tube method (TM), qualitative congo red agar (CRA)) in vitro screening procedures and evaluated in this study to quantify their biofilm forming ability (chap.4, fig. 18). The specificity and sensitivity of methods were found in agreement with several previous studies. TCP method (the gold standard method) was found most sensitive method that indicated greatest number i.e. 96.2% of total isolates as strong biofilm formers with 3.37% as moderate and 0% as weak/no biofilm formers. The number of strong biofilm formers decreased to 67.08% in TM from 962% in TCP with 26.58 and 5.06% bacterial isolates as moderate and weak/none, respectively. Qualitative CRA method was found the least sensitive method with 34.18, 8.18 and 50.63% as strong, moderate and weak/none biofilm formers, respectively. Mathur et al. (2006) obtained similar results where they observed 52.6 and 46.0% isolates as strong biofilm formers where the media was supplemented with glucose and sucrose (23). We also performed this assay with supplementation of dextrose sugar that helps in biofilm development indicating that growth conditions greatly influence the biofilm formation capability of bacteria. The authors found reduced sensitivity of TM and CRA in determining their biofilm capacity as compared to TCP. In our study, the TM did not correlate well with the TCP test for strongly biofilm producing isolates and it was very difficult to discriminate between weak and biofilm negative isolates due to the variability in observed results by different observers. Consequently, high variability was observed and classification in biofilm positive and negative was difficult by TM. Therefore, in accordance with the previous reports, TM cannot be recommended as general screening test to discriminate biofilm producing isolate. Sensitivity of CRA was recorded the least of all the three assays performed in the study so CRA cannot be suggested for confirmed detection of biofilm ability of bacterial isolates. However,

TM should be considered superior in sensitivity compared to CRA. Ruzick et al (2004) also showed TM as better biofilm detection method than CRA in their study as they noted out of total 147 isolates, 53.7 and 43.5% biofilm formers by TM and CRA method, respectively (24). Likewise, Hassan et al. (2013) showed from regional data where 64.7% strong, and 36.3% non or weak biofilm producers were detected by TCP method whereas 49 and 51% as strong and weak/no biofilm formers by TM adding to the validity of TCP (25). Melo et al. (2013) reported sensitivity and specificity as 100% and 25% for TCP and 88.9% and 100% of CRA (26) again referring to the highest sensitivity of TCP. Our data indicates that the TCP method is an accurate and reproducible method for screening and this assay can serve as a reliable quantitative tool for determining biofilm formation of bacterial isolates.

Dominant bacterial species isolated from different biofilms and identified biochemically included *Pseudomonas spp., Vibrio spp., Shewanella spp., Providencia spp., Serratia spp., Klebsiella spp., Bacillus spp.* and *Staphylococcus spp*. (cahp. 4, table 3) with most dominant spp. of *Pseudomonas*. Previously, Percival et al. (1990) have reported the presence of mixture of bacteria related to Enterobacteriaceae family and others in Stainless steel pipes associated biofilms i.e. Pseudomonas sp., Merhylobacterium sp., Acinetobacter sp., Corynebacterium /Arthrobacter sp.and Micrococcus sp. (27). In another study carried out by Percival et al. (1998), *Pseudomonas* sp., *Alcaligenes* sp. and *Corynebacterium/Arthrobacter* sp. were detected as dominant species in SS biofilms (14). Phylogenetic sequencing analysis revealed the presence of several species of nitrifying and denitrifying bacteria in biofilms of different substrates under varying Fe^{3+} concentrations. Significant species in biofilm of control TR included species of genera *Nitrobacter* and *Rhodopseudomonas.* Biofilm on PE at 8.5 mg/l of Fe^{3+} (chap. 4, fig. 15) showed greater diversity of species related to genera *Bradyrhizobium, Nitrobacter and Rhodopseudomonas in addition to the species of genera Nitrospira* and *Nitrosomonas* depicted at 6.5 mg/l of Fe^{3+}(chap. 4, fig. 14). *Nitrosomoas europeae* strain present at 6.5 mg/l concentration of ferric iron was absent at 8.5 mg/l concentration of ferric iron. Biofilm on TR at Fe-6.5 mg/l showed a great diversity of AOB (cahp. 4, fig. 16). These included three different strains of Nitrosomonas sp. i.e; *Nitrosomonas sp. Is79A3, Nitrosomonas sp. AL212* and *Nitrosomonas europaea ATCC 19718*, five different uncultured *Nitrosomonadales* bacterium clones, *Nitrosomonas europaea*

ATCC 19718, *Nitrosospira multiformis* ATCC 25196 and *Thermodesulfovibrio yellowstonii* DSM *11347*. Amplified nucleotide sequence for genus *Nitrobacter* showed the presence of *Nitrobacter hamburgensis* X14, *Nitrobacter winogradskyi* Nb-255 sp. in biofilm microbial community grown on TR in ABBR at 8.5 mg/l concentration of $Fe(OH)_3$ that match to the corresponding species of genus *Nitrobacter* in biofilm on TR from control. Yet, higher (8.5 mg/l) content of Fe^{3+} supported the growth of some additional species of genus *Nitrobacter* i.e. *Nitrobacter* sp. clone NA20, *Nitrobacter* sp. clone NA14, *Nitrobacter* sp. strain R6 and some uncultured *Nitrobacter* sp. which were not found in biofilm on TR from control ABBR (chap. 4, fig. 12). These results of the conducted study, thereby, contribute towards the validity of our hypothesis that substratum surface properties do exert an impact on the microbial community structure of biofilms under varying concentrations of Fe^{3+}. Confocal laser scanning microscope (CLSM) results of this study for *in situ* detection of total population of eubacteria, beta and gamma proteobacteria also established the effect of different concentration of Fe^{3+} and surface characteristics on the community profile of microorganisms within the biofilms. As comparative quantification analysis indicated, there was a linear positive relationship between the cell density of eubacteria (3.00E+01 cells/cm^2 at 2.5 mg/ to 1.05E+02 cells/cm^2 at 8.5 mg/l) and beta proteobacteria (8.10E+01 cells/cm^2 at 2.5 mg/l to 1.42E+02 cells/cm^2 at 8.5 mg/l) and Fe^{3+} concentration whereas, gamma proteobacteria displayed an inverse relation between cell enumeration and Fe^{3+} additions (7.30E+01 cells/cm^2 at 2.5 mg/ to 3.40E+01 cells/cm^2 at 8.5 mg/l). Very related study was conducted by Kim et al. (2014) to investigate the impact of substratum surface property change on biofilm community structure using laboratory biological aerated filter (BAF) reactors and found that the two plastic surfaces different from the perspective of surface roughness and hydrophobicity resulted in different biofilm microbial communities in the BAF reactors. The authors reported majority of microbial populations in test and control reactors belonged to Burkholderiales and Rhodocyclales orders of the Betaproteobacteria class where species of Burkholderiales were more in test reactor compared to control. Previous work has shown that the Betaproteobacteria were commonly found to be the most dominant class in biological wastewater treatment processes (28). Kim and coworkers (2014) deduced that the abundance of Burkholderiales and Rhodocyclales in the

reactors might be due to the presence of organic substrate such as sucrose that was also the cause of small microbial diversity in the reactors and the abundance level of dominant order in test reactor compared to control was due to microbial interplay among multiple species. Comamomonas sp. (from Bulkholderiales) is found in biofilm processes (29) but not as a major species in activated sludge processes, however, its abundance in test reactor further corroborated the notion of impact of modified surfaces. This illustrates one more point that surface effect changes the abundance of microbial species associated with suspended growth in attached growth i.e. biofilms.

Hybridization of biofilm bacteria with fluorescently labelled probes (FISH) coupled with confocal laser scanning microscope (CLSM) provided information on the cohabitation of β and γ proteobacteria and eubacteria and their altered spatial distribution in different biofilms in accordance with the previous reports (chap. 4, fig. 40). Manz et al. (1993) indicated coexistence of β and γ-proteobacteria in water biofilms and microcolonies as an integral part of their survival mechanism (30). Barringuet et al. (2004) found mixed populations of beta and gamma subclasses of Proteobacteria in very early stages of development of biofilm in microcolonies in his FISH study (31). Likewise, Dolinsek et al. (2013) applied oligonucleotide probes to determine the existence of heterotrophic and autotrophic bacterial populations in biofilms (32). All biofilm samples gave positive hybridization with the probe Eub-338 (I,II,III), Bet42 and Gam42.Those results were considered as positive that gave good signals with target cells. The results indicated the potential of this technique as a rapid screening method for bacterial identification and quantification. In the conventional identification of bacteria, time consuming series of physiological and biochemical tests are necessary, the identification of isolated bacteria using FISH and molecular phylogenetic probes targeting 16S- or 23S-rRNA is rapid (Bhavanath *et al.,* 2009).
Gradients of substrates within biofilms create an intricate landscape of microhabitats, resulting in a structured localization of microbial communities there. It was not easy to distinguish growth from attachment of cells. However, it may be possible that dark areas in the CLSM images representing voids with rough surfaces were filled with deposited cells. Some previous studies have also specified presence of such base layer and suggested that growth of biofilms starts from the base laterally (33).

A biofilm is generally considered either consisting of a homogeneous, planar, smooth structure with continuous layers or a heterogeneous patchy structure having voids, channels and aggregates (34). Scanning electron micrographs of biofilms on different support materials grown at varying Fe^{3+} concentrations in this study proved heterogeneous structure of biofilms. On PVC at Fe-8.5 mg/l, small and large rod shaped bacteria, diatoms, chains and clusters of cocci, coccobacilli, spiral shaped bacteria, yeasts and filamentous bacteria attached to the plastic surface individually and in clusters associated with microcolonies were observed at X10,000 and X20,000 (chap. 4, fig. 34). In control, cocci and rod shaped bacilli were also present but bacilli predominated (chap. 4, fig. 3). In control PVC biofilm, microbial diversity seemed l**ess** compared to the density of microbial populations in PVC biofilm at Fe-8,5 mg/l indicating the effect of Fe(III) supplementation on microbial diversity and density. Voids and channels were clearly obvious in both Fe-8.5 mg/l PVC and PVC control biofilms at X1,000. The voids and channels play role in substrate transfer and provide protection to microorganisms against predators and environmental stress such as nutrient depletion and pH change. SEM micrographs displayed differences in biofilm cover (in terms of uneven covering over whole areas with crevices, furrows, grooves, patches and small flocs) on TR of control and 8.5 mg/l. There was greater microbial diversity and density in control biofilm (rosette shaped filamentous organisms and innumerable rods, cocci, peritrichous cells) on TR than at 8.5 mg/l (chap. 4, fig. 36, 37) yet there was no significant difference of EPS contents between the two biofilms. SEM results of more cells in control biofilm than at higher Fe^{3+} contents match with CFU results of this study. Cells in both biofilms differed also in their sizes. Cells were embedded within abundant extracellular polymeric matrix (X25,00, X5,000 and X10,000) in both types of biofilms that is either secreted by sessile microorganisms mainly or attached from immediate environment (medium). Some fibrous projections in different biofilms might be artifacts due to limitations of drying steps during sample preparation. Scanning electron micrographs results correlated well with microbial density and diversity as indicated by other techniques. Previously Muhammad et al. (2013) and Lazarova et al. (2013) have reported in their SEM study that the biofilm is not comprised of uniform, simple and continuous bacterial layers instead it consists of microbial cells encased in glycocalyx i.e. an extracellular matrix of polymers with heterogeneous surface morphology (35), (36). SEM images proved

heterogeneous nature of biofilms as previously indicated by several authors e.g. Li et al. (2013) and Osman et al. (2013) that described biofilm morphology as an irregular, uneven texture with porous network (37), (38).

Fourier transform infrared (FTIR) spectra of EPS of biofilms indicated more proteinaceous contents in TR biofilm at 2.5 (94% transmittance) and 6.5 mg/l (1644.38 and 1636.49 cm^{-}) than at Fe3+ 8.5 mg/l (chap. 4, fig. 29) where there was dominance of ether and esters with peaks at 1035.03 cm^{-} whereas biofilm of control TR depicted a very different spectrum showing the presence of alkanes, ethers and esters (1452.90 cm^{-} and 1049.94 cm^{-}).COOH attributed to carboxylic acids was present at all concentrations of Fe^{3+} in biofilms of PVC, Fe and PE with difference of percent transmittance in the range of 3270 cm^{-}-3384.2 cm^{-} (chap. 4, fig. 32, 31, 28). Predominance of amines and carboxylic acids was observed in biofilms of SS at no/lower (0, 2.5 mg/l) and higher (6.5 and 8.5 mg/l) concentration of Fe^{3+}, respectively. The percentage transmittance varied greatly to different extents depending on the abundance of moieties presence. Some peaks appeared at one concentration of Fe^{3+} disappeared at the same concentration on other surface(s) or at its other concentrations for same surface material. The results were comparable with the findings of Huang et al. (2014) that found dominance of amide group in the biofilm with strongest absorption at wavenumber of 3390 cm^{-} representing N–H and O–H stretching vibration and exhibiting the characteristics of amines and alcohols (or phenols) (39). A weak absorption at 2920 cm^{-} was assigned to asymmetrical C–H stretching vibration of an aliphatic CH_2 group indicating the presence of sugar content in EPS (40). In a study related to foulant analysis of membranes conducted by Jeong et al. (2013), the wavenumbers of 2850 cm^{-} and 1400 cm^{-} revealed stretching vibration, scissoring and bending vibration of C–H group related to alkanes (41) and wavenumber of 874 cm^{-} instructed C–H bending vibration of alkenes. The absorption at 1650 cm^{-} was attributed to stretching vibration of alkenes (39). IR spectra also supported previous findings that environmental conditions (here, Fe^{3+} concentrations and support material properties) change the components of EPS, under which biofilms are grown.

To our knowledge, this is the first direct demonstration of the impacts of ferric iron concentration and substratum surface properties on biofilm community structures and reactor treatment performance in an aerobic batch mode biofilm process. Previous

studies on clinically relevant biofilms were exclusively focused on the interaction between substratum surfaces and single bacterial strains, while studies on wastewater treatment processes that involved mixed microbial communities have predominantly focused on biomass density, distribution, and the resulting treatment performance. The data presented here can serve for the selection of microbial strain combinations for application in waste water treatment processes and bioaugmentation, can be a useful tool to control biofilm development, may provide a basis for further experimental design and facilitate the rational designing of new generations of substrata for improved biofilm based biological treatment processes.

The study led us to a solid understanding that the density and microbial diversity of biofilm is highly influenced by the variability in the concentration of ferric iron in association with substratum properties. Polyethylene, a plastic based material featured the highest microbial biomass as compared to other surfaces at the highest applied concentration of $Fe(OH)_3$ indicating its utility in processes where biofilm is desirable e.g. attached growth membrane processes for waste water treatment whereas Polyvinyl chloride (PVC) and Iron supported the least bacterial density with an increasing concentration of Fe^{3+} revealing their potential application to control biofilms in areas where biofilms need practicing mitigation strategies e.g. water distribution systems . Nitrogen removal is a key to successful wastewater treatment in this age. Biofilms from selected surfaces demonstrated a variable potential towards nitrification/denitrification activity relative to the Fe(III) concentration. Stainless steel (SS), Tire rubber (TR) and Iron (Fe) indicated improved NH_4^+-N and NO_2^--N oxidation with increasing Fe^{3+} concentration compared to Polyethylene (PE) and Polyvinyl chloride (PVC) biofilms.

Furthermore, molecular sequencing analysis, Fourier transform infrared (FTIR) spectroscopy, FISH combined with coaggregation analysis of confocal laser scanning microscopic (CLSM) images and scanning electron microscopy (SEM) of biofilms revealed alterations in the biofilm community structures, spatiotemporal distribution of biofilm microbial consortia and molecular fingerprints of EPS of biofilms on different support materials under the influence of varying Fe(III) concentrations.

Research in the field of "biofilmology" is proceeding in several areas all over the world with special emphasis on elucidation and regulation of gene(S) expressed by biofilm forming microorganisms and their application in areas spanning from environmental biotechnology to medical and industrial biotechnology.

- Further studies should focus on the application of biofilm support materials used in this study and other cost effective and sustainable bio carriers in pilot scale biofilm reactors for waste water treatment. The same can be further imitated under anaerobic conditions to compare the differences and efficiency of the process. Role of trivalent cations such as Al^{3+} and divalent to trivalent ratio of cations e.g. Fe^{2+} to Fe^{3+} in biofilm improvement can be explored according to the recommendations of divalent cation bridging (DCB) theory. Further studies can be undertaken to reveal the Interactions of Fe(III) and other metallic cations with different surfaces under stressed conditions e.g. pH, nutrients, temperature etc.
- Fe mitigation of lead and other toxic compounds also needs to be investigated.
- Very little is known previously about the effect of iron on the behavior of iron associated gene(s) in multispecies biofilms. Quorum sensing (QS) is the key to biofilm regulation. Genes involved in QS can be targeted to modify genetic models based on QS and to understand the dynamics of genes expression in biofilm.
- Addition of iron alters the topography and architectural features of biofilms that can be visualized by confocal laser scanning microscope (CLSM). An improved understanding of molecular mechanisms of cohesion and adhesion phenomena in biofilms would definitely assist to develop and implement biofouling control strategies in wastewater treatment technologies.
- The importance of interspecies interactions, either cooperative, competitive, or both, during surface colonization and biofilm formation has been underestimated. Multispecies biofilms in oligotrophic environments can be studied with fluorescence-labeled, rRNA-targeted oligonucleotide probes. In the future, they could provide information on the spatial distribution and activity of phylogenetically defined populations and thereby could greatly enhance our understanding of the structure-function correlation in biofilms. More detailed studies are necessary to examine similarities between the surface-associated and planktonic communities. This could help answer the following important questions related to drinking water safety. Is shedding of bacteria from biofilms an important source of drinking water contamination? Do pathogenic bacteria really survive and multiply within biofilms in drinking water systems?
- Nitrification served as a proxy to the activity of nitrifying populations in this study. Further studies can be designed based on inoculum preparations for the isolation, characterization and utilization of nitrifying bacterial strains. Bacterial strains isolated during this study may be subjected to 16S rRNA molecular technique for their complete identification and application in processes. Membrane associated proteins can be isolated as amoA and amoB subunits from the amo operon of ammonia oxidizing populations of bacteria. The process can be operated in Sharon,

anammox (anaerobic ammonium oxidation) and Sharon-anammox mode to compare the efficiency of the processes in nitrogen removal.

- Fe(OH)3 can be checked for improved current generation in microbial fuel cells as it has been shown for its ability to reduce the cathode resistance.
- PCR combined with DGGE may be employed to document the altered microbial community structure of biofilms and explain the mechanisms involved in microbially influenced corrosion (MIC) ignored previously.

1. Almstrand R, Daims H, Persson F, Sörensson F, Hermansson M. 2013. New methods for analysis of spatial distribution and coaggregation of microbial populations in complex biofilms. Appl. Environ. Microbiol. 79:5978–87.

2. Naz I, Batool SA, Ali N, Khatoon N, Atiq N, Hameed A, Ahmed S. 2013. Monitoring of growth and physiological activities of biofilm during succession on polystyrene from activated sludge under aerobic and anaerobic conditions. Environ. Monit. Assess. 185:6881–92.

3. Shafahi M, Vafai K. 2009. Biofilm affected characteristics of porous structures. Int. J. Heat Mass Transf. 52:574–581.

4. Donlan RM, Costerton JW. 2002. Biofilms: Survival mechanisms of clinically relevant microorganisms. Clin. Microbiol. Rev. 15:167–193.

5. Calderón K, Martín-Pascual J, Poyatos JM, Rodelas B, González-Martínez A, González-López J. 2012. Comparative analysis of the bacterial diversity in a lab-scale moving bed biofilm reactor (MBBR) applied to treat urban wastewater under different operational conditions. Bioresour. Technol. 121:119–26.

6. Zacheus OM, Iivanainen EK, Nissinen TK, Lehtola MJ, Martikainen PJ. 2000. bacterial biofilm formation on polyvinyl chloride , polyethylene and stainless steel exposed to ozonated water 34.

7. Karunakaran E, Mukherjee J. 2011. " Biofilmology ": a multidisciplinary review of the study of microbial biofilms 1869–1881.

8. Ren L, Tokash JC, Regan JM, Logan BE. 2012. Current generation in microbial electrolysis cells with addition of amorphous ferric hydroxide, Tween 80, or DNA. Int. J. Hydrogen Energy 37:16943–16950.

9. Du Z, Li H, Gu T. 2007. A state of the art review on microbial fuel cells : A promising technology for wastewater treatment and bioenergy 25:464–482.

10. Lim CK, Aris A, Neoh CH, Lam CY, Abdul Majid Z, Ibrahim Z. 2014. Evaluation of macrocomposite based sequencing batch biofilm reactor (MC-SBBR) for decolorization and biodegradation of azo dye Acid Orange 7. Int. Biodeterior. Biodegradation 87:9–17.

11. Gomez J, Bodalo a, Gomez E, Hidalgo a, Gomez M, Murcia M. 2008. A transient design model of a continuous tank reactor for removing phenol with immobilized soybean peroxidase and hydrogen peroxide. Chem. Eng. J. 145:142–148.

12. Park C, Fang Y, Murthy SN, Novak JT. 2010. Effects of floc aluminum on activated sludge characteristics and removal of 17-alpha-ethinylestradiol in wastewater systems. Water Res. 44:1335–40.

13. Nicolella C, van Loosdrecht MC, Heijnen JJ. 2000. Wastewater treatment with particulate biofilm reactors. J. Biotechnol. 80:1–33.

14. Haseborg E, Zamora TM, Fröhlich J, Frimmel FH. 2010. Bioresource Technology Nitrifying microorganisms in fixed-bed biofilm reactors fed with different nitrite and ammonia concentrations. Bioresour. Technol. 101:1701–1706.

15. Phong T, Hilal N, Hankins NP, Novak JT. 2008. The relationship between cation ions and polysaccharide on the floc formation of synthetic and activated sludge 227:94–102.

16. Phong T, Hilal N, Hankins NP, Novak JT. 2008. Characterization of synthetic and activated sludge and conditioning with cationic polyelectrolytes 227:103–110.

17. Luostarinen S, Luste S, Valentín L, Rintala J. 2006. Nitrogen removal from on-site treated anaerobic effluents using intermittently aerated moving bed biofilm reactors at low temperatures. Water Res. 40:1607–1615.

18. Pynaert K, Smets BF, Wyffels S, Beheydt D, Siciliano SD, Verstraete W. 2003. Characterization of an Autotrophic Nitrogen-Removing Biofilm from a Highly

Loaded Lab-Scale Rotating Biological Contactor Characterization of an Autotrophic Nitrogen-Removing Biofilm from a Highly Loaded Lab-Scale Rotating Biological Contactor.

19. Di Trapani D, Mannina G, Torregrossa M, Viviani G. 2010. Quantification of kinetic parameters for heterotrophic bacteria via respirometry in a hybrid reactor. Water Sci. Technol. 61:1757–1766.

20. V. Lazarova JM. 1995. Pergamon IN WATER A N D WASTEWATER TREATMENT. Wat. Res. 29:2227–2245.

21. Wijeyekoon S, Mino T, Satoh H, Matsuo T. 2004. Effects of substrate loading rate on biofilm structure. Water Res. 38:2479–88.

22. De Beer D, Stoodley P, Roe F, Lewandowski Z. 1994. Effects of biofilm structures on oxygen distribution and mass transport. Biotechnol. Bioeng. 43:1131–1138.

23. Costerton JW, Lewandowski Z, Caldwell DE, Korber DR, Lappin-Scott HM. 1995. Microbial biofilms. Annu Rev Microbiol 49:711–45.

24. Kwok WK, Picioreanu C, Ong SL, Van Loosdrecht MCM, Ng WJ, Heijnen JJ. 1998. Influence of biomass production and detachment forces on biofilm structures in a biofilm airlift suspension reactor. Biotechnol. Bioeng. 58:400–407.

25. Yang S, Ngwenya BT, Butler IB, Kurlanda H, Elphick SC. 2013. Coupled interactions between metals and bacterial biofilms in porous media: Implications for biofilm stability, fluid flow and metal transport. Chem. Geol. 337-338:20–29.

26. Appenzeller BMR, Yan C, Jorand F, Block J. 2005. Advantage Provided by Iron for Escherichia coli Growth and Cultivability in Drinking Water 71:5621–5623.

27. Ngwenya BT, Sutherland IW, Kennedy L. 2003. Comparison of the acid-base behaviour and metal adsorption characteristics of a gram-negative bacterium with other strains. Appl. Geochemistry 18:527–538.

28. Brennan A. 2012. Investigating Pilot Scale Performance Of An Activated Sludge Wastewater Treatment System With A High Rate Anaerobic Side Stream Reactor.

29. Beech IB, Sunner J. 2004. Biocorrosion: towards understanding interactions between biofilms and metals. Curr. Opin. Biotechnol. 15:181–6.

30. Niquette P, Servais P, Savoir R. 2000. RESEARCH NOTE IMPACTS OF PIPE MATERIALS ON DENSITIES OF FIXED BACTERIAL BIOMASS IN A DRINKING WATER DISTRIBUTION SYSTEM 34:1952–1956.

31. Percival SL, Knapp JS, Edyvean RGJ, Wales DS. 1998. BIOFILMS , MAINS WATER AND STAINLESS STEEL 32:2187–2201.

32. Kim L, Pagaling E, Zuo YY, Yan T. 2014. Impact of substratum surface on microbial community structure and treatment performance in biological aerated filters. Appl. Environ. Microbiol. 80:177–183.

33. Sharp KH, Distel D, Paul VJ. 2012. Diversity and dynamics of bacterial communities in early life stages of the Caribbean coral Porites astreoides. ISME J. 6:790–801.

34. Manz W, Szewzyk U, Ericsson P, Amann R, Schleifer KH, Stenström T a. 1993. In situ identification of bacteria in drinking water and adjoining biofilms by hybridization with 16S and 23S rRNA-directed fluorescent oligonucleotide probes. Appl. Environ. Microbiol. 59:2293–8.

35. Zhang W, Zhang X, Wang D, Koga Y, Rouse JD, Furukawa K. 2011. Bioresource Technology Trace elements enhance biofilm formation in UASB reactor for solo simple molecule wastewater treatment. Bioresour. Technol. 102:9296–9299.

36. Ojeda JJ, Romero-González ME, Bachmann RT, Edyvean RGJ, Banwart SA. 2008. Characterization of the cell surface and cell wall chemistry of drinking water bacteria by combining XPS, FTIR spectroscopy, modeling, and potentiometric titrations. Langmuir 24:4032–4040.

37. Rasamiravaka T, Labtani Q, Duez P, Jaziri M El. 2014. The formation of biofilms by Pseudomonas aeruginosa : a review of the natural and synthetic compounds interfering with control mechanisms 1–48.

38. Garrett TR, Bhakoo M, Zhang Z. 2008. Bacterial adhesion and biofilms on surfaces. Prog. Nat. Sci. 18:1049–1056.

39. Andersson S. 2009. Characterization of Bacterial Biofilms for Wastewater Treatment.

40. Cui B. 2012. Phenotypic and Genotypic Characterisation of Biofilm Formation in Staphylococcus capitis. Portfolio, Technology.

41. Andersson S, Dalhammar G, Kuttuva Rajarao G. 2011. Influence of microbial interactions and EPS/polysaccharide composition on nutrient removal activity in biofilms formed by strains found in wastewater treatment systems. Microbiol. Res. 166:449–57.

42. Andersson S, Nilsson M, Dalhammar G, Rajarao GK. 2008. Assessment of carrier materials for biofilm formation and denitrification. Vatten 64:201–207.

43. Hassan A, Usman J, Kaleem F, Omair M, Khalid A, Iqbal M. 2011. Evaluation of different detection methods of biofilm formation in the clinical isolates. Brazilian J. Infect. Dis. 15:305–311.

44. Lyautey E, Jackson CR, Cayrou J, Rols J-L, Garabétian F. 2005. Bacterial community succession in natural river biofilm assemblages. Microb. Ecol. 50:589–601.

45. Flemming HC, Neu TR, Wozniak DJ. 2007. The EPS matrix: The "House of Biofilm Cells." J. Bacteriol.

46. Denkhaus E, Meisen S, Telgheder U, Wingender J. 2007. Chemical and physical methods for characterisation of biofilms. Microchim. Acta.

47. Van Der Veen S, Abee T. 2010. Dependence of continuous-flow biofilm formation by Listeria monocytogenes EGD-e on SOS response factor YneA. Appl. Environ. Microbiol. 76:1992–1995.

48. Habimana O, Meyrand M, Meylheuc T, Kulakauskas S, Briandet R. 2009. Genetic features of resident biofilms determine attachment of Listeria monocytogenes. Appl. Environ. Microbiol. 75:7814–7821.

49. Kjelleberg S, Molin S. 2002. Is there a role for quorum sensing signals in bacterial biofilms? Curr. Opin. Microbiol.

50. Caiazza NC, O'Toole GA. 2003. Alpha-toxin is required for biofilm formation by Staphylococcus aureus. J. Bacteriol. 185:3214–3217.

51. Davies DG, Parsek MR, Pearson JP, Iglewski BH, Costerton JW, Greenberg EP. 1998. The involvement of cell-to-cell signals in the development of a bacterial biofilm. Science 280:295–298.

52. De Kievit TR. 2009. Quorum sensing in Pseudomonas aeruginosa biofilms. Environ. Microbiol.

53. Ma S. 2014. CONTROLLING Pseudomonas aeruginosa BIOFILMS AND PERSISTER CELLS BY MANIPULATING CELL-CELL SIGNALING.

54. Li YH, Tian X. 2012. Quorum sensing and bacterial social interactions in biofilms. Sensors.

55. Patriquin GM, Banin E, Gilmour C, Tuchman R, Greenberg EP, Poole K. 2008. Influence of quorum sensing and iron on twitching motility and biofilm formation in Pseudomonas aeruginosa. J. Bacteriol. 190:662–71.

56. Bollinger N, Hassett DJ, Iglewski BH, Costerton JW, Dermott TRMC. 2001. Gene Expression in Pseudomonas aeruginosa : Evidence of Iron Override

Effects on Quorum Sensing and Biofilm-Specific Gene Regulation 183:1990–1996.

57. Lade H, Paul D, Kweon JH. 2014. Isolation and molecular characterization of biofouling bacteria and profiling of quorum sensing signal molecules from membrane bioreactor activated sludge. Int. J. Mol. Sci. 15:2255–73.

58. Belapurkar R, Tale VS, Madkaikar R, Hastings JW, Juan E. 2014. Original Research Article Exploiting Quorum Sensing to inhibit the Bacterial Pathogens 3:453–458.

59. Dunny GM, Leonard BA. 1997. Cell-cell communication in gram-positive bacteria. Annu Rev Microbiol 51:527–564.

60. Federle MJ, Bassler BL. 2003. Interspecies communication in bacteria. J. Clin. Invest.

61. Kay E, Humair B, Dénervaud V, Riedel K, Spahr S, Eberl L, Valverde C, Haas D. 2006. Two GacA-dependent small RNAs modulate the quorum-sensing response in Pseudomonas aeruginosa. J. Bacteriol. 188:6026–6033.

62. Ventre I, Goodman AL, Vallet-Gely I, Vasseur P, Soscia C, Molin S, Bleves S, Lazdunski A, Lory S, Filloux A. 2006. Multiple sensors control reciprocal expression of Pseudomonas aeruginosa regulatory RNA and virulence genes. Proc. Natl. Acad. Sci. U. S. A. 103:171–176.

63. Goodman AL, Kulasekara B, Rietsch A, Boyd D, Smith RS, Lory S. 2004. A signaling network reciprocally regulates genes associated with acute infection and chronic persistence in Pseudomonas aeruginosa. Dev. Cell 7:745–754.

64. Katarzyna L, Sai G, Singh OA. 2015. Non-enclosure methods for non-suspended microalgae cultivation: literature review and research needs. Renew. Sustain. Energy Rev. 42:1418–1427.

65. Jahid IK, Ha S-D. 2014. The Paradox of Mixed-Species Biofilms in the Context of Food Safety. Compr. Rev. Food Sci. Food Saf. 13:990–1011.

66. Lee KWK, Periasamy S, Mukherjee M, Xie C, Kjelleberg S, Rice S a. 2014. Biofilm development and enhanced stress resistance of a model, mixed-species community biofilm. ISME J. 8:894–907.

67. Lehtola MJ, Miettinen IT, Keinänen MM, Kekki TK, Laine O, Hirvonen A, Vartiainen T, Martikainen PJ. 2004. Microbiology, chemistry and biofilm development in a pilot drinking water distribution system with copper and plastic pipes. Water Res. 38:3769–79.

68. Badireddy AR, Chellam S, Gassman PL, Engelhard MH, Lea AS, Rosso KM. 2010. Role of extracellular polymeric substances in bioflocculation of activated sludge microorganisms under glucose-controlled conditions. Water Res. 44:4505–4516.

69. Metcalf E, Eddy H. 2003. Wastewater engineering: treatment and reuseWastewater Engineering, Treatment, Disposal and Reuse. Techobanoglous G, Burton FL, Stensel HD (eds). Tata McGraw-Hill Publishing Company Limited, 4th edition. New Delhi, India.

70. Sheng G, Yu H, Li X. 2010. Extracellular polymeric substances (EPS) of microbial aggregates in biological wastewater treatment systems : A review. Biotechnol. Adv. 28:882–894.

71. Götz F. 2002. Staphylococcus and biofilms. Mol. Microbiol.

72. Sheng GP, Yu HQ, Li XY. 2010. Extracellular polymeric substances (EPS) of microbial aggregates in biological wastewater treatment systems: a review. Biotechnol Adv 28:882–894.

73. Romaní AM, Fund K, Artigas J, Schwartz T, Sabater S, Obst U. 2008. Relevance of polymeric matrix enzymes during biofilm formation. Microb. Ecol. 56:427–436.

74. Park C, Novak JT. 2009. Characterization of lectins and bacterial adhesins in activated sludge flocs. Water Environ. Res. 81:755–764.

75. Mayer C, Moritz R, Kirschner C, Borchard W, Maibaum R, Wingender J, Flemming HC. 1999. The role of intermolecular interactions: studies on model systems for bacterial biofilms. Int. J. Biol. Macromol. 26:3–16.

76. Saravanan V, Sreekrishnan TR. 2006. Modelling anaerobic biofilm reactors--a review. J. Environ. Manage. 81:1–18.

77. Wijeyekoon S, Mino T, Satoh H, Matsuo T. 2004. Effects of substrate loading rate on biofilm structure. Water Res. 38:2479–88.

78. Yang X, Beyenal H, Harkin G, Lewandowski Z. 2000. Quantifying biofilm structure using image analysis. J. Microbiol. Methods 39:109–19.

79. Mutombo DT. 2004. Internal circulation reactor: pushing the limits of anaerobic industrial effluents treatment technologies. Proc. 2004 Water Inst. South. Africa Bienn. Conf. Cape Town, South Africa. 608–616.

80. Donati G. 1999. Batch and semibatch catalytic reactors (from theory to practice). Catal. Today 52:183–195.

81. Boltz JP, Morgenroth E, Daigger GT, deBarbadillo C, Murthy S, Sørensen KH, Stinson B. 2012. Method to identify potential phosphorus rate-limiting conditions in post-denitrification biofilm reactors within systems designed for simultaneous low-level effluent nitrogen and phosphorus concentrations. Water Res. 46:6228–38.

82. Fang HHP, Chui HK, Li YY. 1995. Effect of degradation kinetics on the microstructure of anaerobic biogranules. Water Sci. Technol. 32:165–172.

83. Guiot SR, Pauss A, Costerton JW. 1992. A structured model of the anaerobic granule consortium. Water Sci. Technol.

84. Schink B. 1997. Energetics of syntrophic cooperation in methanogenic degradation. Microbiol. Mol. Biol. Rev. 61:262–280.

85. Nougués JM, Grau MD, Puigjaner L. 2001. Parameter estimation with genetic algorithm in control of fed-batch reactors. Chem. Eng. Process. 41:303–309.

86. Shukla SK, Rao TS. 2013. Effect of calcium on Staphylococcus aureus biofilm architecture: a confocal laser scanning microscopic study. Colloids Surf. B. Biointerfaces 103:448–54.

87. Silverstein J, Hernandez M. 2005. Effects of Soluble Ferri - Hydroxide Complexes on Microbial Neutralization of Acid Mine Drainage 39:7826–7832.

88. Musk DJ, Banko D a, Hergenrother PJ. 2005. Iron salts perturb biofilm formation and disrupt existing biofilms of Pseudomonas aeruginosa. Chem. Biol. 12:789–96.

89. Ku¨sel K, Dorsch T. 2000. Effect of supplemental electron donors on the microbial reduction of Fe(III), sulfate, and CO2 in mining–impacted freshwater lake sediments. Microb. Ecol. 40:238–249.

90. Küsel K, Dorsch T, Acker G, Stackebrandt E. 1999. Microbial reduction of Fe(III) in acidic sediments: Isolation of Acidiphilium cryptum JF-5 capable of coupling the reduction of fe(III) to the oxidation of glucose. Appl. Environ. Microbiol. 65:3633–3640.

91. Bowman RS. 1997. Aqueous Environmental Geochemistry. Eos, Trans. Am. Geophys. Union.

92. Massonet C, Pintens V, Merckx R, Anné J, Lammertyn E, Van Eldere J. 2006. Effect of iron on the expression of sirR and sitABC in biofilm-associated Staphylococcus epidermidis. BMC Microbiol. 6:103.

93. Teng F, Guan YT, Zhu WP. 2008. Effect of biofilm on cast iron pipe corrosion in drinking water distribution system: Corrosion scales characterization and microbial community structure investigation. Corros. Sci. 50:2816–2823.

94. Chyan J-M, Senoro D-B, Lin C-J, Chen P-J, Chen I-M. 2013. A novel biofilm carrier for pollutant removal in a constructed wetland based on waste rubber tire chips. Int. Biodeterior. Biodegradation 85:638–645.

95. Sen SK, Raut S. 2015. Journal of Environmental Chemical Engineering Microbial degradation of low density polyethylene (LDPE): A review. Biochem. Pharmacol.

96. Seth AD, Edyvean RGJ. 2006. The function of sulfate-reducing bacteria in corrosion of potable water mains. Int. Biodeterior. Biodegrad. 58:108–111.

97. Van der Kooij D, Vrouwenvelder HS, Veenendaal HR. 1995. Kinetic aspects of biofilm formation on surfaces exposed to drinking water. Water Sci. Technol. 32:61–65.

98. Park C. 2007. Extracellular Polymeric Substances in Activated Sludge Flocs: Extraction, Identification, and Investigation of Their Link with Cations and Fate in Sludge.

99. Yin X, Han P, Lu X, Wang Y. 2004. A review on the dewaterability of bio-sludge and ultrasound pretreatment. Ultrason. Sonochem.

100. Nguyen TP, Hankins NP, Hilal N. 2007. A comparative study of the flocculation behaviour and final properties of synthetic and activated sludge in wastewater treatment. Desalination 204:277–295.

101. Nguyen TP, Hilal N, Hankins NP, Novak JT. 2008. Determination of the effect of cations and cationic polyelectrolytes on the characteristics and final properties of synthetic and activated sludge. Desalination 222:307–317.

102. Leentvaar J. 1982. Effect of magnesium a n d calcium precipitation on coagulation-flocculation with lime 16.

103. Peeters B, Dewil R, Lechat D, Smets IY. 2011. Quantification of the exchangeable calcium in activated sludge flocs and its implication to sludge settleability. Sep. Purif. Technol. 83:1–8.

104. Higgins MJ, Novak JT. 1997. Characterization of Exocellular Protein and Its Role in Bioflocculation. J. Environ. Eng.

105. Das A, Caccavo F. 2000. Dissimilatory Fe(III) oxide reduction by Shewanella alga BrY requires adhesion. Curr. Microbiol. 40:344–347.

106. Christopher Dustin Muller. 2001. High-Intensity Shear as a Wet Sludge Disintegration Technology and a Mechanism for Floc Structure Analysis.

107. Lim S, Kim S, Yeon KM, Sang BI, Chun J, Lee CH. 2012. Correlation between microbial community structure and biofouling in a laboratory scale membrane bioreactor with synthetic wastewater. Desalination 287:209–215.

108. Miura Y, Watanabe Y, Okabe S. 2007. Membrane biofouling in pilot-scale membrane bioreactors (MBRs) treating municipal wastewater: Impact of biofilm formation. Environ. Sci. Technol. 41:632–638.

109. Dolinšek J, Lagkouvardos I, Wanek W, Wagner M, Daims H. 2013. Interactions of nitrifying bacteria and heterotrophs: identification of a Micavibrio-like putative predator of Nitrospira spp. Appl. Environ. Microbiol. 79:2027–37.

110. Nogueira R, Elenter D, Brito A, Melo LF, Wagner M, Morgenroth E. 2005. Evaluating heterotrophic growth in a nitrifying biofilm reactor using fluorescence in situ hybridization and mathematical modeling. Water Sci. Technol. 52:135–141.

111. Kindaichi T, Ito T, Okabe S. 2004. Ecophysiological Interaction between Nitrifying Bacteria and Heterotrophic Bacteria in Autotrophic Nitrifying Biofilms as Determined by Microautoradiography-Fluorescence In Situ Hybridization Ecophysiological Interaction between Nitrifying Bacteria and He.

112. Burrell PC, Phalen CM, Hovanec TA, Icrobiol APPLENM. 2001. Identification of Bacteria Responsible for Ammonia Oxidation in Freshwater Aquaria 67:5791–5800.

113. Ma S, Zhang D, Zhang W, Wang Y. 2014. Ammonia stimulates growth and nitrite-oxidizing activity of Nitrobacter winogradskyi. Biotechnol. Biotechnol. Equip. 28:27–32.

114. Cua LS, Stein LY. 2011. Effects of nitrite on ammonia-oxidizing activity and gene regulation in three ammonia-oxidizing bacteria. FEMS Microbiol. Lett. 319:169–75.

115. Norton JM, Alzerreca JJ, Suwa Y, Klotz MG. 2002. Diversity of ammonia monooxygenase operon in autotrophic ammonia-oxidizing bacteria. Arch. Microbiol. 177:139–49.

116. Zou H, Huang J, Fang F, Guo J. 2013. Polygenic analysis of ammonia-oxidizing bacteria for completely autotrophic nitrogen removal 7:1794–1801.

117. Purkhold U. 2003. 16S rRNA and amoA-based phylogeny of 12 novel betaproteobacterial ammonia-oxidizing isolates: extension of the dataset and proposal of a new lineage within the nitrosomonads. Int. J. Syst. Evol. Microbiol. 53:1485–1494.

118. Qiu S, Chen G, Zhou Y. 2010. Abundance and diversity of ammonia-oxidizing bacteria in relation to ammonium in a chinese shallow eutrophic urban lake. Brazilian J. Microbiol. 41:218–226.

119. Cébron A, Garnier J. 2005. Nitrobacter and Nitrospira genera as representatives of nitrite-oxidizing bacteria: detection, quantification and growth along the lower Seine River (France). Water Res. 39:4979–92.

120. Heylen K, Gevers D, Vanparys B, Wittebolle L, Geets J, Boon N, De Vos P. 2006. The incidence of nirS and nirK and their genetic heterogeneity in cultivated denitrifiers. Environ. Microbiol. 8:2012–21.

121. Kolkata E, Bengal W, Saha M, Sarkar A, Bandhophadhyay B. 2013. Development of Molecular Identification of Nitrifying Bacteria in Water 5:1–5.

122. Shore JL, M'Coy WS, Gunsch CK, Deshusses M a. 2012. Application of a moving bed biofilm reactor for tertiary ammonia treatment in high temperature industrial wastewater. Bioresour. Technol. 112:51–60.

123. Gujer W. 2010. Nitrification and me - a subjective review. Water Res. 44:1–19.

124. Singka D, Kumdhitiahutsawakul L, Rekkriangkrai P. 2012. A Simple Method for DNA Extraction from Activated Sludge 39:111–118.

125. Zhou J, Bruns MANN, Tiedje JM. 1996. DNA recovery from soils of diverse composition . These include : DNA Recovery from Soils of Diverse Composition 62.

126. Regan JM, Harrington GW, Noguera DR, Al RET, Icrobiol APPLENM. 2002. Ammonia- and Nitrite-Oxidizing Bacterial Communities in a Pilot-Scale Chloraminated Drinking Water Distribution System 68:73–81.

127. Huang Z, Gedalanga PB, Olson BH. 2010. Distribution of Nitrobacter and Nitrospira Communities in an Aerobic Activated Sludge Bioreactor and their Contributions to Nitrite Oxidation 2390–2403.

128. Li Q, Sun S, Xie H, Zhang W, Feng J, Song C. 2013. Journal of Environmental Biology 34:307–314.

129. Geets J, Cooman M De, Wittebolle L, Heylen K, Vanparys B, Vos P De, Verstraete W, Boon N. 2007. Real-time PCR assay for the simultaneous quantification of nitrifying and denitrifying bacteria in activated sludge 211–221.

130. Juretschko S, Timmermann G, Schmid M, Schleifer K, Pommerening-röser A, Wagner M. 1998. Combined Molecular and Conventional Analyses of Nitrifying Bacterium Diversity in Activated Sludge : Nitrosococcus mobilis and Nitrospira -Like Bacteria as Dominant Populations Combined Molecular and Conventional Analyses of Nitrifying Bacterium Diversity.

131. Nasr R a., AbuShady HM, Hussein HS. 2012. Biofilm formation and presence of icaAD gene in clinical isolates of staphylococci. Egypt. J. Med. Hum. Genet. 13:269–274.

132. Knobloch JK-M, Horstkotte M a, Rohde H, Mack D. 2002. Evaluation of different detection methods of biofilm formation in Staphylococcus aureus. Med. Microbiol. Immunol. 191:101–6.

133. Freeman DJ, Falkiner FR, Patrick S. 1989. New method for detecting slime production by coagulase negative staphylococci 872–874.

134. Christensen GD, Simpson W a., Younger JJ, Baddour LM, Barrett FF, Melton DM, Beachey EH. 1985. Adherence of coagulase-negative staphylococci to plastic tissue culture plates: A quantitative model for the adherence of staphylococci to medical devices. J. Clin. Microbiol. 22:996–1006.

135. Taj Y, Essa F, Aziz F, Kazmi SU. 2012. Study on biofilm-forming properties of clinical isolates of Staphylococcus aureus. J. Infect. Dev. Ctries.

136. Mathur T, Singhal S, Khan S, Upadhyay DJ, Fatma T, Rattan A. 2006. Detection of biofilm formation among the clinical isolates of Staphylococci: an evaluation of three different screening methods. Indian J. Med. Microbiol. 24:25–29.

137. Coates J. 2000. Interpretation of Infrared Spectra, A Practical Approach. Encycl. Anal. Chem. 10815–10837.

138. Amann RI, Krumholz L, Stahl D a. 1990. Fluorescent-oligonucleotide probing of whole cells for determinative, phylogenetic, and environmental studies in microbiology. J. Bacteriol. 172:762–70.

139. Barranguet C, Beusekom SAM Van, Veuger B, Neu TR, Manders EMM, Sinke JJ, Admiraal W. 2004. Studying undisturbed autotrophic biofilms : still a technical challenge 34:1–9.

140. Muhamad MH, Sheikh Abdullah SR, Mohamad AB, Abdul Rahman R, Hasan Kadhum AA. 2013. Application of response surface methodology (RSM) for optimisation of COD, NH3-N and 2,4-DCP removal from recycled paper wastewater in a pilot-scale granular activated carbon sequencing batch biofilm reactor (GAC-SBBR). J. Environ. Manage. 121:179–90.

141. Yun M-A, Yeon K-M, Park J-S, Lee C-H, Chun J, Lim DJ. 2006. Characterization of biofilm structure and its effect on membrane permeability in MBR for dye wastewater treatment. Water Res. 40:45–52.

142. Lo IW, Lo KV, Mavinic DS, Shiskowski D, Ramey W. 2010. Contributions of biofilm and suspended sludge to nitrogen transformation and nitrous oxide emission in hybrid sequencing batch system. J. Environ. Sci. 22:953–960.

143. Woznica A, Nowak A, Beimfohr C, Karczewski J, Bernas T. 2010. Monitoring structure and activity of nitrifying bacterial biofilm in an automatic biodetector of water toxicity. Chemosphere 78:1121–8.

144. Osman WHW, Abdullah SRS, Mohamad AB, Kadhum AAH, Rahman RA. 2013. Simultaneous removal of AOX and COD from real recycled paper wastewater using GAC-SBBR. J. Environ. Manage. 121:80–86.

145. Li X, Xing M, Yang J, Lu Y. 2013. Properties of biofilm in a vermifiltration system for domestic wastewater sludge stabilization. Chem. Eng. J. 223:932–943.

146. Huang H, Ren H, Ding L, Geng J, Xu K, Zhang Y. 2014. Aging biofilm from a full-scale moving bed biofilm reactor: characterization and enzymatic treatment study. Bioresour. Technol. 154:122–30.

147. Melo PDC, Ferreira LM, Filho AN, Zafalon LF, Isa H, Vicente G, Souza V De. 2013. Comparison of methods for the detection of biofilm formation by Staphylococcus aureus isolated from bovine subclinical mastitis 124:119–124.

148. Rehman, A. et al., 2012. Sequential Application of Plastic Media- Trickling Filter and Sand Filter for Domestic Wastewater Treatment at Low Temperature Condition. *British Biotechnology Journal*, 2(4), pp.179–191.

149. Růžička, F. et al., 2004. Biofilm detection and the clinical significance of Staphylococcus epidermidis isolates. *Folia Microbiologica*, 49(5), pp.596–600.

150. Oliveira, R. et al., 2001. The role of hydrophobicity in bacterial adhesion.*bioline*, pp.11–22. Available at http://repositorium.sdum.uminho.pt/handle/1822/6706.

151. Osman, W.H.W. et al., 2013. Simultaneous removal of AOX and COD from real recycled paper wastewater using GAC-SBBR. *Journal of Environmental Management*, 121, pp.80–86.

152. Lipponen, M.T.T., Suutari, M.H. & Martikainen, P.J., 2002. Occurrence of nitrifying bacteria and nitrification in Finnish drinking water distribution systems. *Water research*, 36(17), pp.4319–29. Available at: http://www.ncbi.nlm.nih.gov/pubmed/12420937.

153. Kavita, K., Mishra, A. & Jha, B., 2011. Isolation and physico-chemical characterisation of extracellular polymeric substances produced by the marine bacterium Vibrio parahaemolyticus. *Biofouling*, 27(3), pp.309–317.

154. Andersson, S., Kuttuva Rajarao, G., et al., 2008. Biofilm formation and interactions of bacterial strains found in wastewater treatment systems. *FEMS Microbiology Letters*, 283, pp.83–90.

Table 1. Chart showing CFU/ml from different biofilm support materials under varying Fe(III) concentrations.

	Polyethylene(PE)	Fe	Stainless steel (SS)	Tire rubber (TR)	Polyvinylchloride (PVC)
Fe2.5	7.120E+07	2.300E+06	2.000E+06	3.400E+07	4.000E+06
	5.280E+08	1.080E+08	1.800E+07	1.360E+08	3.300E+08
	5.040E+09	2.480E+09	1.300E+08	9.200E+08	2.000E+09
	3.490E+10	3.500E+09	8.000E+09	5.200E+09	1.450E+10
	4.310E+11	7.300E+10	5.000E+10	1.200E+10	9.000E+10
Fe6.5	7.120E+07	2.800E+06	1.000E+07	3.000E+08	7.000E+07
	8.120E+08	1.950E+08	8.000E+08	1.500E+09	3.570E+08
	6.760E+09	2.340E+09	6.000E+09	8.390E+09	2.350E+09
	4.760E+10	8.100E+09	4.000E+10	3.930E+10	1.300E+09
	3.760E+11	1.000E+10	2.000E+11	1.600E+11	1.100E+10
Fe8.5	1.104E+08	3.400E+06	6.560E+07	3.500E+08	5.600E+07
	5.440E+08	7.000E+06	5.120E+08	2.567E+09	4.300E+07
	5.000E+09	1.000E+07	4.680E+09	1.900E+10	3.200E+08
	4.800E+10	1.000E+0	4.440E+10	1.324E+1	1.000E+09

		8		1	
	8.320E+11	1.000E+09	2.200E+11	8.250E+10	3.000E+09
Control	6.920E+07	8.320E+07	9.460E+08	6.160E+07	8.190E+07
	6.160E+08	7.050E+08	7.760E+07	4.520E+08	6.400E+08
	5.000E+09	6.500E+09	4.500E+08	4.200E+09	4.000E+09
	5.600E+10	4.300E+10	2.000E+09	3.150E+10	1.440E+10
	4.100E+11	2.100E+11	9.700E+10	2.150E+11	8.700E+10

Table 2. Two way ANOVA without Replication Applied on CFU data

SUMMARY	*Count*	*Sum*	*Average*	*Variance*
Fe2.5	5	1.14E+08	22700000	9.19E+14
	5	1.12E+09	2.24E+08	4.18E+16
	5	1.06E+10	2.11E+09	3.52E+18
	5	6.61E+10	1.32E+10	1.64E+20
	5	6.56E+11	1.31E+11	2.89E+22
Fe6.5	5	4.54E+08	90800000	1.47E+16
	5	3.66E+0	7.33E+08	2.57E+1

		9		7
	5	2.58E+10	5.17E+09	7.39E+18
	5	1.36E+11	2.73E+10	4.41E+20
	5	7.57E+11	1.51E+11	2.31E+22
Fe8.5	5	5.85E+08	1.17E+08	1.84E+16
	5	3.67E+09	7.35E+08	1.11E+18
	5	2.9E+10	5.8E+09	5.99E+19
	5	2.26E+11	4.52E+10	2.9E+21
	5	1.14E+12	2.28E+11	1.22E+23
Control	5	1.24E+09	2.48E+08	1.52E+17
	5	2.49E+09	4.98E+08	6.39E+16
	5	2.02E+10	4.03E+09	4.97E+18
	5	1.47E+11	2.94E+10	4.68E+20
	5	1.02E+12	2.04E+11	1.69E+22
PLASTIC	20	2.26E+12	1.13E+11	4.95E+22
Fe	20	3.61E+11	1.81E+10	2.37E+21

stainless steel	20	6.75E+11	3.38E+10	4.27E+21		
TR	20	7.16E+11	3.58E+10	3.88E+21		
PVC	20	2.32E+11	1.16E+10	7.13E+20		
ANOVA						
Source of Variation	*SS*	*df*	*MS*	*F*	*P-value*	*F crit*
Rows	5.07E+23	19	2.67E+22	3.131105	0.000216	1.725029
Columns	1.33E+23	4	3.32E+22	3.898145	0.006216	2.492049
Error	6.48E+23	76	8.52E+21			

Table 3: Average CFU/ml from different supports under varying Fe(III) concentrations.

	Biofilm Support Materials									
Fe Concentration	Stainless Steel	Std. Error	TR	Std. Error	Iron	Std. Error	PVC	Std. Error	PE	Std. Error
Fe-2.5	1.163E+10	9.698E+09	1.806E+10	2.287E+09	1.58E+10	7.06E+09	2.14E+10	1.73E+10	9.43E+10	4.21E+10
Fe-6.5	4.936E+10	3.831E+10	4.190E+10	3.031E+10	4.13E+09	1.84E+09	3.02E+09	2.03E+09	8.62E+10	3.85E+10
Fe-8.5	5.393E+10	4.226E+10	4.736E+10	2.592E+10	2.24E+08	1E+08	8.84E+08	5.56E+08	1.77E+11	7.91E+10
Contr	2.009	1.920	2.959	21679	5.21	2.32	2.12	1.66	9.43	4.21

ol	E+10	E+10	E+09	49326	E+10	E+10	E+10	E+10	E+10	E+10

Table 4. Light microscopy examination of selected bacteria isolated from activated sludge and biofilms developed under varying Fe(III) concentration on different support materials.

Biofilm			Activated Sludge		
No.	**Isolate No.**	**Gram Staining**	**No.**	**Isolate No.**	**Gram Staining**
1	Iq7	gram positive, long Bacilli	1	Iq1	gram negative, Bacilli
2	Iq11	gram positive, Bacilli	2	Iq2	gram negative, Bacilli
3	Iq15	gram positive, cocci (diplococcic)	3	Iq5	gram negative Bacilli, thin and short
4	Iq20	gram negative, chains of large Bacilli	4	Iq6	gram negative Bacilli, chains
5	Iq26	gram positive, Bacilli	5	Iq7	gram negative, Bacilli
6	Iq26	gram negative, Bacilli	6	Iq9	gram positive, Bacilli
7	Iq54	gram positive, Bacilli	7	Iq12	gram positive, cocci
8	Iq87	gram negative, short Bacilli	8	Iq13	gram negative, short Bacilli
9	Iq88	gram negative, Bacilli	9	q14	Gram variable
10	Iq89	gram positive, Bacilli	10	Iq15	gram negative, Bacilli

11	Iq89	gram negative, Bacilli	11	Iq17	gram negative, coccobacilli
12	Iq91	gram negative, Bacilli	12	Iq18	gram negative, Bacilli
13	Iq93	gram positive, Bacilli	13	Iq23	gram negative, thin rods
14	Iq98	gram negative, Bacilli	14	IqB23	gram positive, clustered
15	Iq99	gram negative, Bacilli	15	Iq24 (Orange)	gram positive, Bacilli, chains
16	Iq101	gram positive, short rods (may be coccobacilli)	16	Iq26	gram positive, cocci
17	Iq104	gram negative, Bacilli	17	Iq18	gram negative, Bacilli
18	Iq106	gram negative, short Bacilli (may be coccobacilli)	18	Iq23	gram negative, Bacilli
19	Iq109	gram negative, Bacilli	19	IqB23	gram positive, clustered
20	Iq115	gram negative, Bacilli			
21	Iq118	gram positive, Bacilli			
22	Iq121	gram negative, Bacilli			

Table 5: Concentrations (mg/l) and % Increase/decrease of nitrite in stainless steel.

Stainless steel - NO_2^-										
Fe Concentration	0 (X1)	A	15 (X2)	A	ΔX	% red./Inc.	30 (X3)	A	ΔX	% red./Inc.
2.5	0.0501	0.02839	0.17025	0.12231	0.12015	70.57268722	0.2904	0.4122	0.2403	82.747 9339
6.5	0.083	0.231479	0.1667	0.10012	0.0837	50.20995801	0.2505	0.35 14	0.1675	66.866 2675
8.5	0.0401		0.1101	0.09675	0.07	63.57856494	0.1603	0.2035	0.1202	74.984 4042
Control	0.0668	0.04342	0.0334	0.00431	0.0334	50	0	-0.04741	0.0668	100

Table 6: Concentrations (mg/l) and % Increase/decrease of nitrate in stainless steel.

Stainless steel - NO_3^-										
Fe Concentration	0 (X1)	A	15 (X2)	A	ΔX	% red./ Inc.	30 (X3)	A	ΔX	% red./ Inc.
2.5	Undetectable	-0.08851	1.56312	0.15342	1.56312	100	3.126407	0.02405	3.126407	100
6.5	Undetectable	2.7889	1.3944	0.1221	1.3944	100	2.7889	0.01173	2.7889	100
8.5	Undetectable	-0.07551	0.5579	0.06423	0.5579	100	1.1155	0.01521	1.1155	100
Control	Undetecable	-0.11523	1.5789	0.15213	1.5789	100	3.1581	0.02505	3.1581	100

Table 7: Concentrations (mg/l) and % Increase/decrease of nitrite in PVC.

PVC - NO_2^-										
Fe Concentration	0 (X1)	A	15 (X2)	A	ΔX	% red./Inc.	30 (X3)	A	ΔX	% red./Inc.
2.5	0.083	0.05845	0.1083	0.1528	0.0253	23.36103416	0.1336	0.17 29	0.0506	37.8742515
6.5	0.083	0.231479	0.099995	0.14721	0.016995	16.99584979	0.1169	0.15 06	0.0339	28.9991446
8.5	0.0401	0.10213	0.1101	0.1621	0.07	63.57856494	0.1603	0.20 35	0.1202	74.9844042
Control	0.0668	0.04342	0.0334	0.081243	0.0334	50	0	-0.04741	0.0668	100

Table 8. Concentrations (mg/l) and % Increase/decrease of nitrate in PVC biofilm.

PVC-NO_3^-										
Fe Concentration	0 (X1)	A	15 (X2)	A	ΔX	% red./Inc.	30 (X3)	A	ΔX	% red./Inc.
2.5	0.835	5.53208	1.225947	0.11101	0.390947	31.88938837	2.7889	0.04312	1.9539	70.0598802
6.5	<0.835	2.7889	0.1235	0.11789	0.7115	85.20958084	0.2788	0.12024	0.5562	66.6107784
8.5	<0.02004	0.00312	0.8366	4.6784	0.81656	97.60459001	1.6733	0.14195	1.65326	98.8023666
Control	Undetectable	-0.0835	1.3939	1.321	1.3939	100	2.7889	0.04342	2.7889	100

Table 9: Concentrations (mg/l) and % Increase/decrease of nitrite in Fe biofilm

Fe-NO_2^-										
Fe Concentration	0 (X1)	A	15 (X2)	A	ΔX	% red./Inc.	30 (X3)	A	ΔX	% red./Inc.
2.5	0.58 45	0.52 772	1.00 2	2.000 11	0.41 75	41.666 66667	1.4 195	2.16 97	0.83 5	58.823 5294
6.5	0.05 1	0.04 521	0.16 74	0.450 001	0.11 64	69.534 05018	0.2 839	0.23 547	0.23 29	82.035 9281
8.5	0.04 711	0.03 125	0.12 41	0.420 01	0.07 699	62.038 67849	0.2 01	0.23 145	0.15 389	76.562 1891
Control	0.58 45	0.31 1	0.35 905	0.845 32	0.22 545	38.571 42857	0.1 336	0.15 61	0.45 09	77.142 8571

Table 10. Concentrations (mg/l) and % Increase/decrease of nitrate in Iron biofilm

Fe-NO_3^-										
Fe Concentration	0 (X1)	A	15 (X2)	A	ΔX	% red./ Inc.	30 (X3)	A	ΔX	% red./ Inc.
2.5	Undetectable	0.03 173	0.697 225	0.93 21	0.697 225	100	1.39 445	0.11 356	1.39 445	100
6.5	Undetectable	0.00 021	1.786 7	2.54 321	1.786 7	100	3.62 55	0.25 718	3.62 55	100
8.5	Undetectable	0.00 331	1.670 8	2.33 672	1.670 8	100	3.67 45	0.25 612	3.67 45	100
Control	Undetecable	0.03 34	0	0	0	0	0	0	0	0

Table 11: Concentrations (mg/l) and % Increase/decrease of nitrite in PE biofilm.

PE- NO_2^-

Fe Concentration	0 (X1)	A	15 (X2)	A	ΔX	% red./Inc.	30 (X3)	A	ΔX	% red./Inc.
2.5	0.0835	0.0501	0.167	0.092122	0.0835	50	0.25005	0.35514	0.167	66.666 6667
6.5	0.0835	0.232873	0.12525	0.040 01	0.04175	33.3333 3333	0.167	0.2062	0.2329	139.46 1078
8.5	0.10 02	0.0668	0.13 36	1.673 21	0.03 34	25	0.167	0.22 86	0.06 68	40
Control	0.0835	0.056 78	0.12 525	1.321	0.04 175	33.3333 3333	0.167	0.22 02	0.08 35	50

Table 12. Concentrations (mg/l) and % Increase/decrease of nitrate in PE biofilm

PE-NO_3^-

Fe Concentration	0 (X1)	A	15 (X2)	A	ΔX	% red./Inc.	30 (X3)	A	ΔX	% red./Inc.
2.5	Undetectable	0.02839	0.11 1556	0.07214	0.11 1556	100	0.22 3112	0.06012	0.22 3112	100
6.5	Undetectable	2.78 89	0.55 62	0.62 11	0.55 62	100	1.11 55	0.10 521	1.11 55	30.76 81699
8.5	<.0116 9	0.91	1.39 29	2.78 321	1.38 121	99.160 74377	2.78 89	0.04 175	2.77 721	99.58 08383
Control	Undetecable	0.00 334	1.39 44	2.77 321	1.39 44	100	2.78 89	0.07 181	2.78 89	100

Table 13: Concentrations (mg/l) and % Increase/decrease of nitrite in TR biofilm

TR- NO_2^-										
Fe Concentration	0 (X1)	A	15 (X2)	A	ΔX	% red./Inc.	30 (X3)	A	ΔX	% red./Inc.
2.5	0.099981	0.074378	0.6785	0.8211	0.578519	85.26440678	2.0004	3.87	1.900419	95.0019496
6.5	0.4175	1.164366	1.8036	2.76821	1.3861	76.85185185	3.1897	4.9447	2.7722	86.9109948
8.5	0.0668	0.0334	0.054275	0.00687	0.012525	18.75	0.04175	0.2761	0.02505	37.5
Control	0.0835	0.05678	0.1008	0.47011	0.0173	17.16269841	0.1336	0.1561	0.0501	37.5

Table 14: Concentrations (mg/l) and % Increase/decrease of nitrate in TR biofilm

TR- NO_3^-										
Fe Concentration	0 (X1)	A	15 (X2)	A	ΔX	% red./Inc.	30 (X3)	A	ΔX	% red./Inc.
2.5	Undetectable	-0.08421	1.4761	2.10021	1.4761	100	2.643	0.05746	2.643	100
6.5	Undetectable	-0.09853	1.8127	2.34612	1.8127	100	3.6255	1.65497	3.6255	100
8.5	Undetectable	0.02004	1.3944	2.01754	1.3944	100	2.7889	0.06847	2.7889	100
Control	Undetectable	0.0835	1.3349	2.015611	1.3349	100	2.7889	0.04008	2.7889	100

Table 15. Dissolved oxygen (mg/l) profile within the reactors monitored periodically.

No.	Sample	1st reading DO (mg/l)	2nd reading DO (mg/l)	3rd reading DO (mg/l)	Average DO (mg/l)
1	Activated sludge	4.57	4.57	4.56	4.57
2	Fe-2.5	0.4	0.16	.18	0.25
3	Fe-6.5	1.45	0.04	1.21	0.9
4	Fe-8.5	4.21	0.25	1.89	2.12
5	Control	4.06	0.74	1.20	2

Table 16: Comparative analysis of effect of centrifuge and vertex on microbial density

	CFU/ml (24 h)	
Dilution	Sludge without processing	Sludge after centrifugation and vertexing
10^ 1	3.405E+03	4.575E+03
10^ 2	2.130E+03	2.145E+03
10^ 3	1.215E+03	1.800E+03
10^ 4	6.450E+02	7.190E+02
10^ 5	3.660E+02	6.900E+02
10^ 6	2.220E+02	4.050E+02
10^ 7	1.670E+02	1.770E+02

Table 17: Microtiter plate assay chart representing the OD (590nm) of biofilm forming and non-biofilm forming isolates measured by ELISA autoreader (Biorad).

	A	B	C	D	E	F	G	H
1	(11)0.453	(25)0.208	(99)0.241	(86)0.335	(8)0.246	(20)0.168	(119)0.334	0.167

2	(4)0.282	(1)0.369	(111)0.4	(83)0.433	(95)0.468	(22)0.233	(88)0.286	0.189
3	(85)0.213	(23)0.291	(107)0.272	(27)0.56	(91)0.393	(18)0.317	(104)0.243	
4	(113)0.248	(6)0.28	(51)0.426	(118)0.296	(10)0.334	(103)0.328	0.175	
5	(116)0.379	(113)0.752	(81)0.200	(28)0.453	(12)0.255	(26)0.243	0.199	
6	(105)0.211	(33)0.256	(16)0.384	(102)0.264	(51)0.37	(21)0.65	0.277	
7	(45)0.215	(24)0.336	(14)0.698	(89)0.662	(54)0.246	(95)0.341	0.203	
8	(66)0.184	(52)0.268	(82)0.349	(94)0.302	(7)0.38	(unknown)1.199	0.217	
9	(56)0.298	(57)0.471	(5)0.200	(53)0.282	(2)0.227	(110)1.772	0.189	
10	(55)0.316	(115)0.52	(101)0.733	(87)0.262	(15)0.366	(100)0.528	0.262	
11	(92)0.499	(19)0.519	(98)0.838	(93)0.631	(17)0.288	(30)0.441	0.239	
12	(32)0.166	(19)0.37	(108)0.287	(96)0.3	(29)0.535	(3)0.306	0.182	

Table 18: NO_2^- - N concentration (mg/l) in aerobic batch biofilm reactors (ABBRs) during sludge digestion under treated and untreated conditions.

		Nitrite in week 1		**week 2**		**week 3**	
No.	Sample No	Concentration (mg/l)	Absorbance	Concentration (mg/l)	Absorbance	Concentration	Absorbance
1	Control	182	0.231	74	0.099	44	0.063

		week 1		week 2		week 3	
No.	Sample No	Nitrate concentration (mg/l)	Absorbance	Nitrate concentration (mg/l)	Absorbance	Nitrate concentration (mg/l)	Absorbance
1	Control	168.3	0.796	206.6	0.936	163.7	0.78
2	Fe - 2.5	273.7	1.18	258.9	1.126	132.6	0.667
3	Fe - 6.5	220.5	0.986	141.9	0.701	128.1	0.647
4	Fe - 8.5	150.6	0.732	182	0.846	183	0.85
2	Fe - 2.5	55	0.077	17	0.03	27	0.043
3	Fe - 6.5	61	0.084	14	0.027	42	0.061
4	Fe - 8.5	17	0.03	12	Absorbance	61	0.083

Table 19: NO_3^- - N concentration (mg/l) within aerobic batch biofilm reactors (ABBR) during sludge digestion under treated and untreated conditions.

Table 21. pH profile of activated sludge in Aerobic Batch Biofilm Reactors (ABBR).

Fe^{3+} concentration in reactors (mg/l)	Reading1	Reading 2	Reading 3	Reading 4	Average
Control	7.47	7.47	7.31	7.06	7.3275
Fe-2.5	6.44	7.26	7.6	7.47	7.1925
Fe-6.5	6.45	7.33	7.54	7.65	7.2425
Fe-8.5	6.65	7.35	7.79	7.65	7.36